Search for Anomalous Gauge Coupling through Vector Boson Scattering and Development of the GEM Detectors at the CMS Experiment

Ram Krishna Sharma

PhD Reg. No.: SF-1/Ph.D./2574, October 25th 2012

Pre-PhD Seminar

October 8, 2018

Supervisor: Dr. Md. Naimuddin

Advisory Committee: Dr. Ashok Kumar

Prof. T. R. Seshadri

Documentation

Available on CMS information server

CMS AN -2017/236

The Compact Muon Solenoid Experiment

Analysis Note

The content of this note is intended for CMS internal use and distribution only

Internal Analysis Note (CMS AN-2017/236)

04 September 2017 (v7, 05 October 2018)

Search for anomalous electroweak production of $WW/WZ/ZZ$ boson pairs in association with two jets in proton-proton collisions at 13 TeV

Ram Krishna Sharma, Aram Apyan, Andrew Beretvas, Jeffrey Berryhill, Pietro Govoni, Davide V
Green, Md Naimuddin, Jakob Salfeld-Nebgen, Patricia Teles

Abstract

Published Paper on GEM Detector

Nuclear Inst. and Methods in Physics Research, A

journal homepage: www.elsevier.com/locate/nima

ELSEVIER

Technical Notes

Development, characterization and qualification of first GEM foils produced in India

Aashaq Shah [a], Asar Ahmed [a], Mohit Gola [a], Ram Krishna Sharma [a,*], Shivali Malhotra [a], Ashok Kumar [a], Md. Naimuddin [a], Pradeep Menon [b], K. Srinivasan [b]

[a] Department of Physics & Astrophysics, University of Delhi, Delhi, India
[b] Micropack Pvt. Ltd., Bengaluru, India

ARTICLE INFO

Keywords:
GEM
Single-mask
Double-mask

ABSTRACT

The increasing demand for Gas Electron Multiplier (GEM) foils has been driven by their application in many current and proposed high-energy physics experiments. Micropack, a Bengaluru-based company, has established and commercialized GEM foils for the first time in India. Micropack used the double-mask etching technique to successfully produce 10 cm × 10 cm GEM foil. In this paper, we report on the development as well as the ... the size uniformity of the holes and leakage current ... foils are of good quality and satisfy all the necessary

...itutions, including the University of Delhi, are ...tor upgrade project of the CMS experiment [11] ...Collider (LHC). Indian groups are planning to ...ly 20% of the total GEM detectors required for ...de [12] and future GE2/1 upgrade [13] . As a ...D program on GEM detectors has been initiated ...icropack Pvt. Ltd. in Collaboration with Indian ...rked upon the development of GEM foils in

...013, Micropack signed a Transfer of Technology ... CERN for the development of GEM foils in ...efforts, refining of processes and repeated trials, ...ccessful in realizing 10 cm × 10 cm GEM foils, ...dimensional requirements. The foil production ...ith single-mask process. However, after several ...zed that copper removal through the reverse ...allenging. By contrast, the double-mask process ...ast results. The double-mask GEM foils were ... in a similar fashion as produced at the CERN ...ing photo-lithographic techniques in which hole ...d to the copper-clad polyimide substrate using ...ed on the top and bottom of the substrate. A 15

CMS PAPER SMP-18-006

DRAFT
CMS Paper

The content of this note is intended for CMS internal use and distribution only

Paper Draft:
To be submitted in PLB

2018/06/20
Head Id: 465236
Archive Id: 465239P
Archive Date: 2018/06/20
Archive Tag: trunk

Search for anomalous electroweak production of $WW/WZ/ZZ$ boson pairs in association with two jets in proton-proton collisions at 13 TeV

Available on the CMS information server

CMS DN-16-017

CMS Draft Analysis Note

The content of this note is intended for CMS internal use and distribution only

Internal Detector Note:
Test Beam Studies

2018/08/15
Head Id: 373977
Archive Id: 471924
Archive Date: 2016/11/16
Archive Tag: trunk

Test beam studies of Gas Electron Multiplier (GEM) detectors for the upgrade of CMS endcap muon system

Vipin Bhatnagar[3], Brian Dorney[1], Marek Michal Gruchala[4], Priyanka Kumari[3], Ankita Mehta[3], Md Naimuddin[2], Jeremie Alexandre Merlin[1], Archana Sharma[1], Ram Krishna Sharma[2], and J.B. Singh[3]

[1] CERN, Geneva, Switzerland
[2] University of Delhi, INDIA
[3] Panjab University, Chandigarh, INDIA
[4] Ghent University, Belgium

Outline of Talk

- Introduction on LHC, CMS and its features
- Introduction to GEM
- GEM fabrication & characterisation in India
- Test beam studies for CMS muon system upgrade
- Introduction of VBS & aQGC
- Details of Physics analysis
- Conclusions

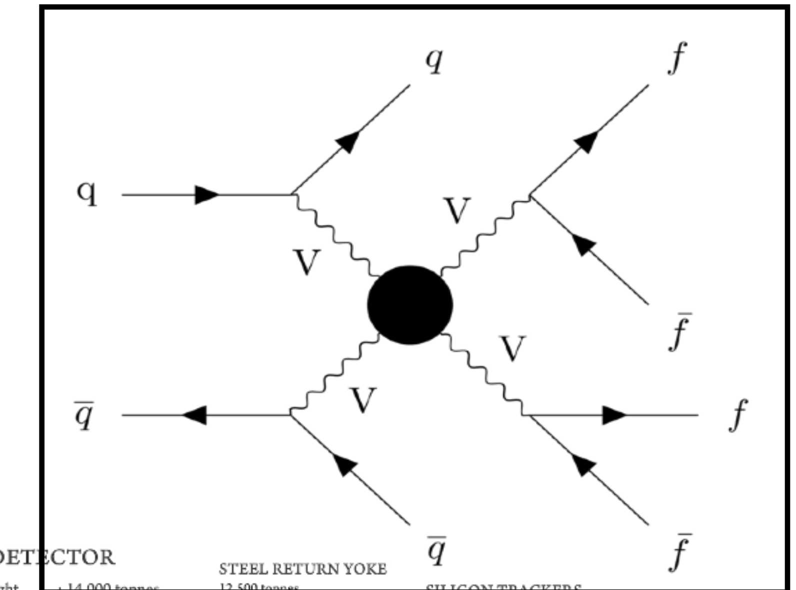

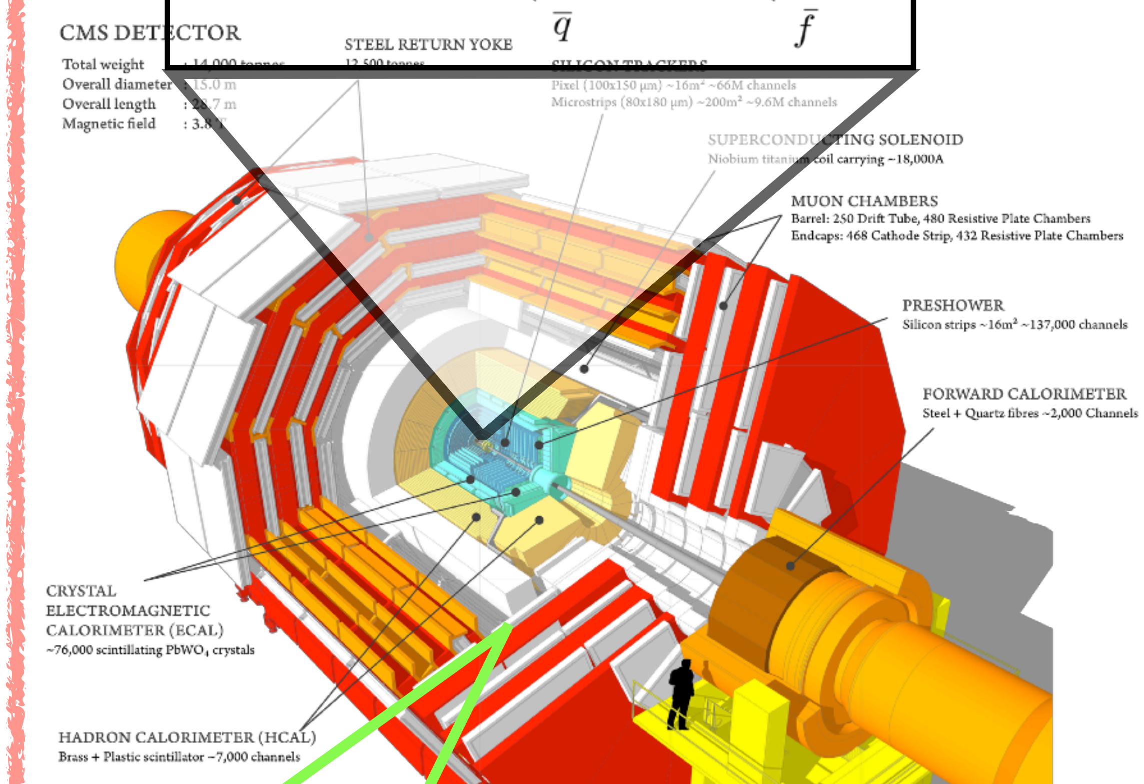

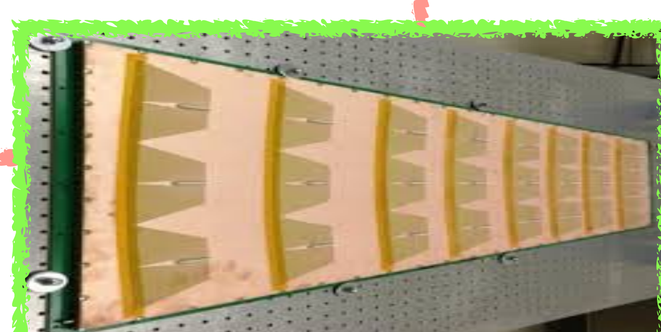

Large Hadron Collider

- World's most powerful particle accelerator & collider.
- Located in a 27 km long tunnel, 100 m underground at Swiss-France border.
- High energy protons travelling in two counter-rotating beams are smashed together to understand the behaviour of particles and their interactions → 40 million times per second.
- Currently, operating at 13 TeV centre of mass energy with peak luminosity, L = 2.1 x 10^{34} $cm^{-2}s^{-1}$.
- Four big experiments located at various interaction points.

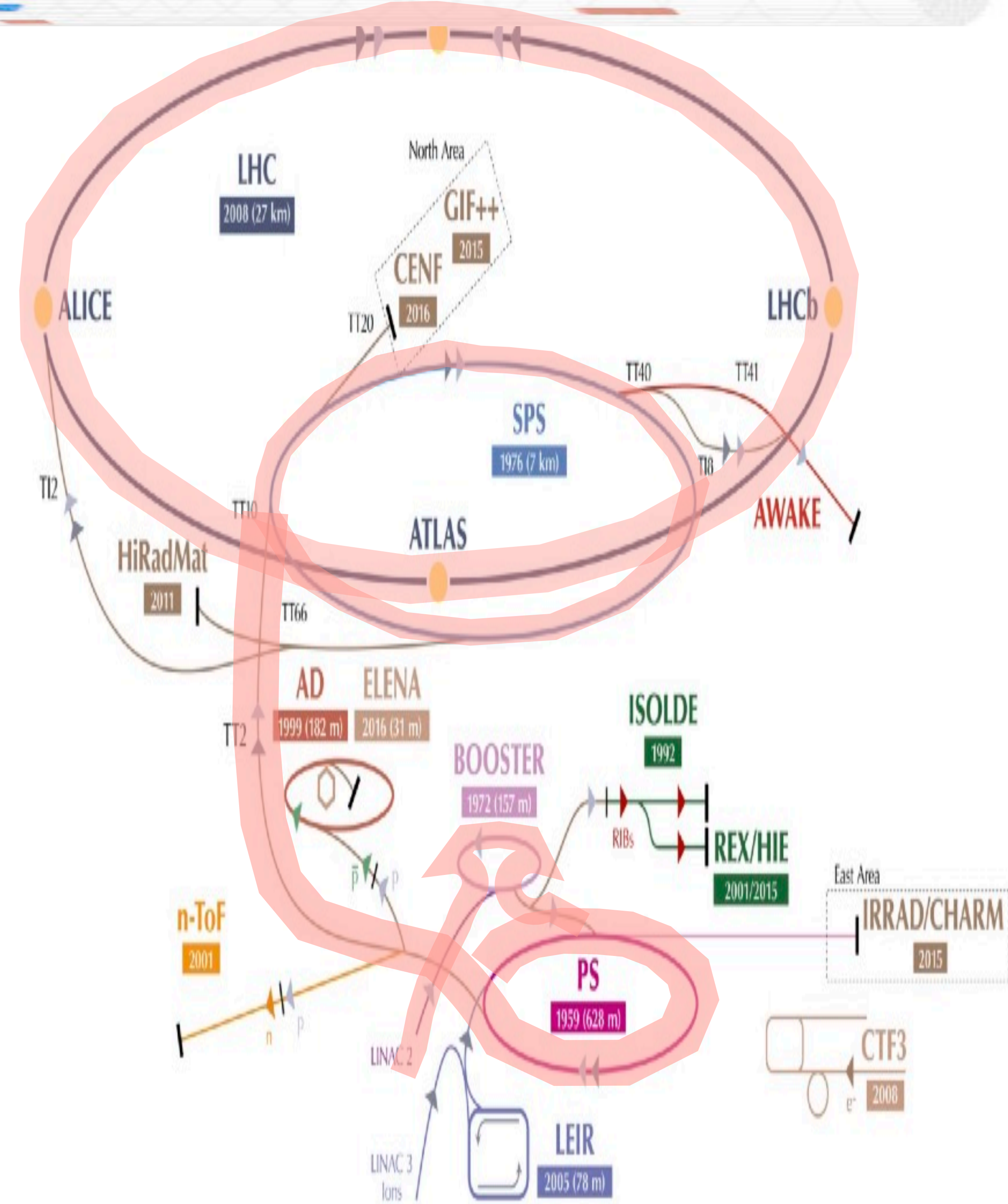

$$\frac{dR}{dt} = \mathscr{L} \,.\, \sigma_p \rightarrow \mathscr{L} = \frac{k_b N_1 N_2 f_{rev}\gamma}{A_{eff}} \rightarrow \mathscr{L}_{int} = \int_0^T L(t')dt' \,,$$

Compact Muon Solenoid (CMS) Experiment

- CMS detector is one of general purpose detector built around the LHC
- Consists of 4 sub-detectors:
  - Tracker
  - Electromagnetic Calorimeter
  - Hadron Calorimeter
  - Muon System

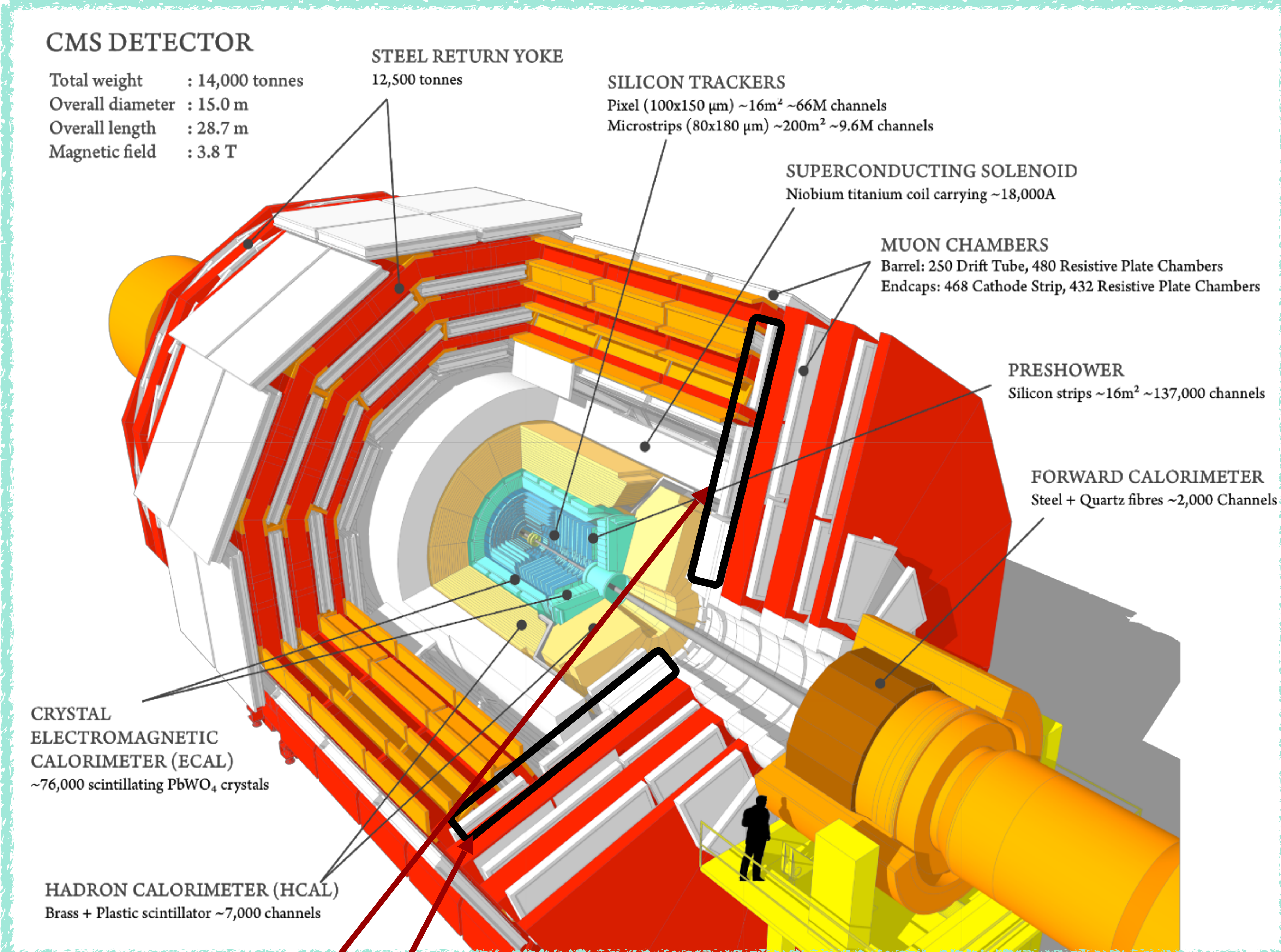

Muon system to be upgraded…

CMS Detector Slice

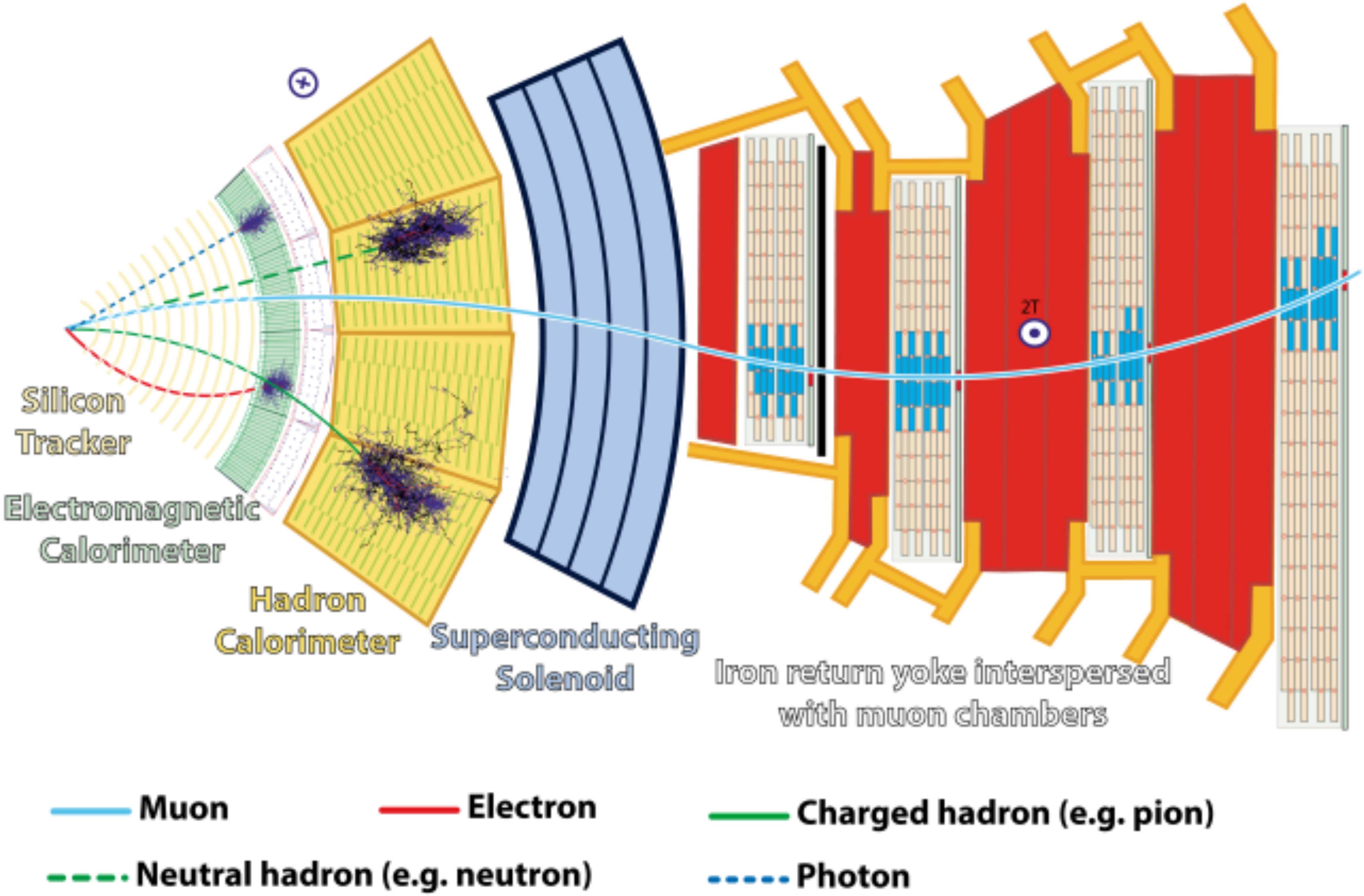

What is GEM?

- GEM ⇒ Gas Electron Multiplier

- A thin polyamide sheet (Kapton) coated with a thin layer of metal (copper)
⇒ chemically pierced with uniform array of holes.

$$E = \frac{V}{d}$$

  - Small potential difference can create high electric field:
  - V ⇒ potential difference, d ⇒ Thickness of polyamide sheet.

- A gaseous detector made using the GEM foil known as the GEM detector.

- **Motivation**: Developed to operate in high rate, and harsh experimental condition.

- Presently in Use:
  - HERA-B tracker,
COMPASS experiment at CERN,
LHCb tracker, TOTEM

GEM Features:
Rate Capability: ~MHz/cm²
Spatial Resolution: ~100 μm
Time Resolution: ~ 5-7ns
Detection Efficiency: > 98%

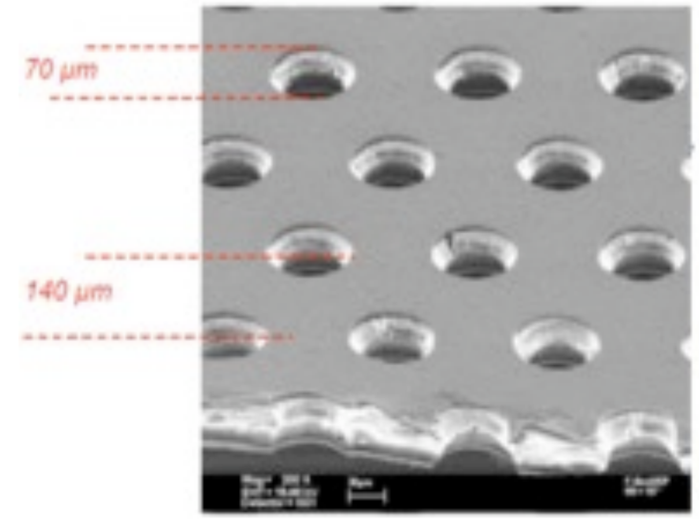

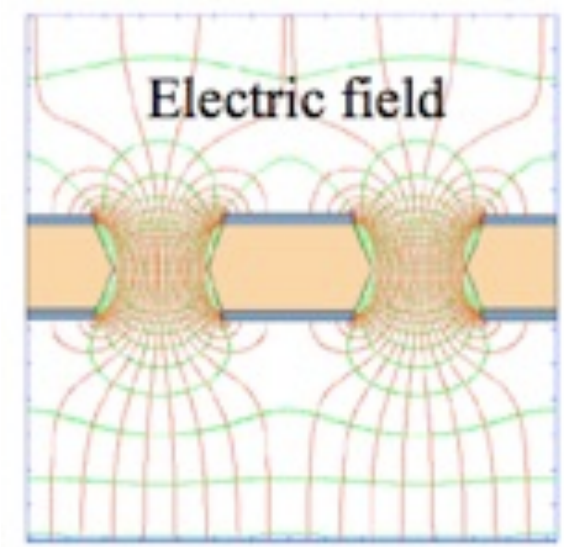

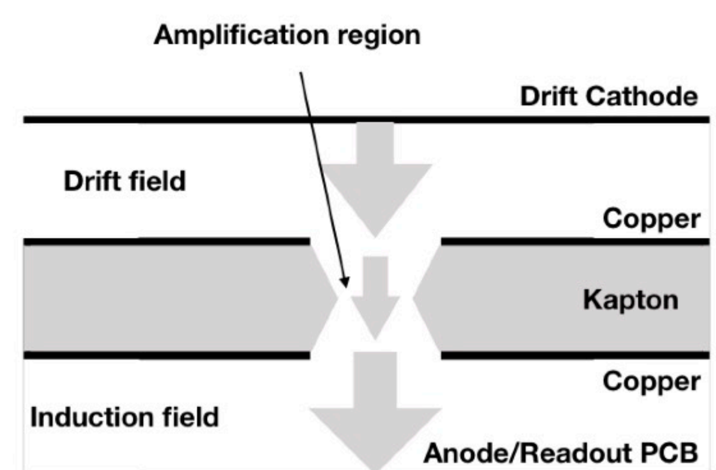

Hardware activities (Delhi University)

- Through Transfer-of-Technology Indian company (Micropack Pvt. Ltd.) got the technology of producing the GEM foil from CERN.
- It successfully produced small GEM foil ($10x10cm^2$).
- Characterisation of GEM foils:
    - Visual inspection
    - Optical Study
    - Electrical behaviour of the foils

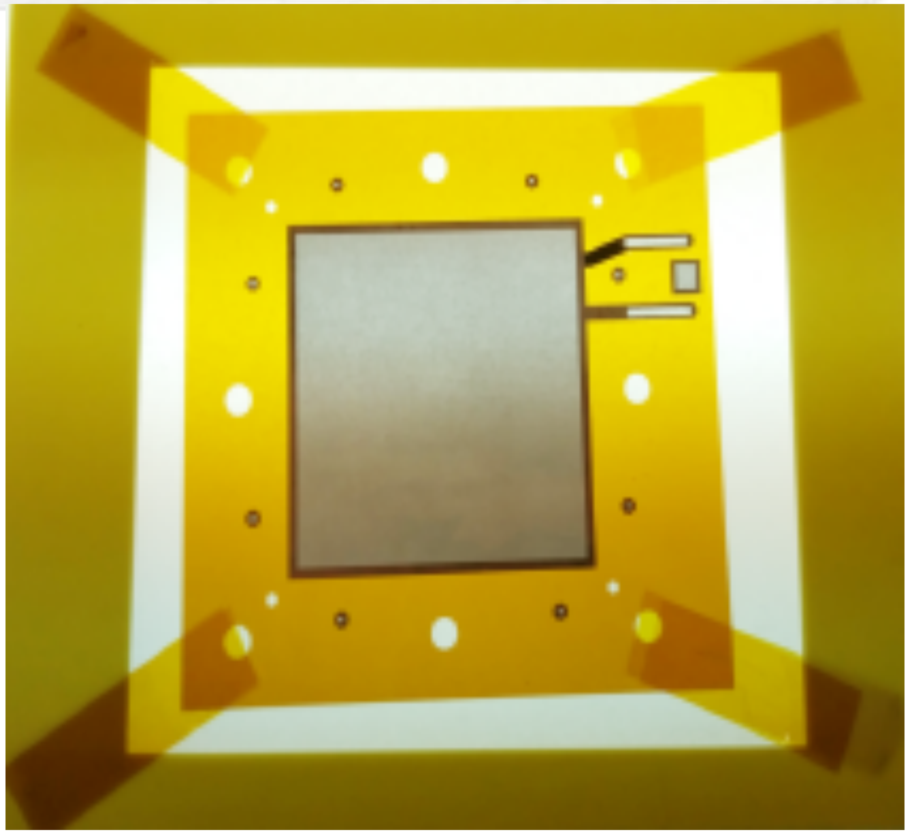

10cmX10cm Micropack Foil with frame

Adhesive Roller

GEM Foil

- GEM foil hole size : 50 μm (inner diameter)
  70 μm (outer diameter)

- Should be exposed *only* in clean rooms
  - Clean room specially designed room for scientific research
  - Maintained at extremely low level of particle per cubic meters.
  - Different classes of clean room can be made as per need. For example:
    - Class-100 clean room : maintains particle per cubic meter = 100
    - Class-1000 clean room: maintains particle per cubic meter = 1000

Clean Room for GEM foil Characterization

(at University of Delhi)

- Clean room class: Class 100
- Dimensions: 14 ft x 12 ft x 8 ft
- Equipped with humidity and temperature controls
- Continues monitored with dust particle counter in real time

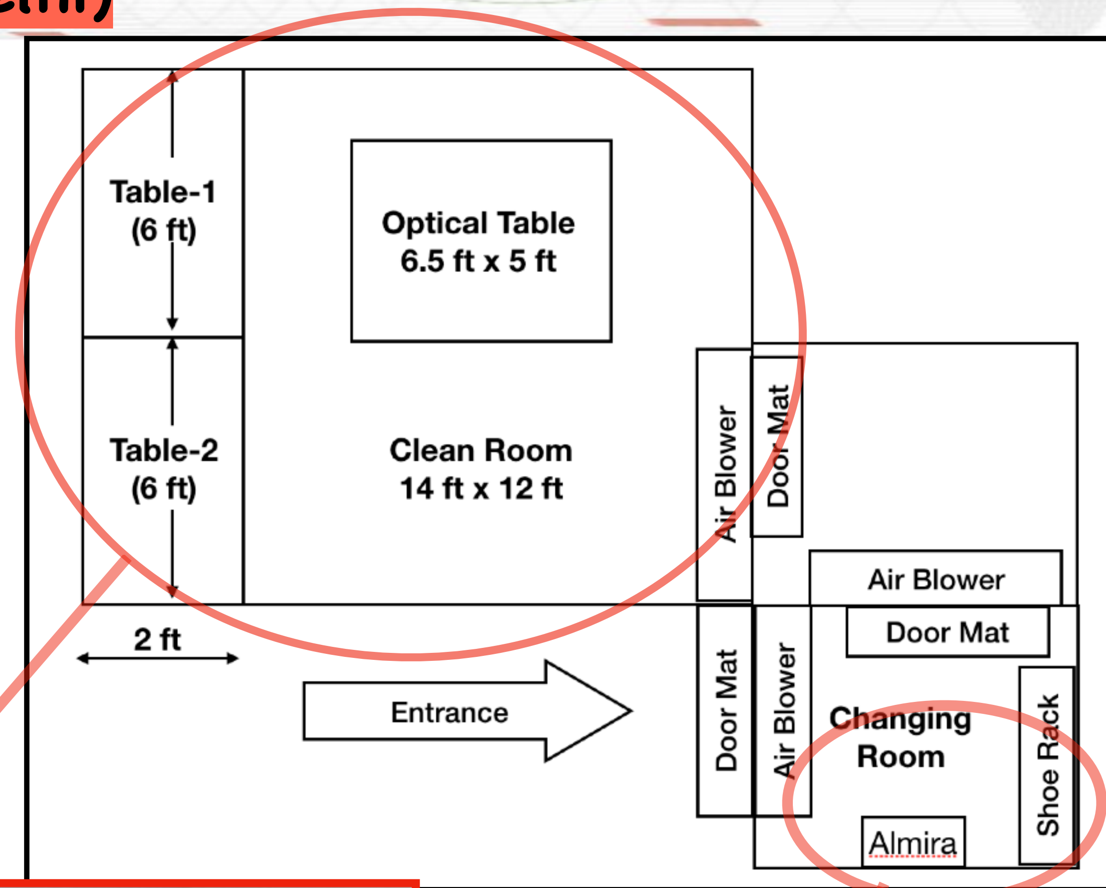

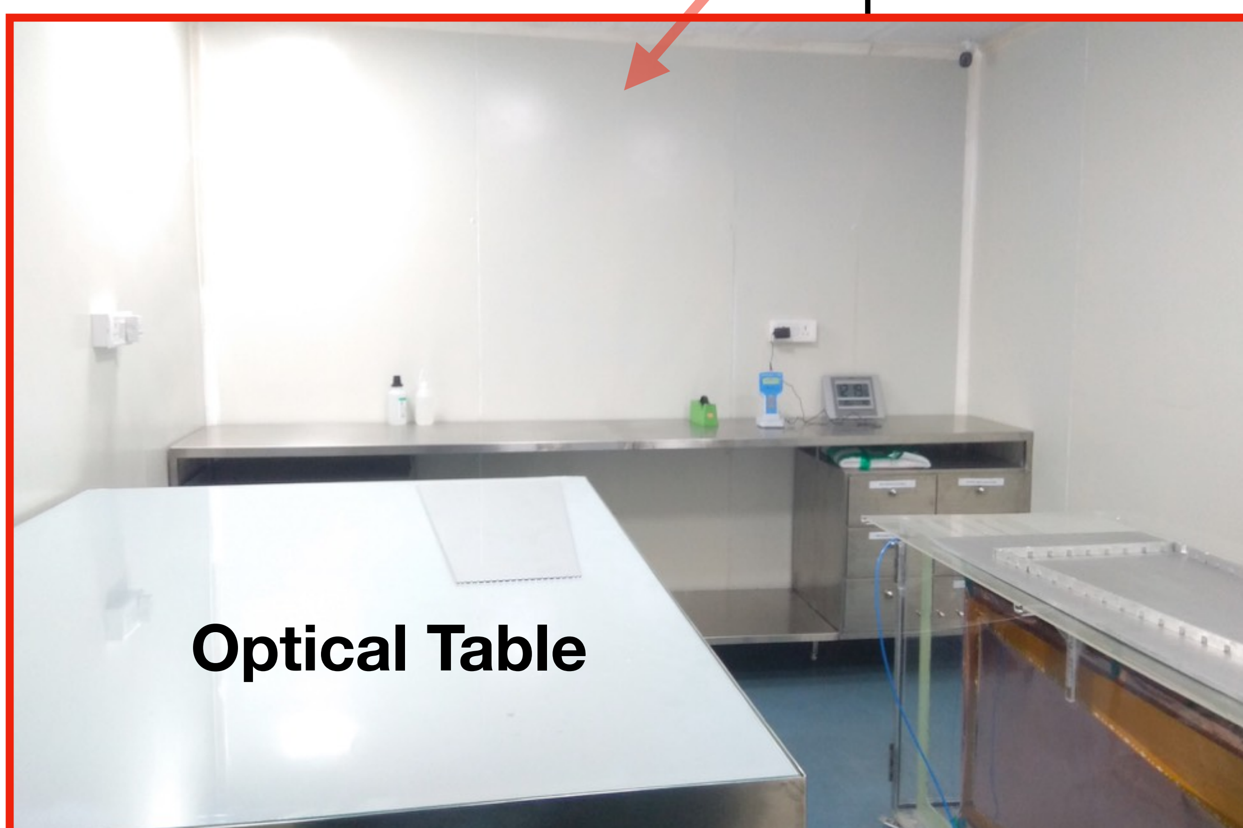

Optical Study of Micropack Foils

Pictures were taken in clean room of class 100
Camera used: AF-S Micro Nikon
Lens : 40mm 1:2.4G

Divided each foil in 9X9 Sectors to take pictures
Images were taken for both sides for outer and inner holes

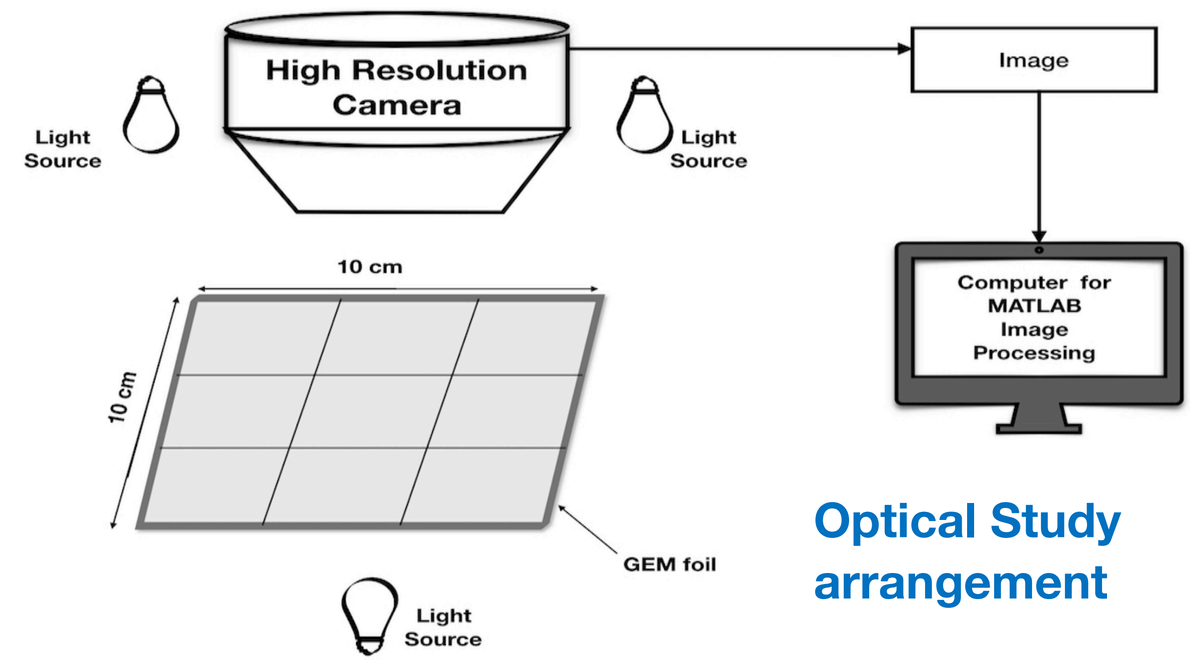

Optical Study arrangement

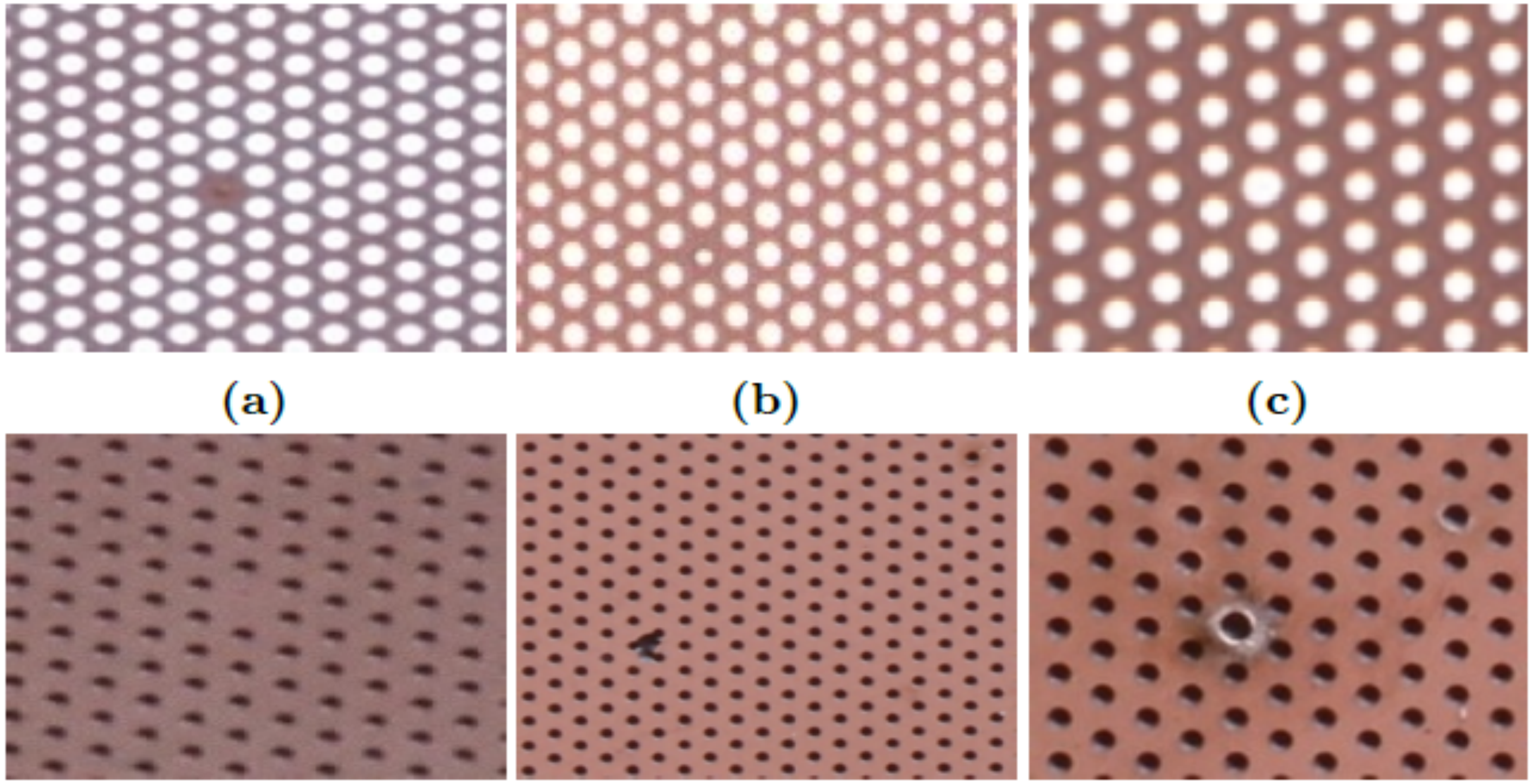

(a) (b) (c)
(d) (e) (f)

Observed Defects:

(a) Un-etched Kapton
(b) Under size
(c) Oversize
(d) Un-etched Copper
(e) Merged holes
(f) Burnt holes

Observed Defects Distribution

Only 0.13% of defects found.

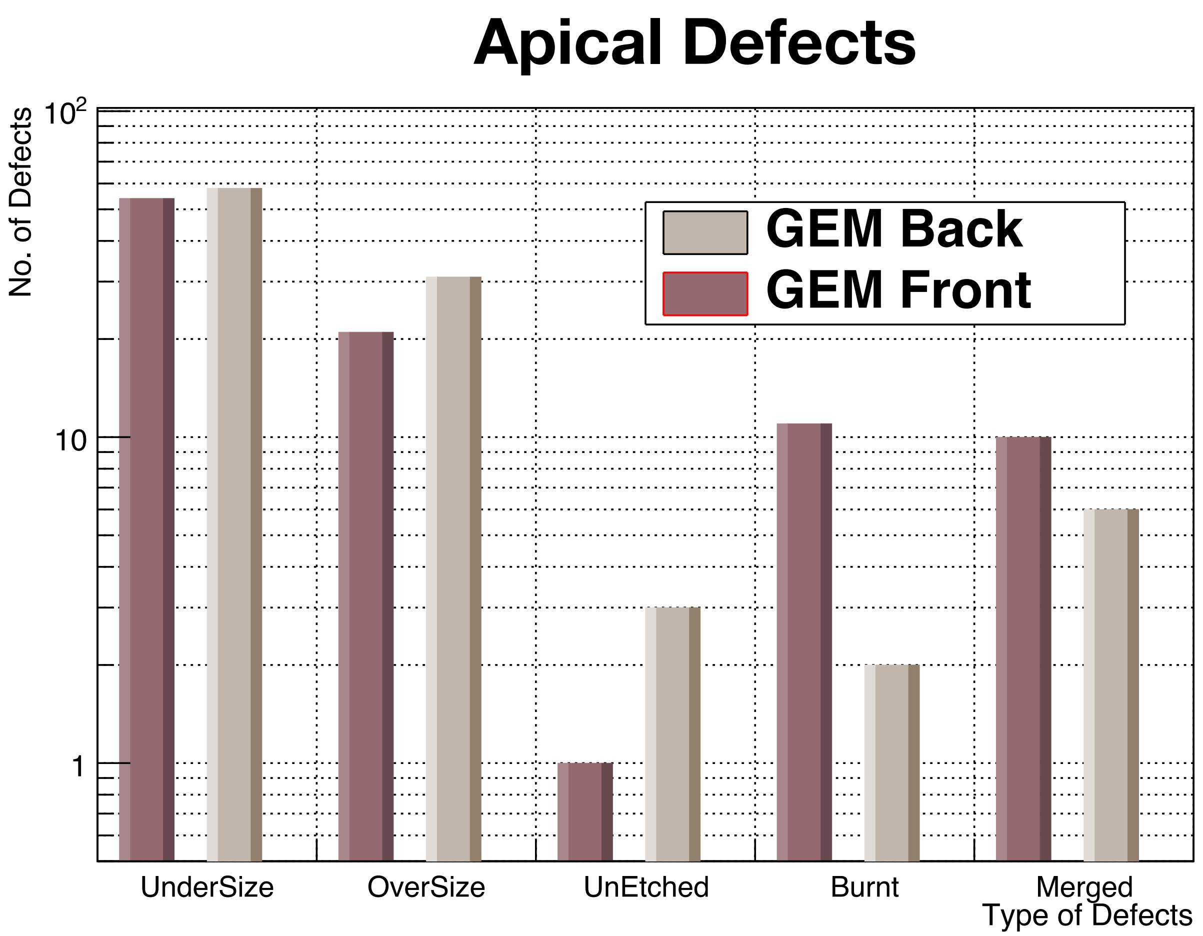

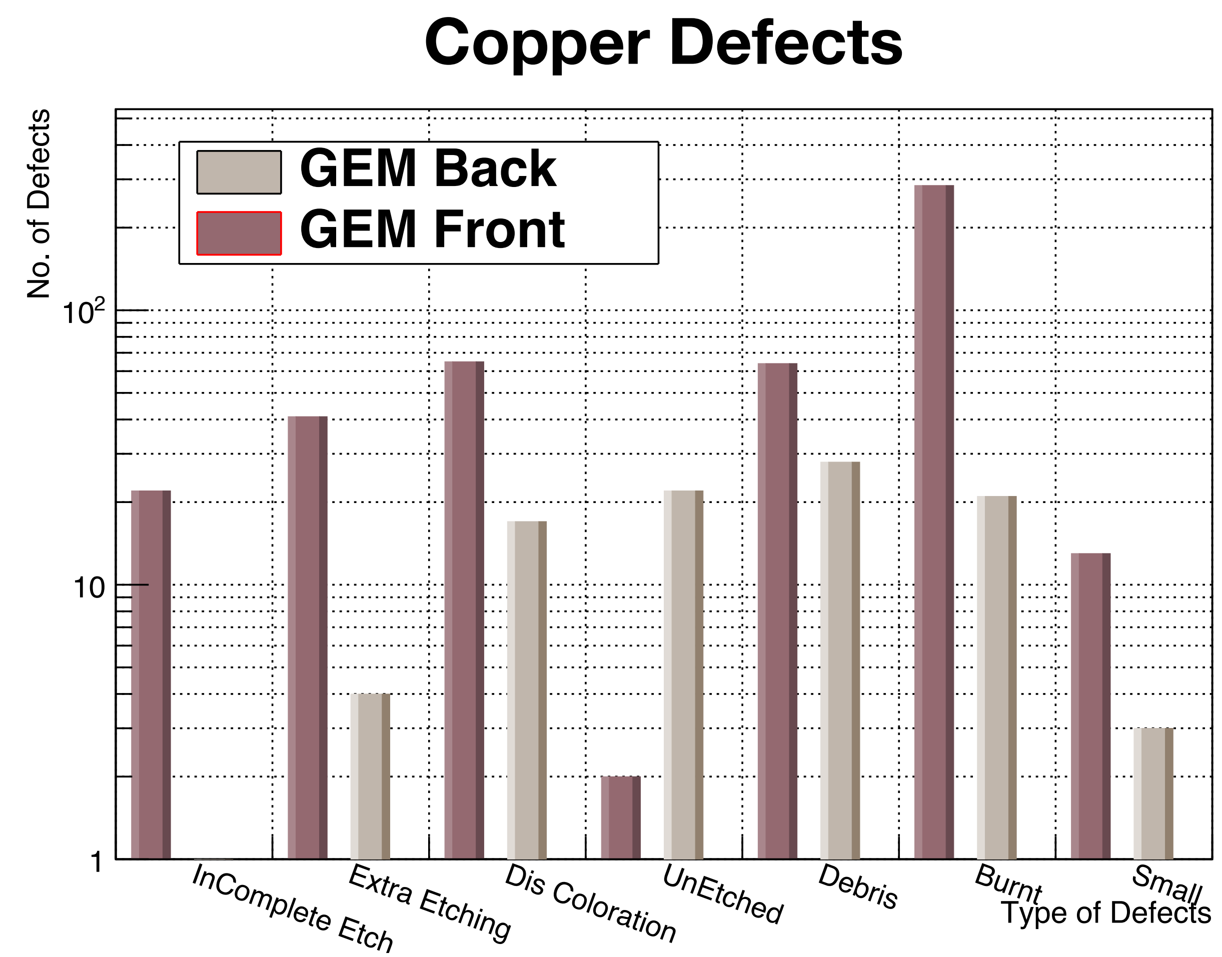

Electrical Characterisation

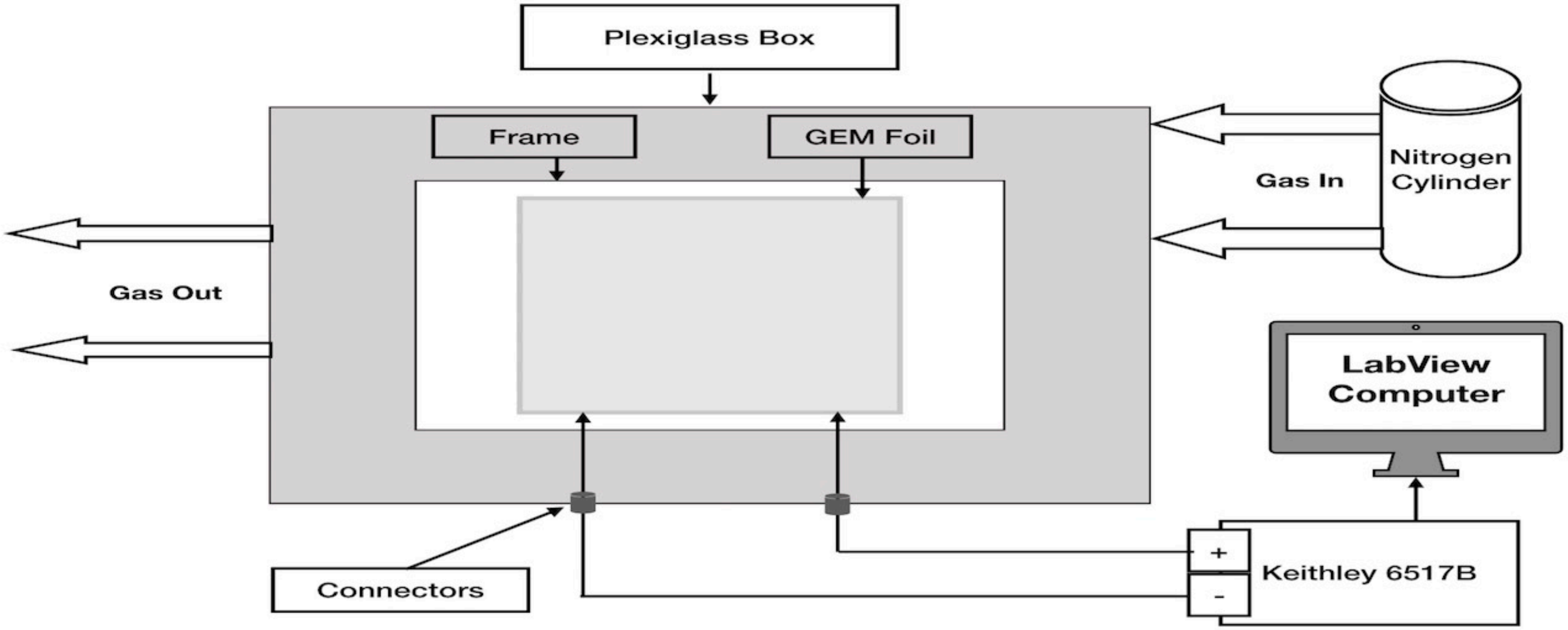

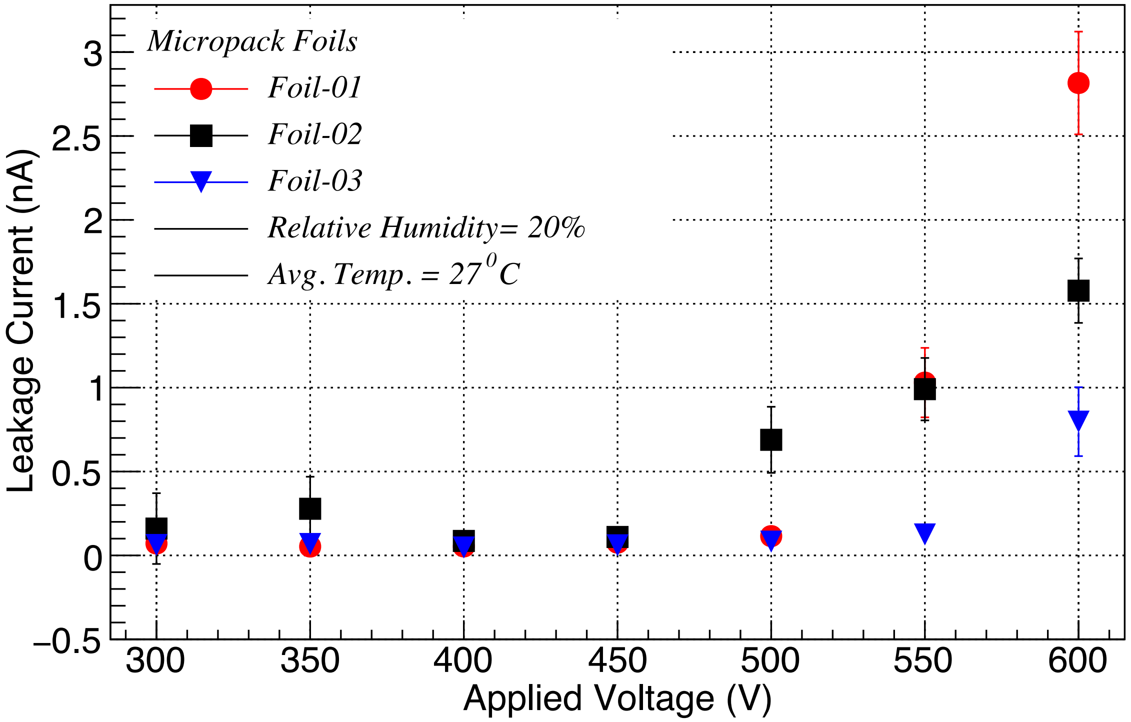

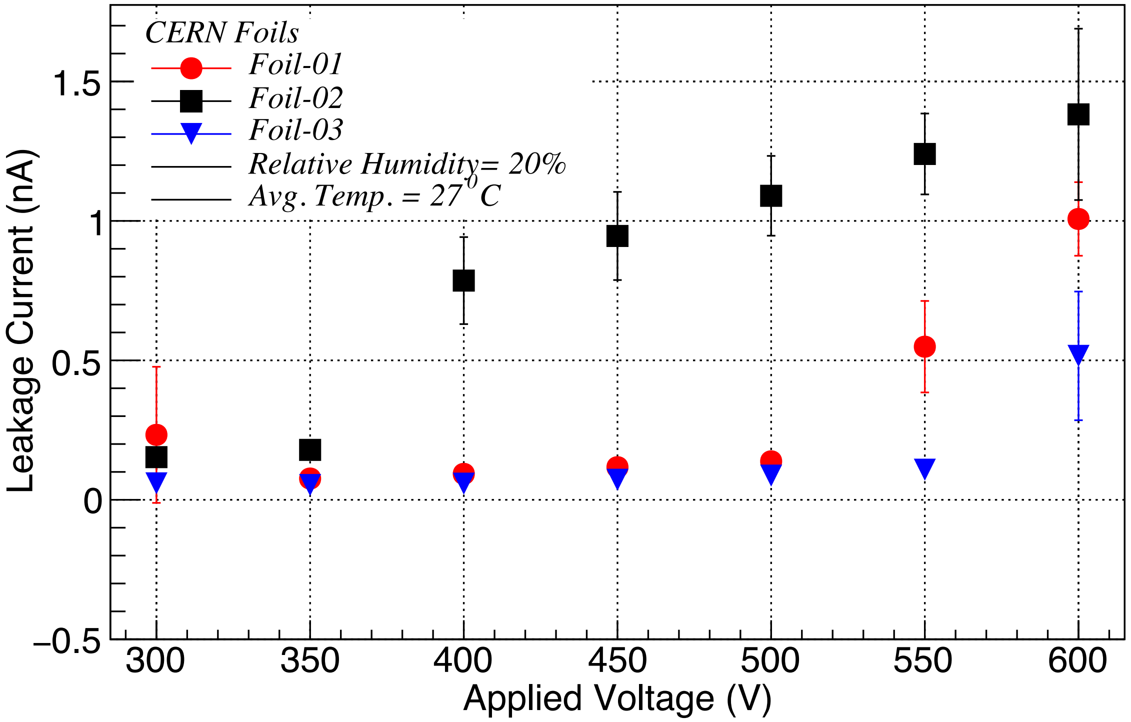

CMS Muon System Upgrade

Test Beam Studies of GEM

The CMS-GEM Project

- Originally CMS muon system was designed with high redundancy
  - Resistive plate chamber (RPC) extended up to |η| = 2.4
- However, at the time of construction CMS RPCs were not validated for rates in forward region
- Solution to handle increased pile-up, particle rate, and backgrounds is to provide the original redundancy CMS was designed with!!
  - Gas Electron Multiplier (GEM) detector.

Advantages of GEM:

- Radiation hardness
- Provides robust tracking and triggering in muon system
- Improve L1 and HLT muon momentum resolution to reduce or maintain global muon trigger rate up to |η| = 2.2
- Ensure maximum trigger efficiency in high PU environment

Phase-I: Install two layers (super-chambers) of triple-GEM chambers in the presently vacant position in front of ME1/1 during Long Shut-down-2.

Ref: 2014 JINST 9 C01053

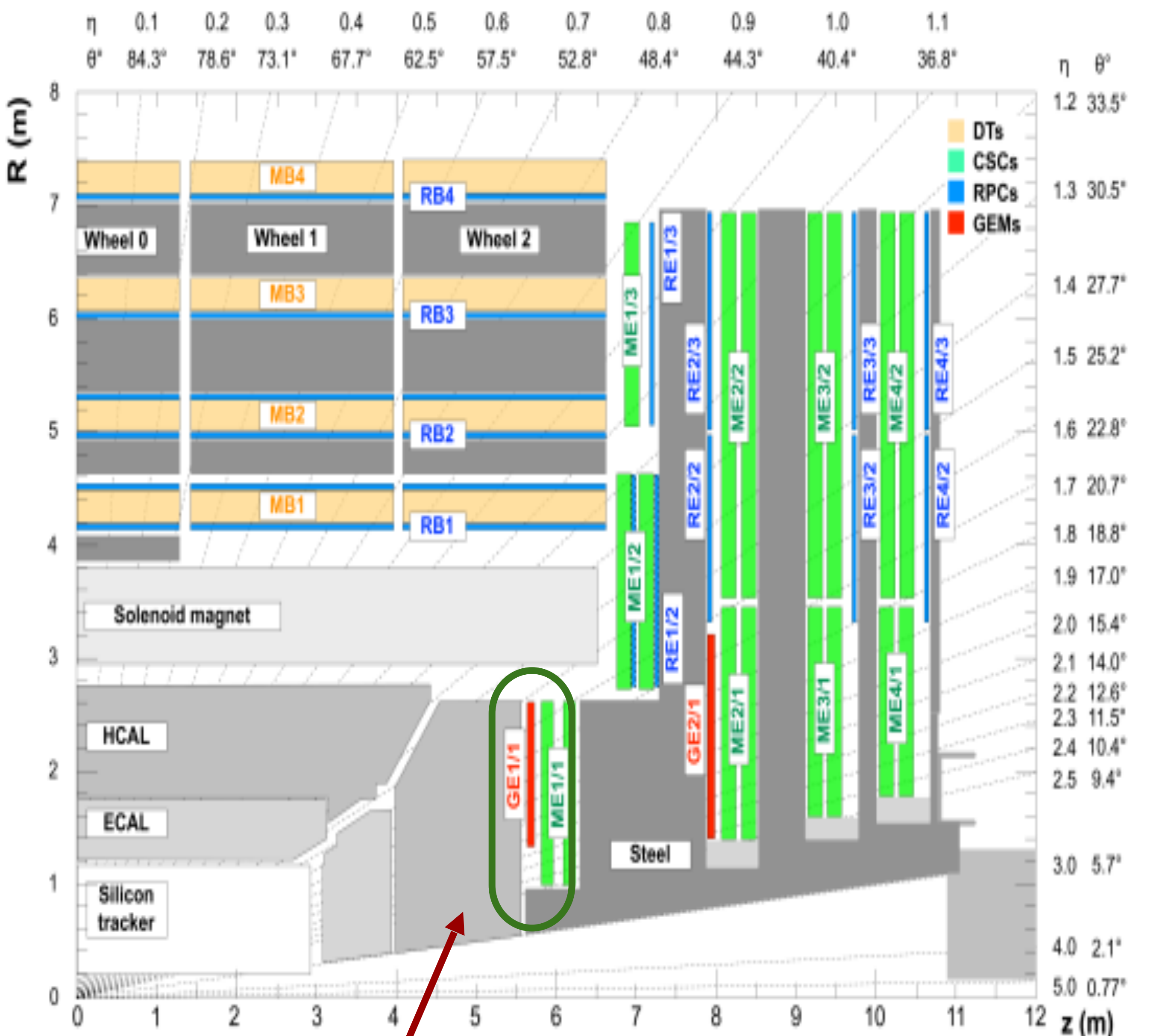

GEM Features:
Rate Capability: 10^5 Hz/cm^2
Spatial/Time Resolution: ~100μm/~4-5ns
Detection Efficiency: > 98%

Introduction To GE1/1

- GE1/1 is the prototype of GEM detector.
    - This is a triple-GEM detector, i.e. it contains 3 GEM foils, with gap configuration 3/1/2/1 mm for Drift/Transfer 1 /Transfer 2/Induction gaps, respectively.
- It is going to support muon system in endcap ($1.6 < \eta < 2.2$) region of CMS after long shutdown 2.

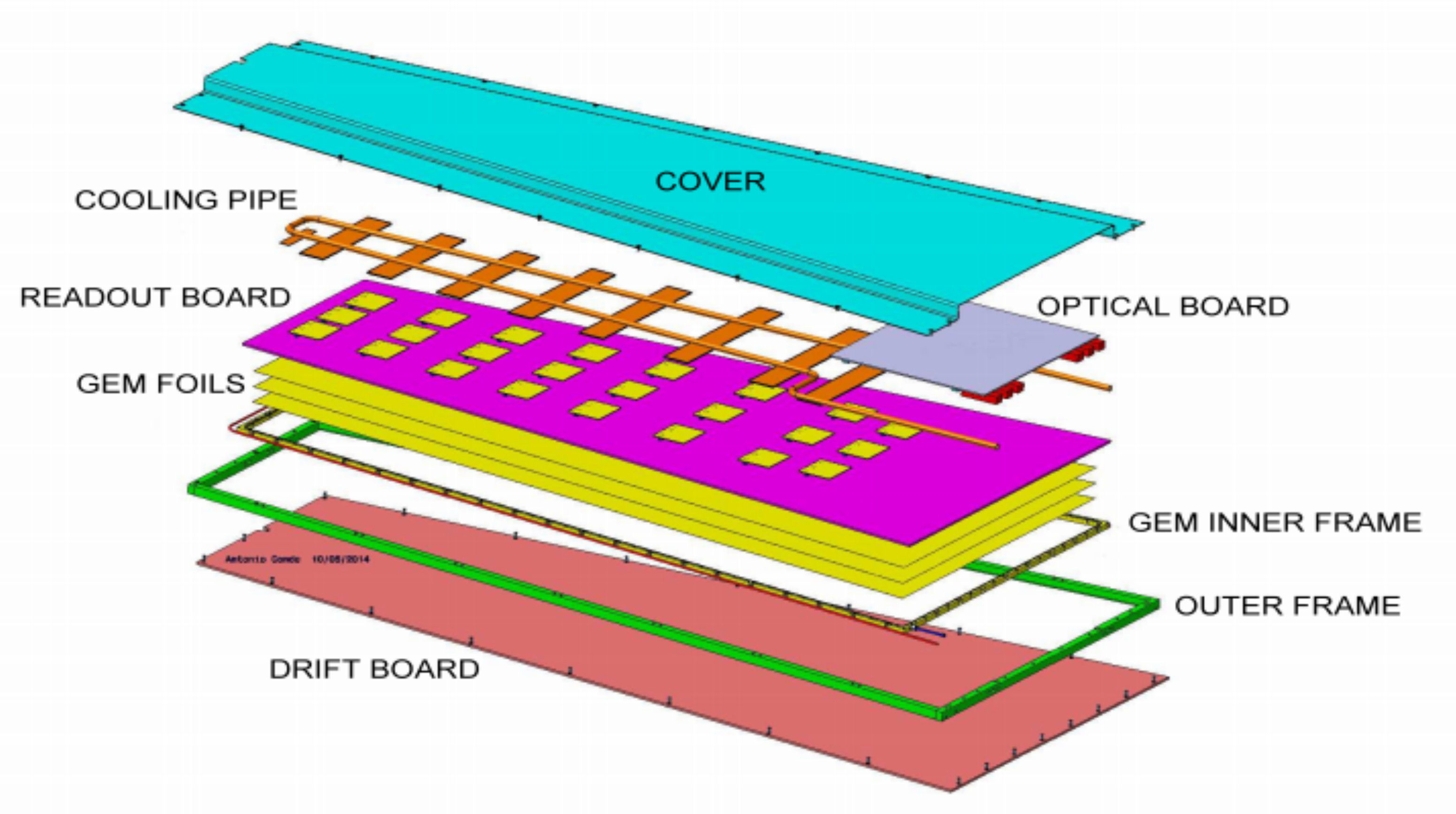

Figure: Mechanical design of GE1/1 chamber.

GEM Test Beam Setup

Beam Details:
- Beam Type : Muon Beam
- Energy. : 120-150 GeV

Experimental Setup Consists of Following Detectors:
- **Three scintillators**: Trigger comes from the coincidence of these scintillators.
- **Three trackers**: Triple-GEM detectors having active area of 10x10 cm^2, with gap configuration 3/2/2/2 mm and 2D readout.
- **GE1/1**: Full size triple-GEM detector (Trapezoidal shape, 990x220-455mm^2) with gap configuration 3/1/2/1 mm having only 1D readout..

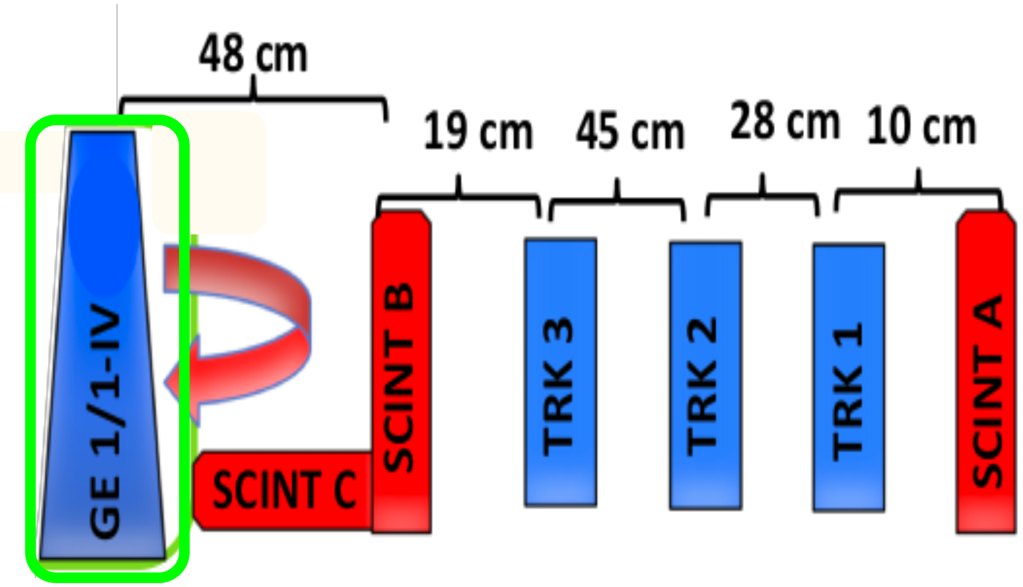

Gas Mixture Used:
- Ar/CO2 (70/30) and Ar/CO2/CF4 (45/15/40)

Electronics Used:
- Front-end electronics: VFAT2 Hybrid
  - On detector electronics, with digital readout
- Back-end electronics: TURBO
  - Off detector electronics, designed for small experiments (test beam) only.

Software:
- Data is taken from TURBO data acquisition software

GE1/1 Detector

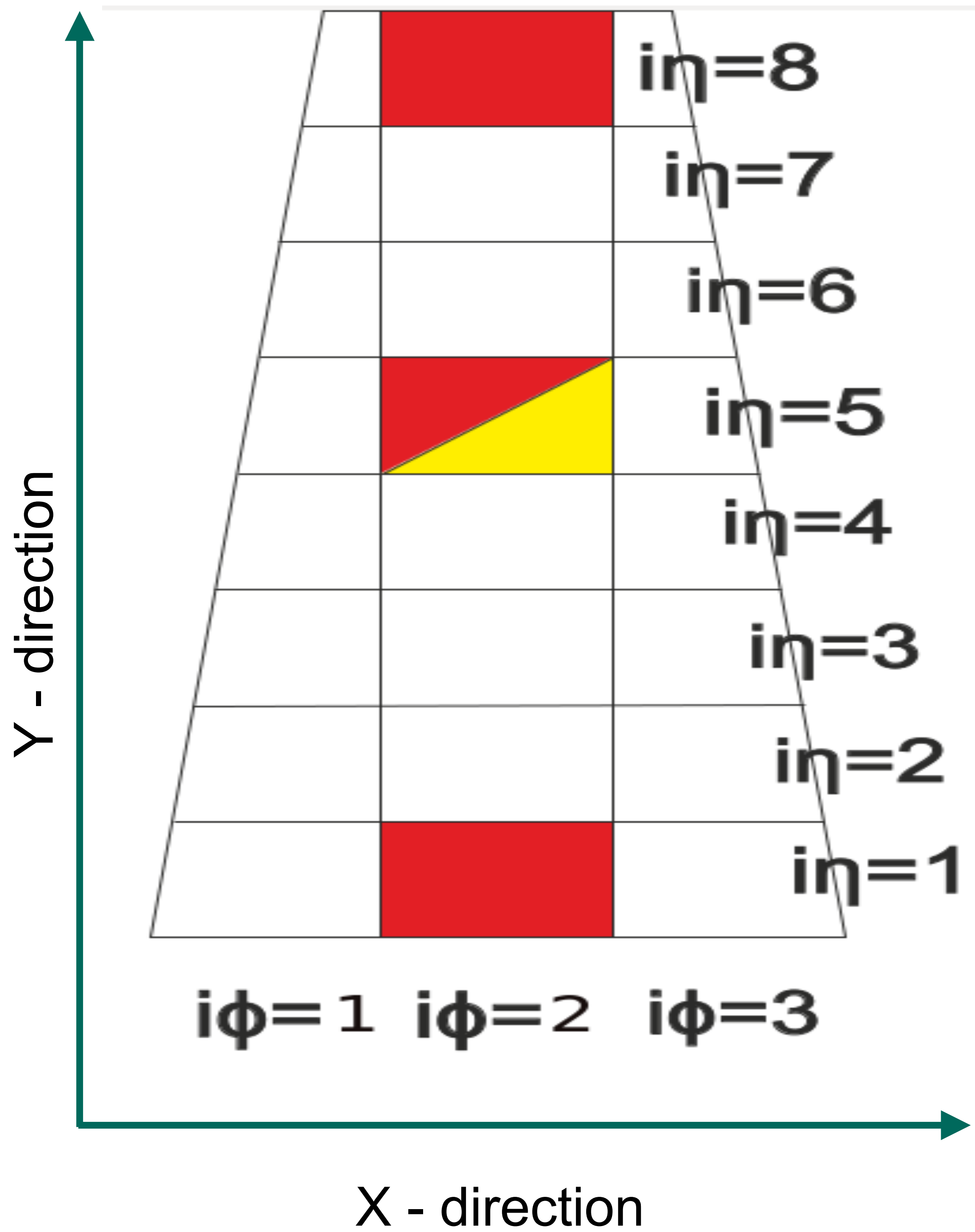

- GE1/1 detector divided into 8 iη regions and 3 iΦ region.
- Scanned three different readout sectors of the GE1/1 detector (iη,iΦ) = {(1,2),(5,2),(8,2)}.
- In the figure colour shows which sectors of GE1/1's are exposed to beam. Red sectors are taken with gas Ar/CO2/CF4 (45/15/40) while yellow section is taken with gas Ar/CO2 (70/30).

Beam Profile Plot

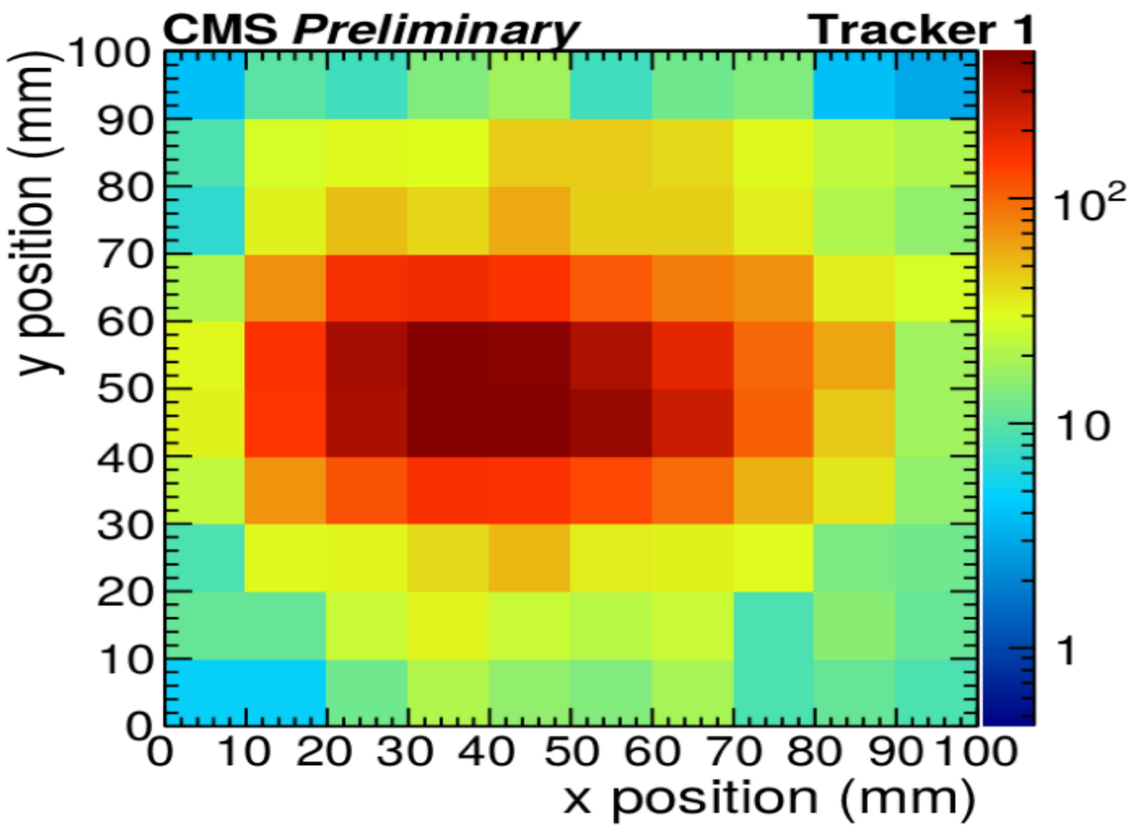

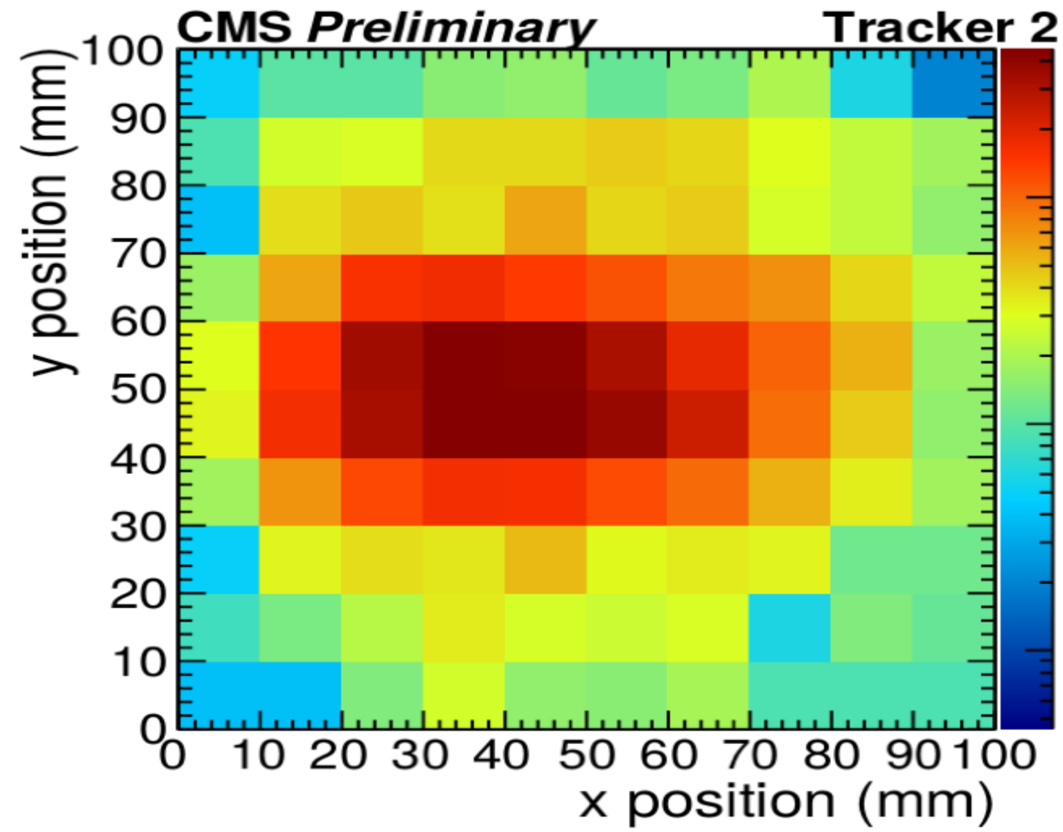

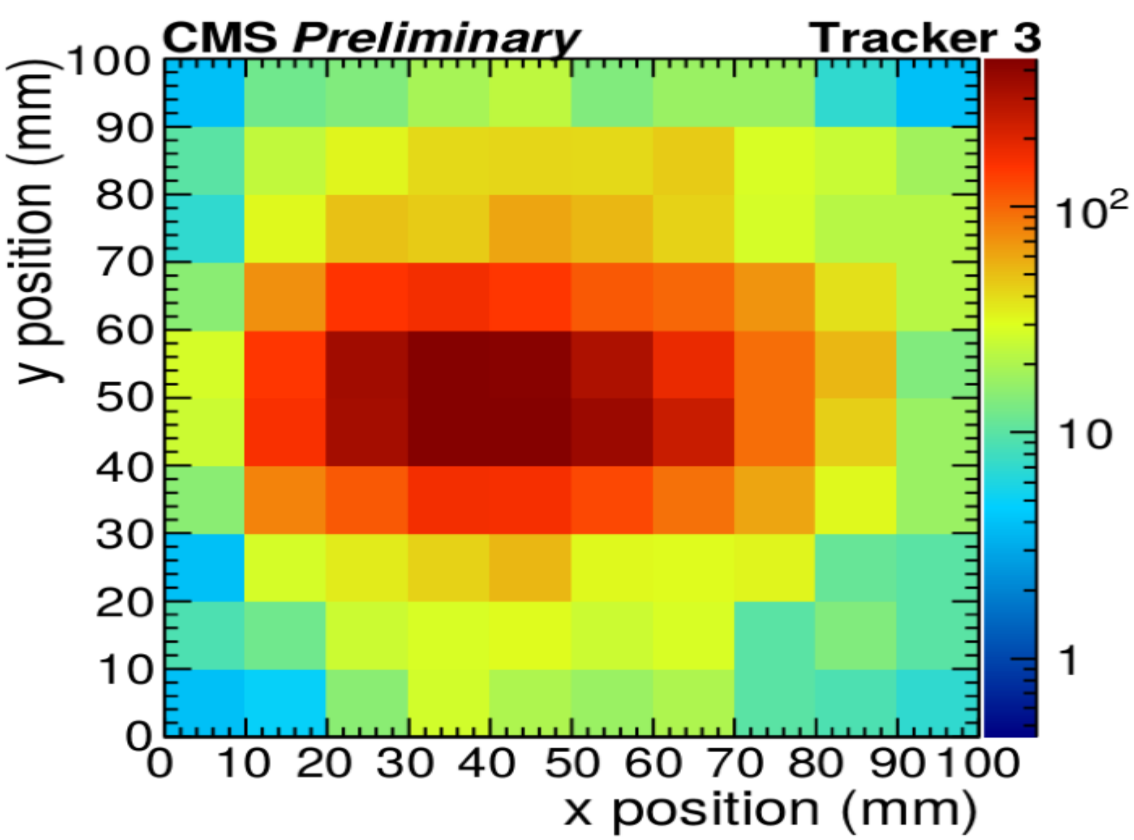

Beam profile for tracker 1, 2 and 3 are shown. Trackers are 10 x 10 cm^2 triple GEMs. This shows beam spot is approximately at the centre of trackers. This is representative of all runs.

Tracker & GE1/1 Hit Distribution

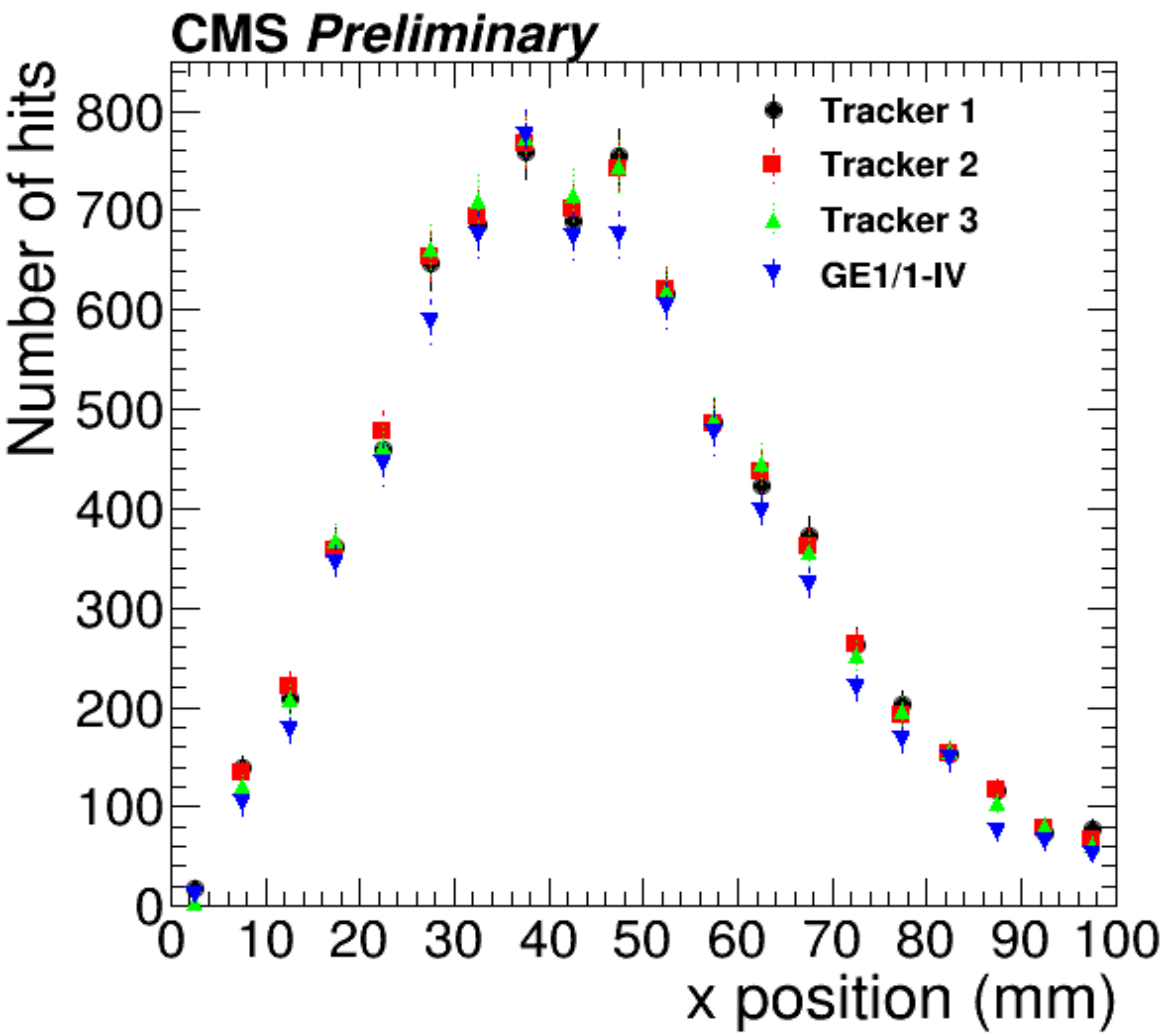

Hit position measured by three trackers and GE1/1 (gap configuration: 3/1/2/1 mm) along x. Here hits in all 4 detectors are comparable and showing that beam is around center of detector.

Hit position measured by three trackers along y. No GE1/1 here since it is with only 1d readout along x. Here hits in all 3 trackers are comparable and showing that beam is approximately at center of detector.

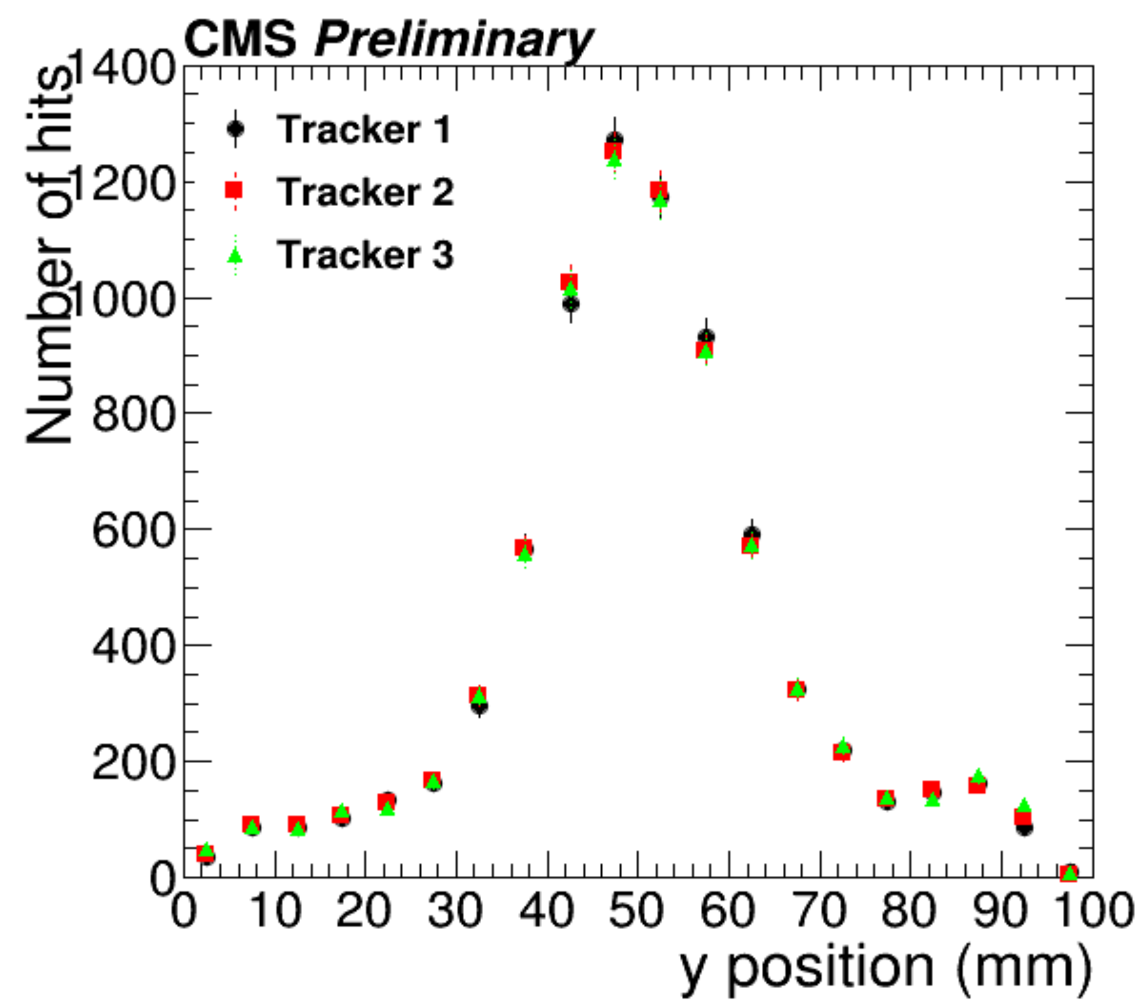

Fiducial Region Selection

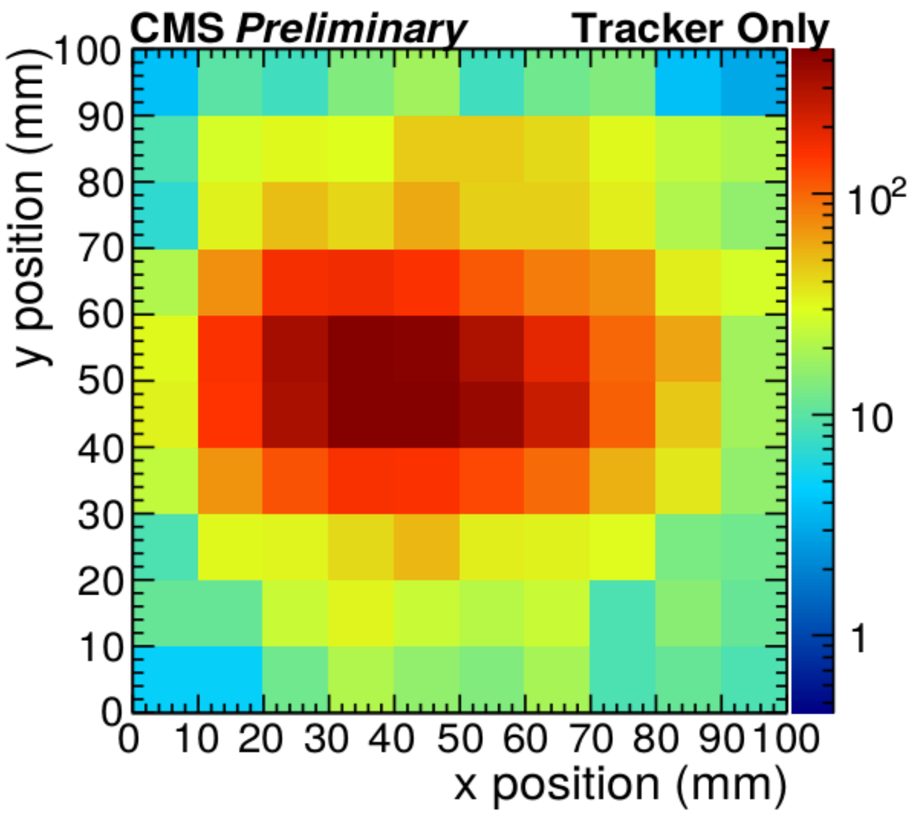

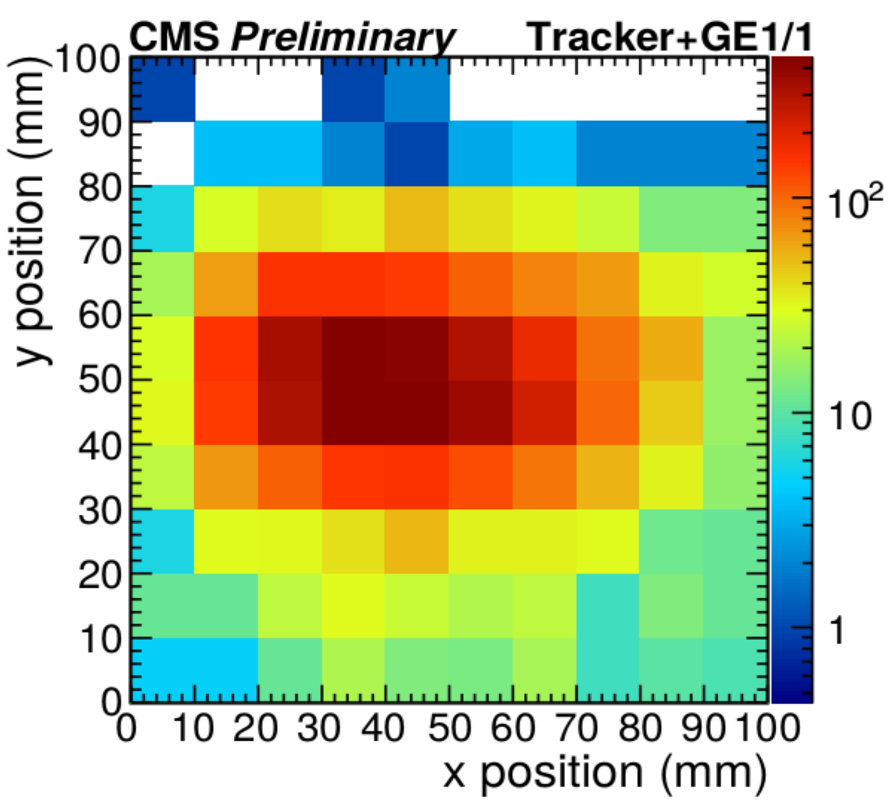

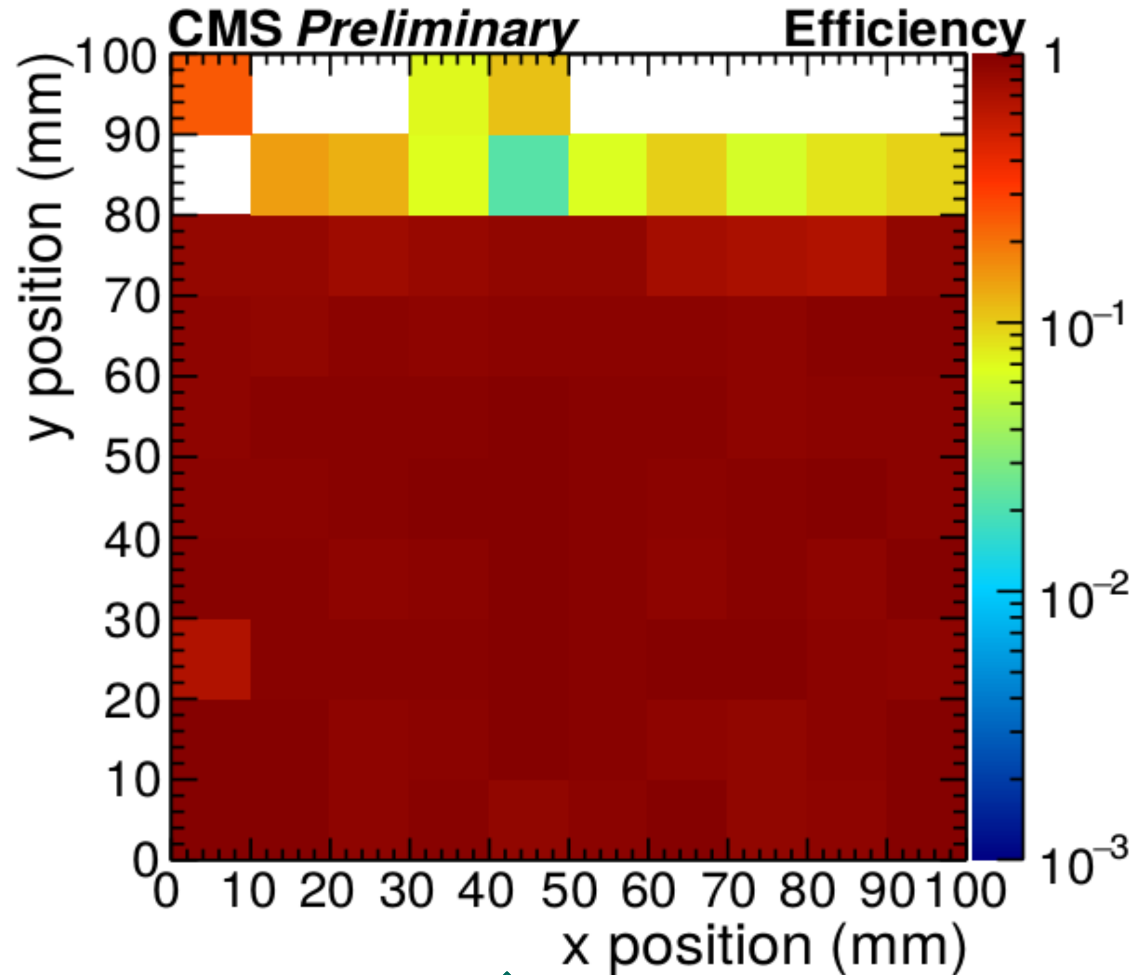

GE1/1 detection efficiency: number of reconstructed muons leaving a hit in GE1/1 divided by the total number of reconstructed muons (i.e. ratio of the top left and bottom left plots).

GE1/1 Detector Performance (Test Beam Measurements)

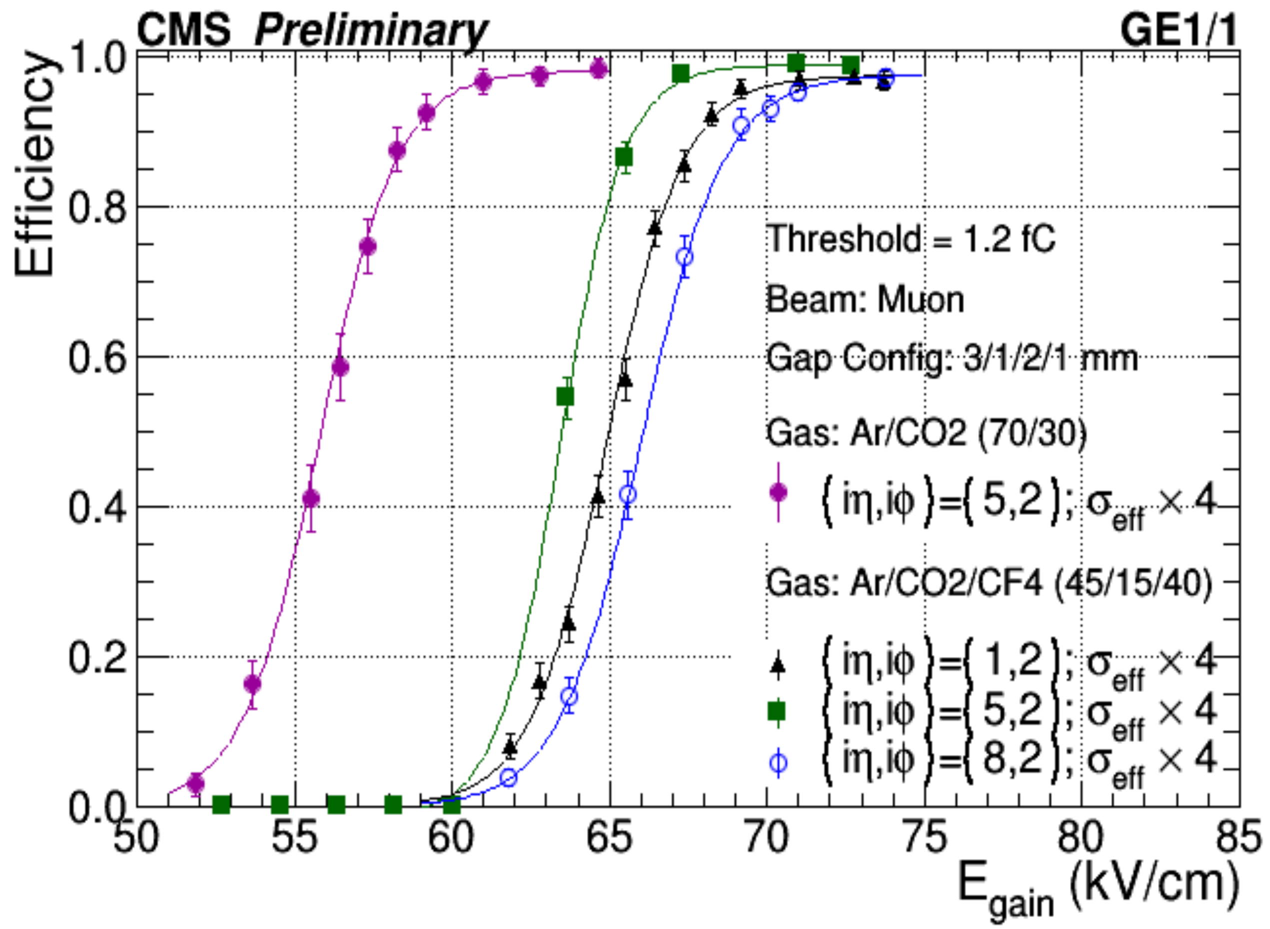

Efficiency of GE1/1

Time resolution of GE1/1

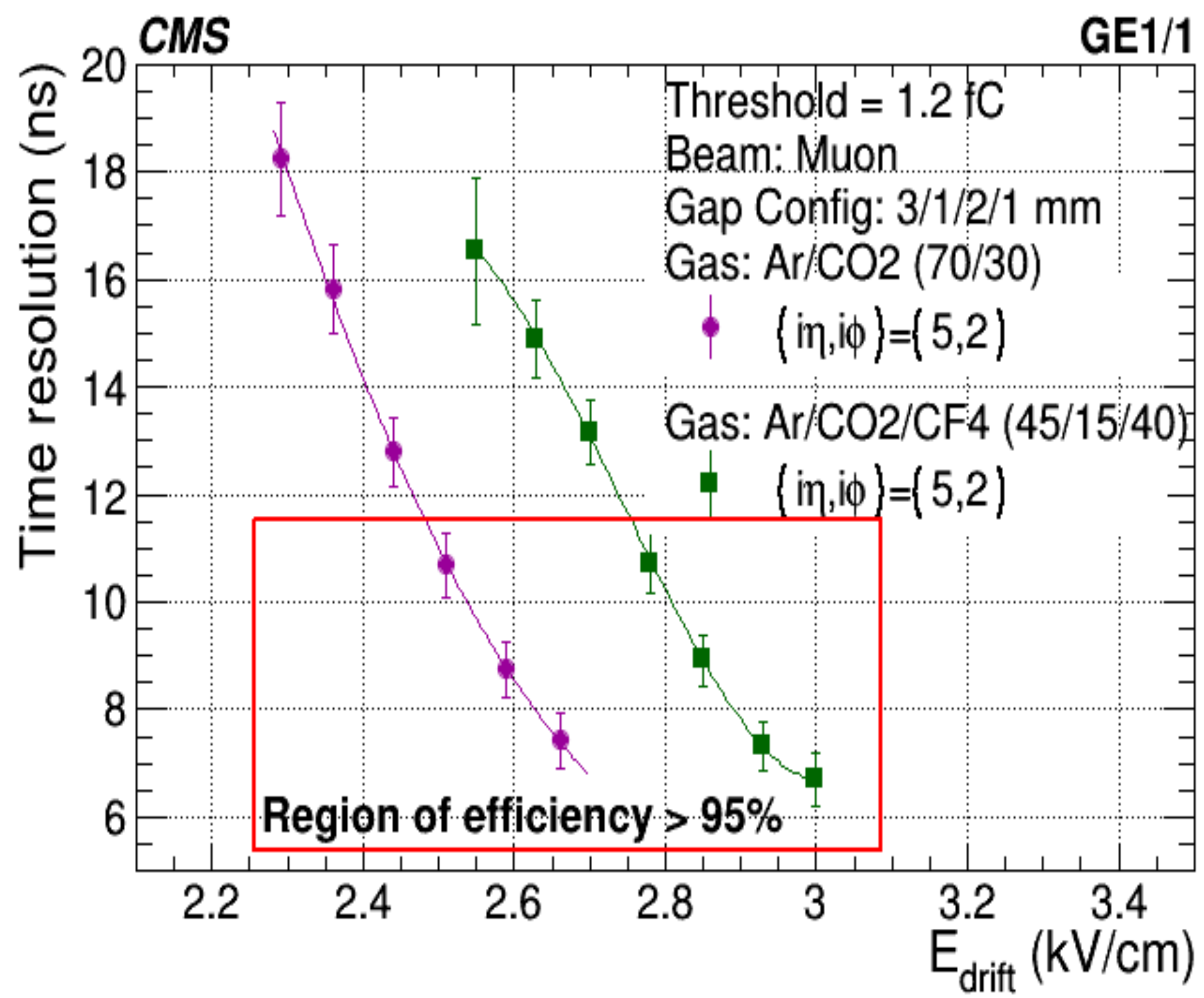

Cluster Size

- Cluster is defined as the number of strips of the readout that surpass the threshold.

Scan of cluster size wrt current supplied to HV divider.

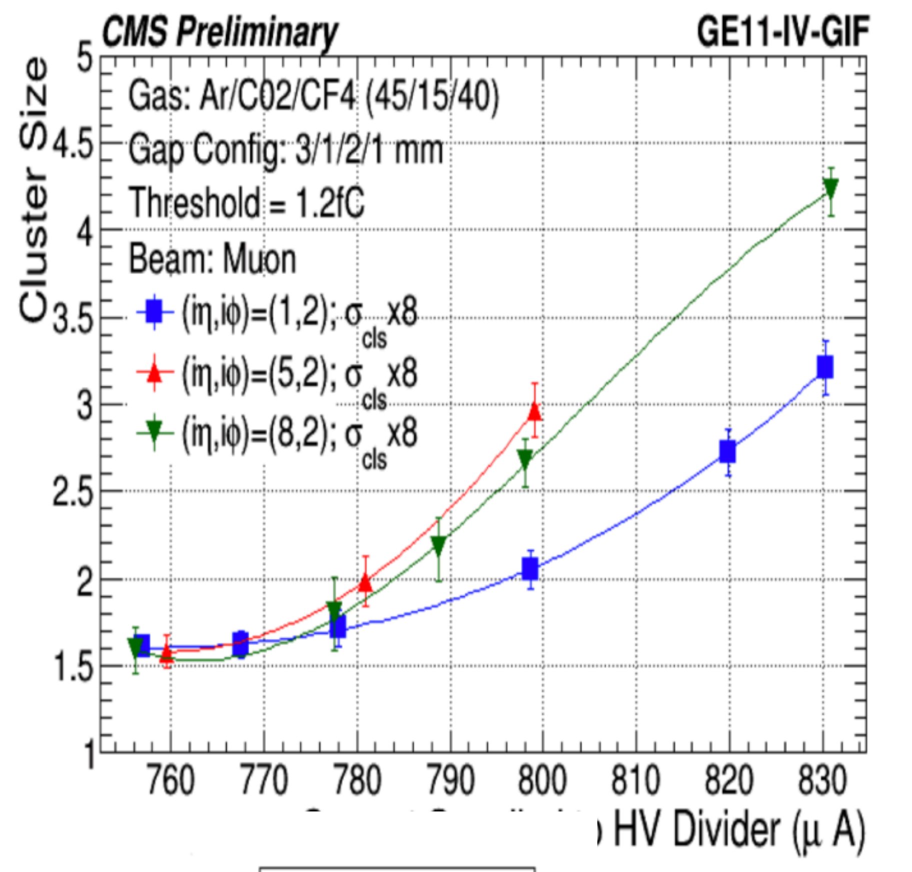

Few individual Cluster size distribution

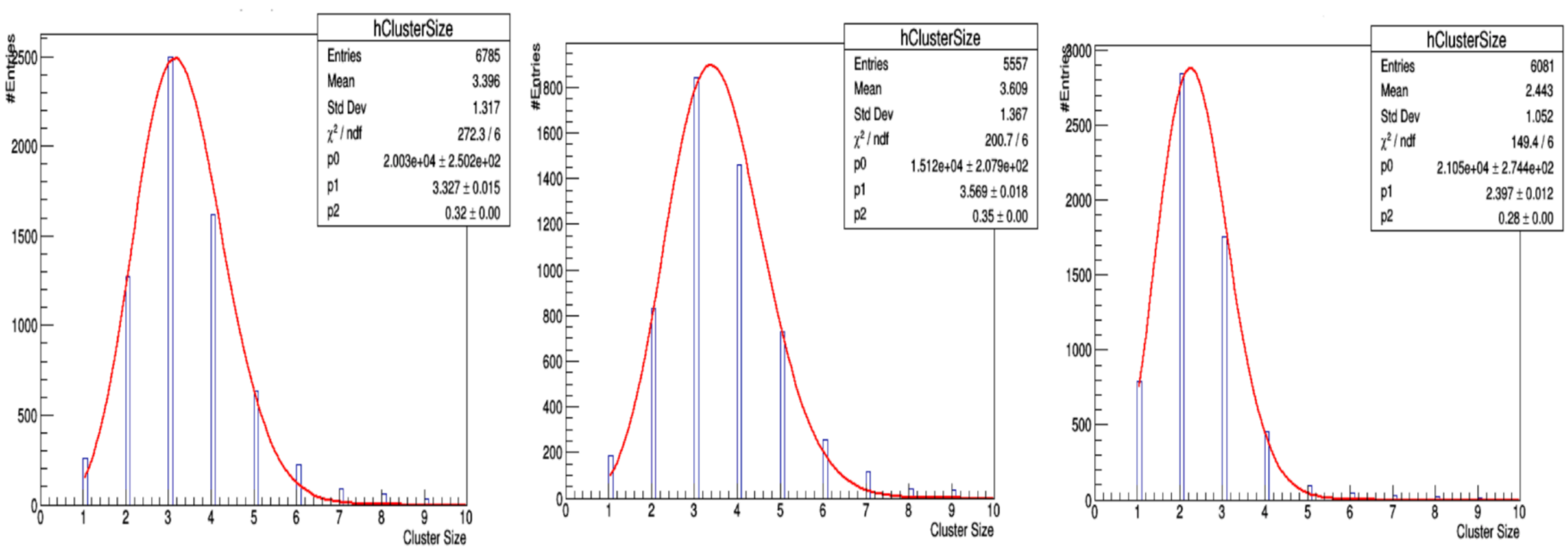

Summary of Detector Work

- GEM foils produced in India shows very good electrical and optical properties
    - Having ≅ 0.13% defects only.
- Triple-GEM provides excellent solution for the forward CMS muon system upgrade.
- Triggering and tracking capability will provide great improvement during Run3.
- Full GE1/1 to be installed during LS2 (2019-2020).
- Test beam analysis performed and it gave us very good results:
    - Efficiency ≥ 98%
    - Time resolution ~5-8 ns
    - Space resolution ~200 μm

Physics Analysis

Introduction

Particle physics is a modern name for the centuries old effort to understand the basic laws of physics.

- Edward Witten

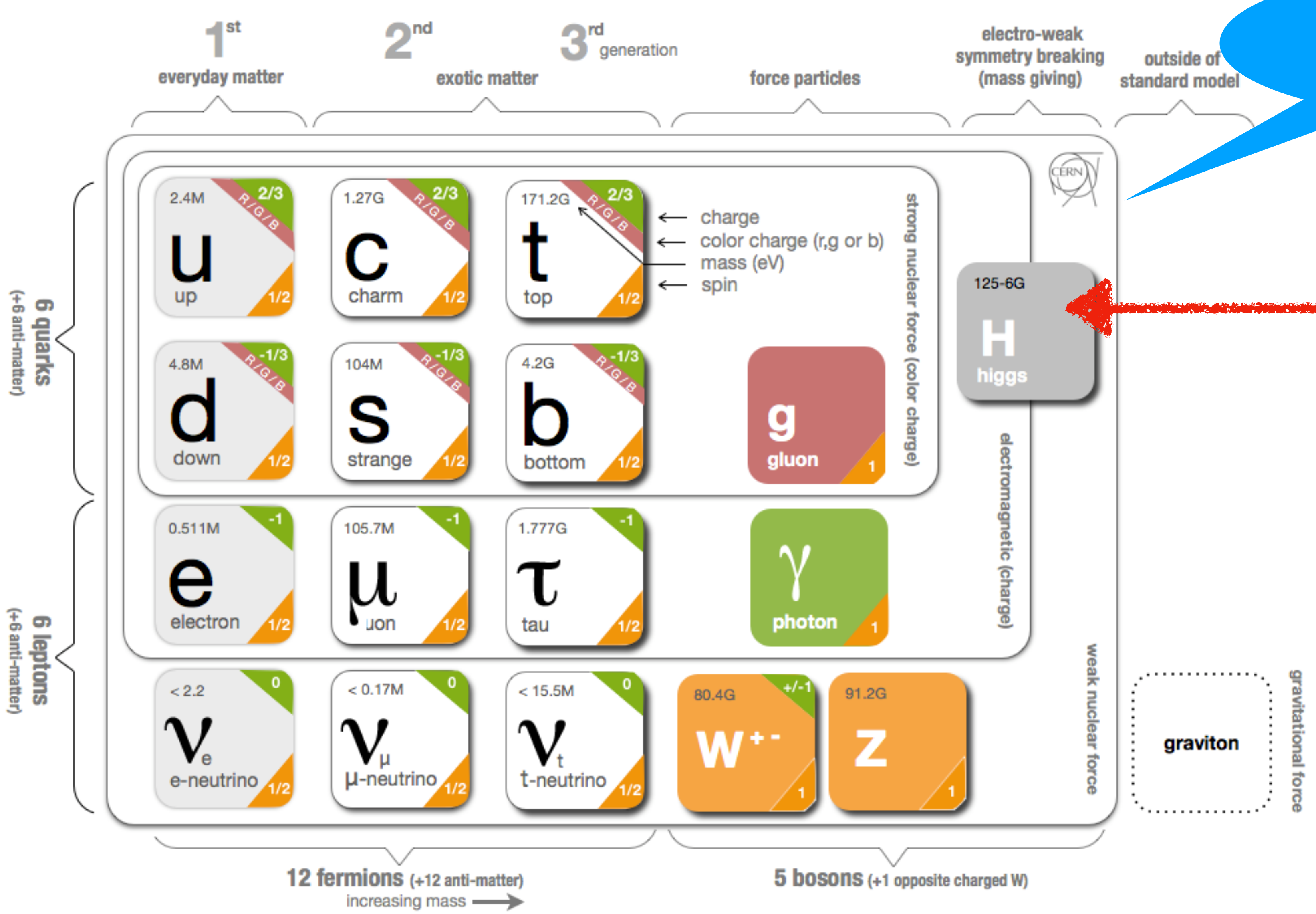

Periodic Table of Standard Model

Last missing piece of SM

Finally observed at CMS & ALTAS detector at LHC, CERN.

After Higgs Discovery???

➡Important task is to understand the mechanism behind the Electroweak Symmetry Breaking!!!

➡Two possible ways:

1. Precision measurement of the Higgs and the vector boson properties.
2. Study of the vector boson scattering.

Vector Boson Scattering

- At LHC the vector boson scattering occurs with the virtual W's emitted by the quarks.
- Importance:
    - Without Higgs its cross-section increases with energy always
        - While leads to unitarity violation.
- Still the SM scattering cross-section is too low to look for it.
    - Another way: Look at the coupling of quartic vertices (Same low cross-section issue is there).
    - EFT: allows us to modify the coupling strength and introduce the neutral vertices.
        - Increases the cross-section.
        - Easy to set the limits on aQGC.

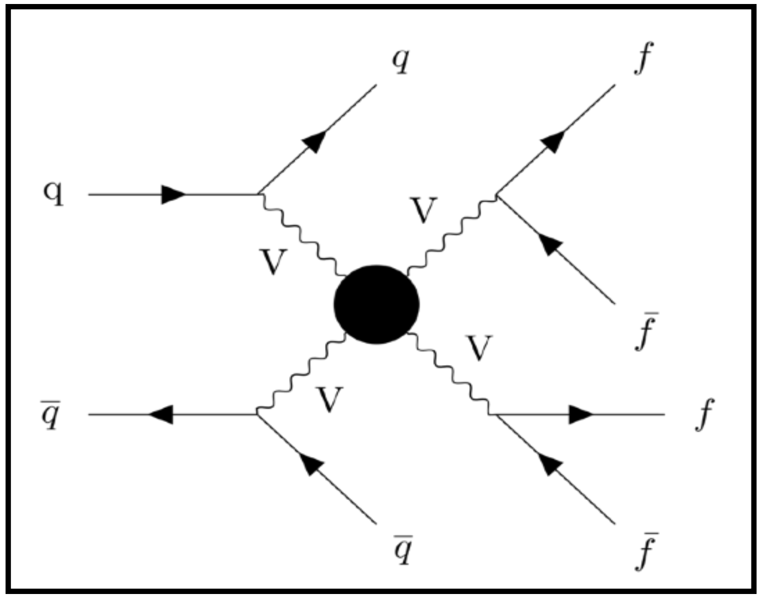

Anomalous Quartic Gauge Coupling-I

- BSM search using model independent way:
  - Modify triple and quartic gauge couplings by redefining SM Lagrangian.

$$L_{SM} \longrightarrow L_{eff} = L_{SM} + \sum_{n=1}^{\infty} \sum_{i} \frac{c_i^{(n)}}{\Lambda^n} \mathcal{O}_I^{(n+4)}$$

  - $\Lambda >> m$ & $L_{eff} \rightarrow L_{sm}$ as $\Lambda \rightarrow \infty$
  - An effective field theory is the low energy approximation to the new physics, where "low" means < Λ
- Sample was generated using MadGraph5 at LO
  - Used reweighting feature to save information about different parameter points for each operator.

	$WWWW$	$WWZZ$	$WW\gamma Z$	$WW\gamma\gamma$	$ZZZZ$	$ZZZ\gamma$	$ZZ\gamma\gamma$	$Z\gamma\gamma\gamma$	$\gamma\gamma\gamma\gamma$
$\mathcal{O}_{S,0}, \mathcal{O}_{S,1}$	✓	✓			✓				
$\mathcal{O}_{M,0}, \mathcal{O}_{M,1}, \mathcal{O}_{M,6}, \mathcal{O}_{M,7}$	✓	✓	✓	✓	✓	✓	✓		
$\mathcal{O}_{M,2}, \mathcal{O}_{M,3}, \mathcal{O}_{M,4}, \mathcal{O}_{M,5}$		✓	✓	✓	✓	✓	✓		
$\mathcal{O}_{T,0}, \mathcal{O}_{T,1}, \mathcal{O}_{T,2}$	✓	✓	✓	✓	✓	✓	✓	✓	✓
$\mathcal{O}_{T,5}, \mathcal{O}_{T,6}, \mathcal{O}_{T,7}$		✓	✓	✓	✓	✓	✓	✓	✓
$\mathcal{O}_{T,8}, \mathcal{O}_{T,9}$					✓	✓	✓	✓	✓

Anomalous Quartic Gauge Coupling-II

- WV/ZV production in association with two jets
    - Semi-leptonic final state with a boosted hadronic W/Z
- Stringent aQGC bounds for WV channel was set by ATLAS using 8 TeV data sample
- **Benefits**:
    - larger branching ratio than same sign analysis.
    - Full WW invariant mass reconstruction (neutrino p_Z calculation by constraining W-boson mass)
    - aQGC contribution from all possible vertex:
        - WWWW, ZZWW, γγWW, γZWW, ZZZZ,…
    - **It should significantly improve the current limits.**

Phys. Rev. D 95 (2017) 032001

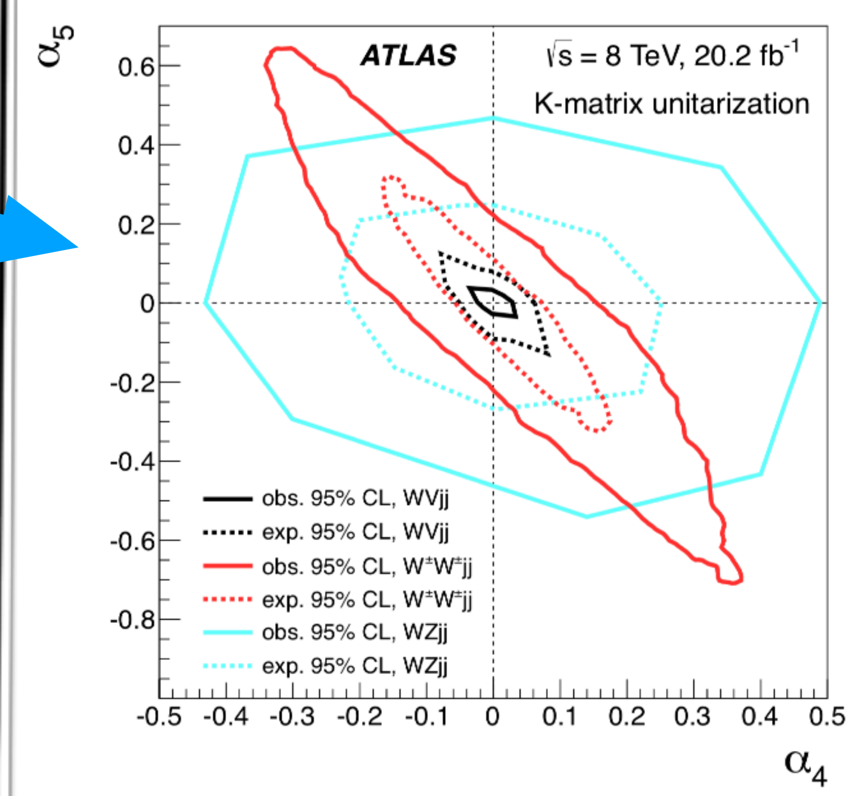

WV Channel

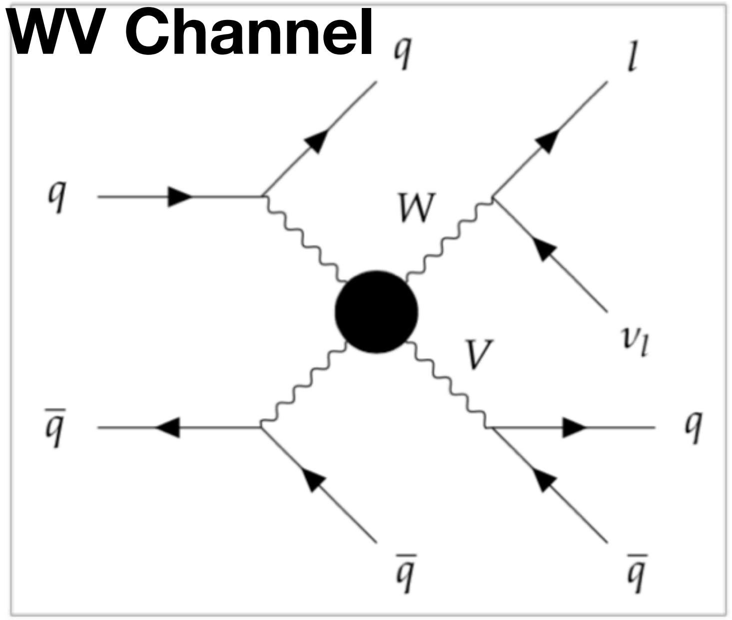

ZV Channel

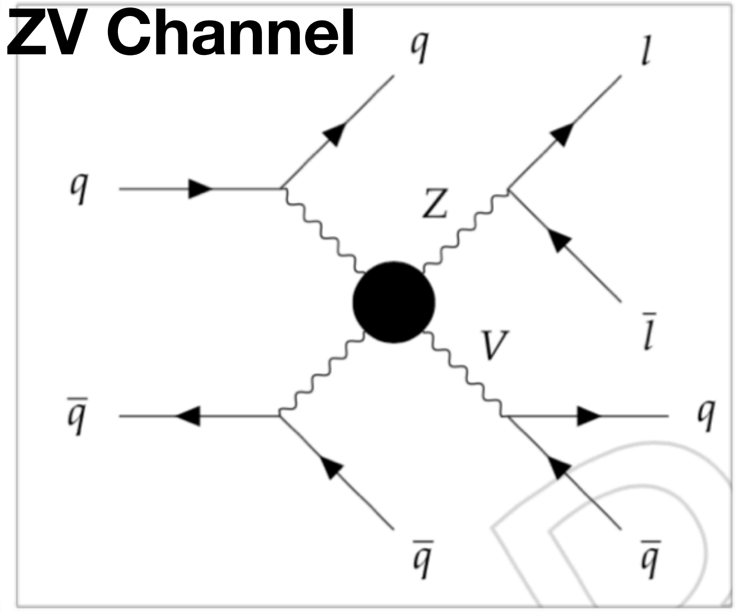

Signal Sample

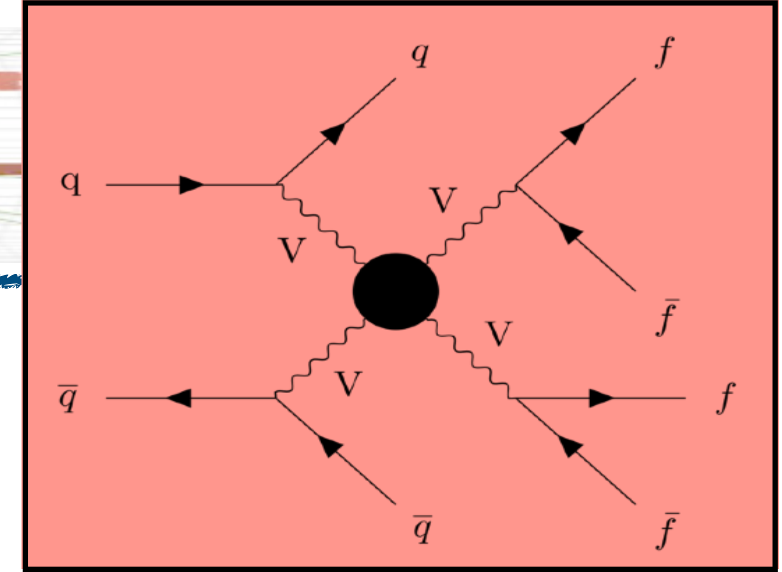

- Analysing two different final state of signal:

  1. WV Case: **1 lepton, 2 VBF jets, 1 Fat jet corresponding to boosted W/Z-boson, and MET.**

  2. ZV Case: **2 lepton, 2 VBF jets, 1 Fat jet corresponding to boosted W/Z-boson**

- Both signal sample (i.e. SM EWK and aQGC) generated with LO MadGraph generator.

- Also, we produced QCD initiated diboson at LO using MadGraph.

aQGC Scaling (M_{WW} Distribution)

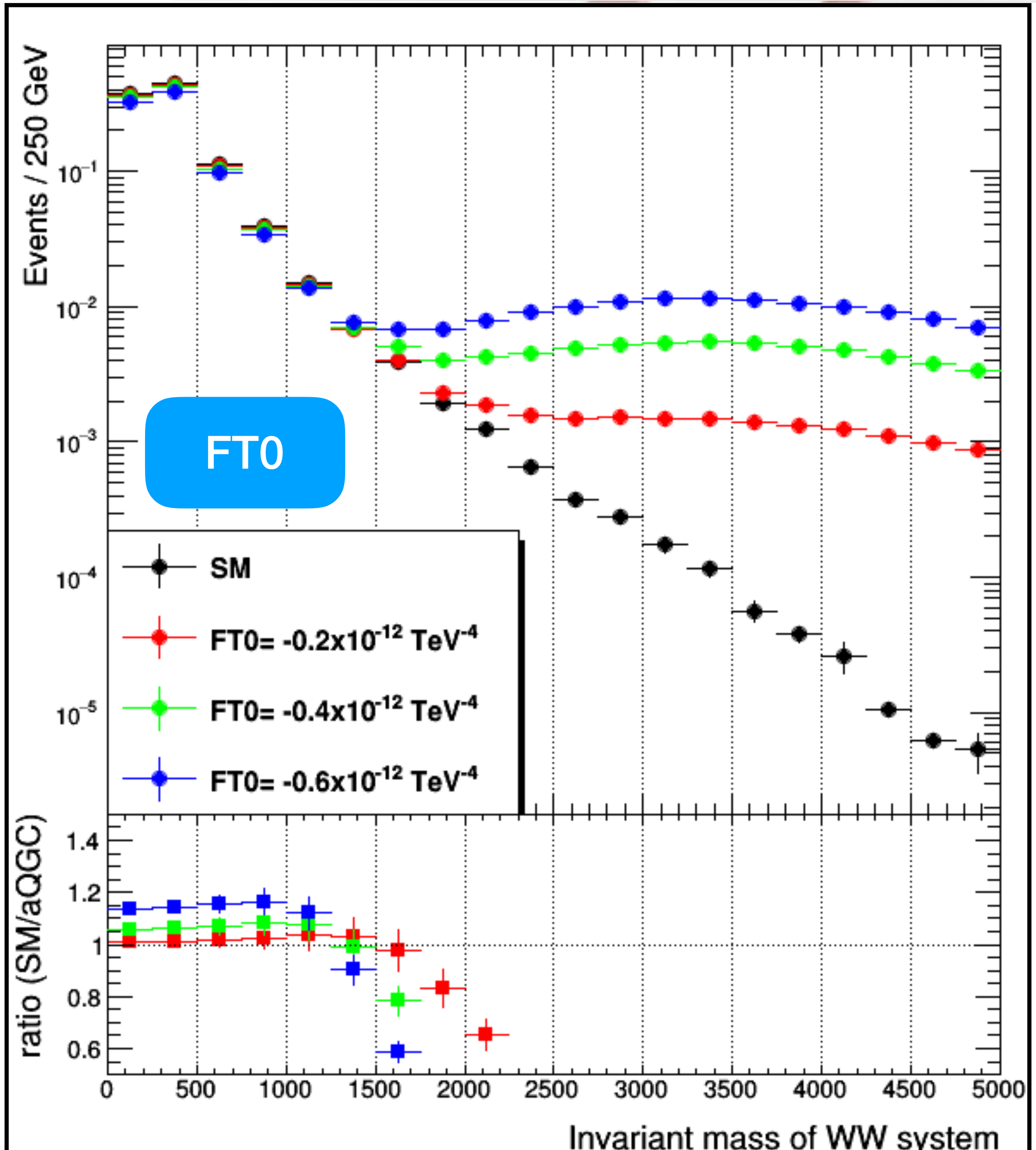

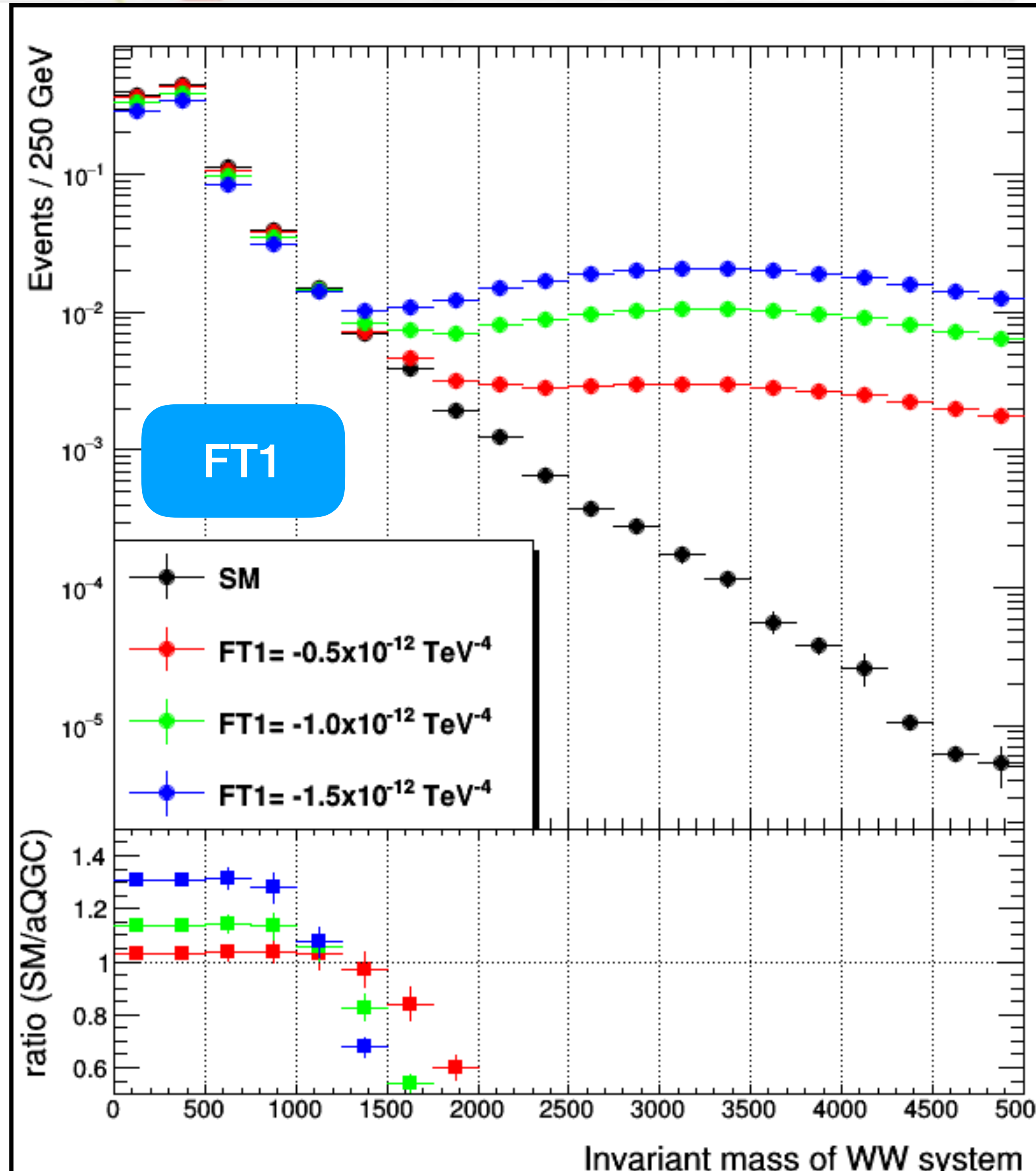

➡**aQGC enhances the production cross-section at large M_{WW}.**

Possible Backgrounds

- The process which can fake signal is known as backgrounds.
- It may be of two types:
    - Bremsstrahlung process: The process where the W boson are radiated by quark or anti-quark partons, and which do not contribute to VV scattering.
    - Process which fake a VV final state.

- **W+Jets:** Most dominating background. W decays to lν.
- **VVJJ (QCD initiated)**: This is irreducible background for analysis.
- tt **Jets**: Top quark always decays to one b-quark and one W boson. So, $t\bar{t}.\rightarrow bWbW \rightarrow bl\nu l\nu$, if we mis-measure one lepton and one b quark form jets.
- **Drell-Yan:** Z/Gamma decays to l^+l^- and we mis-measure one l because of acceptance or inefficiency effects, gives missing energy.
- **Single top production**: Here $t \rightarrow bW \rightarrow bl\nu$, and 3 fake jets is reconstructed or we get some from ISR or FSR.

Analysis Strategy

Pre-Selection:

- Should have exactly one lepton (or two, in case of ZV channel)
- Should have MET (only for WV channel)
- At least one Fat Jet (having radius parameter 0.8)
  - 40< m_W < 150
  - pt>200 GeV, |η| < 2.4
  - |ΔR(Fat Jet, lepton) | > 1.0
  - Fat jet Closest to W-boson mass
- At least two small jets (having radius parameter 0.4)
  - pT > 30 GeV, Mjj > 500 GeV
  - |ΔR(Small Jet, lepton) | > 0.3
  - |ΔR(Fat Jet, AK4jet) | > 0.8
  - Select highest m_{jj} pair
- Small radius jet is tagged as b-tag if it has secondary vertex:
  - pT > 30 GeV, |η| < 2.4

Boson Centrality (Phys. Rev. D 95, 032001)

$$\xi_V = min\{\Delta\eta_-, \Delta\eta_+\}$$

where,

$$\Delta\eta_- = min\{\eta(V_{had}), \eta(V_{lep})\} - min\{\eta_{j1}, \eta_{j2}\},$$
$$\Delta\eta_+ = max\{\eta_{j1}, \eta_{j2}\} - max\{\eta(V_{had}), \eta(V_{lep})\}$$

- **ζ > 0 : Both W's should be within VBF jets**
- **ζ < 0 : One or both lepton are at larger |η| than the VBF jets**

Zeppenfeld w.r.t. Leptonic W (Phys. Rev. D 54, 6680)

$$Z_{Wlep} = \frac{\eta_{Wlep} - \frac{\eta_{j1} + \eta_{j2}}{2}}{|\eta_{j1} - \eta_{j2}|}$$

Event Selection

WV Channel

- Final Selection Electrons (Muons)
  - Exactly 1 lepton
  - For Electrons exclude region $1.4442 < \eta < 1.566$
  - MET > 80 GeV (50 GeV)
  - Fat Jet (having radius parameter 0.8):
    - $65 < m_W < 105$, **Tau2/Tau1** < 0.55
  - VBF jets (having radius parameter 0.4):
    - $m_{jj} > 800$ GeV, dEta > 4.0
  - Boson-Centrality > 1.0
  - Leptonic zeppenfeld < 0.3
  - Hadronic zeppenfeld < 0.3
  - $m_{WV} > 600$

ZV Channel

- Final Selection
  - Exactly 2 leptons
  - $76 < m_{LL} < 107$
  - Large radius parameter jet:
    - $65 < m_Z < 105$, **Tau2/Tau1** < 0.55
  - VBF jets:
    - $m_{jj} > 800$ GeV, dEta > 4.0
  - $m_{ZV} > 600$
- Fit m_{VV} distribution to get limits

Ratio of sub-jet Momenta

WV/ZV Signal Extraction

- We used M_{WW} distribution to get the limits for both WV and ZV channel.
    - SM EWK production is treated as background.

Final state	WV	ZV
Data	—	—
V+jets	199 ± 12	53.1 ± 4.5
top	120 ± 10	0.16 ± 0.03
SM QCD VV	34 ± 6	6.4 ± 1.3
SM EW VV	18 ± 1	2.4 ± 0.2
Total bkg.	372 ± 13	62 ± 5
$f_{T2}//Lambda^4 = -0.5, -2.5\ \text{TeV}^{-4}$	22 ± 1	7.6 ± 0.6
$m_H = 500\ \text{GeV}, s_h = 0.5$	40 ± 1	4.3 ± 0.1

- Before doing this we estimated W+jets (for WV channel) and Z+jets (for ZV channel) in data driven way.

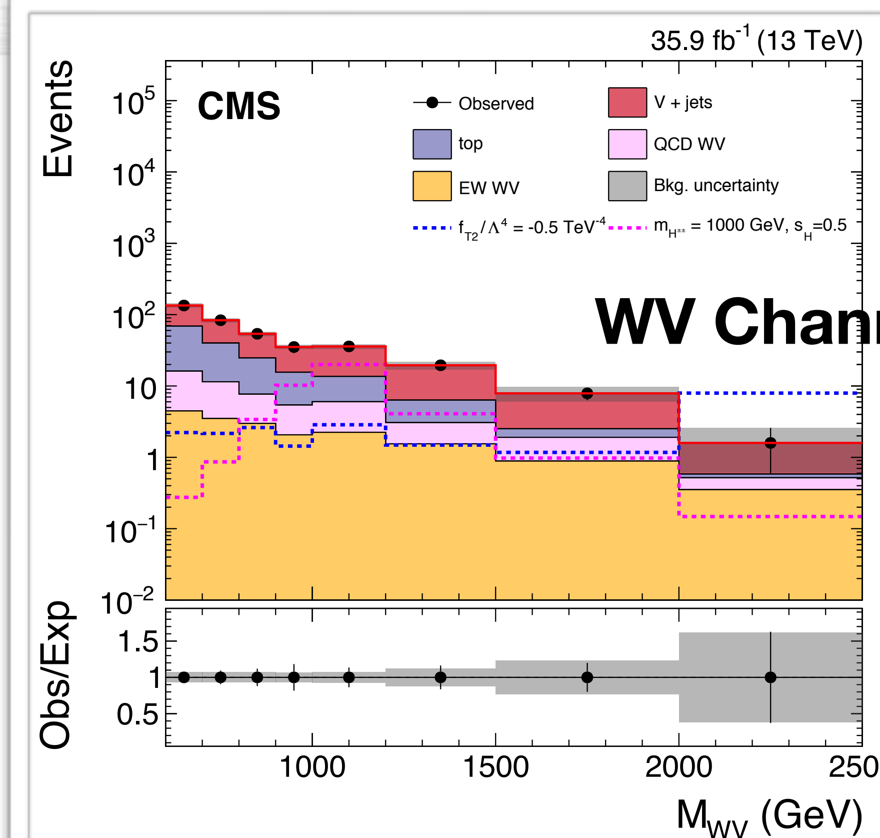

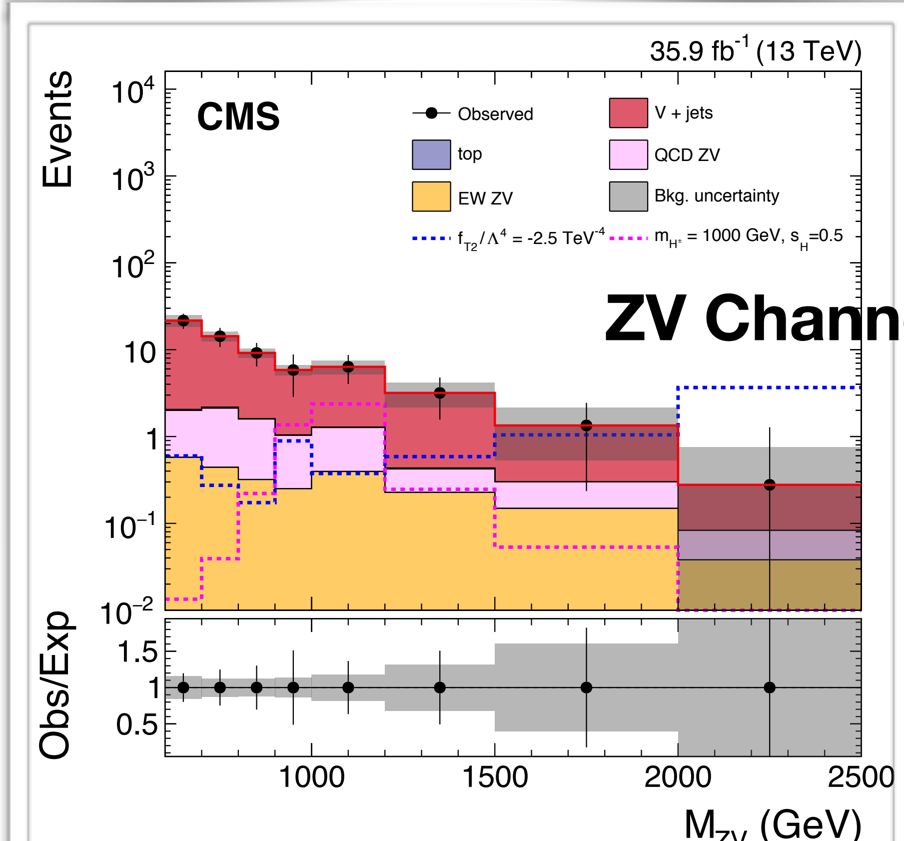

Control Region

- TTbar Control Region
  - Number of medium b-tag AK4 jets > 0

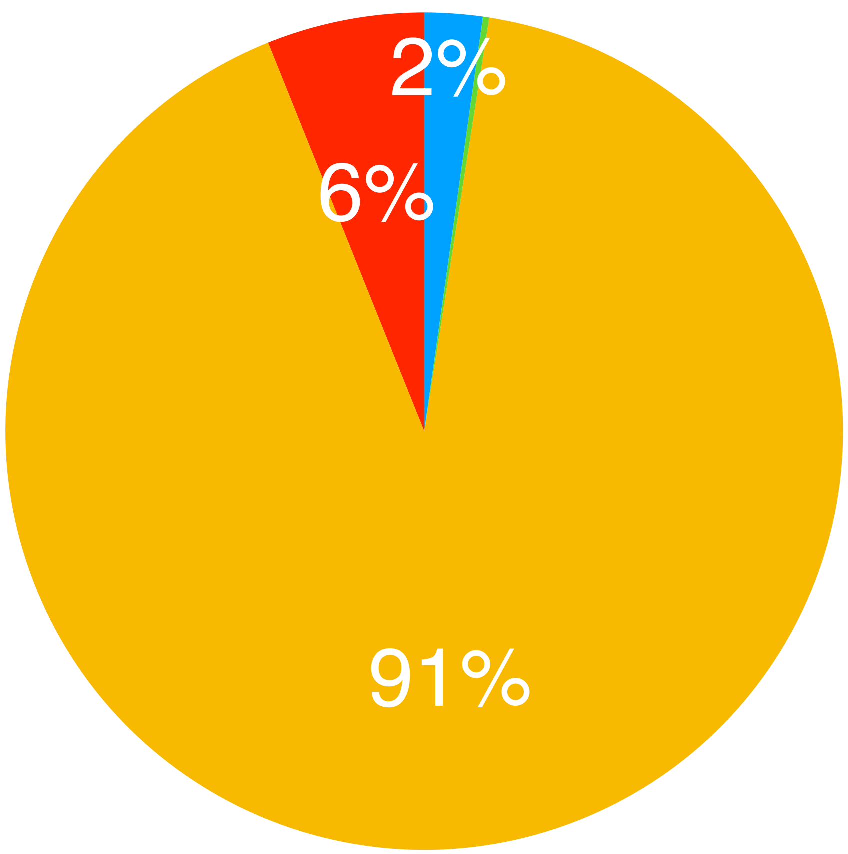

- W+jet Control Region
  - $40 < m_W < 65$ or
  - $105 < m_W < 150$

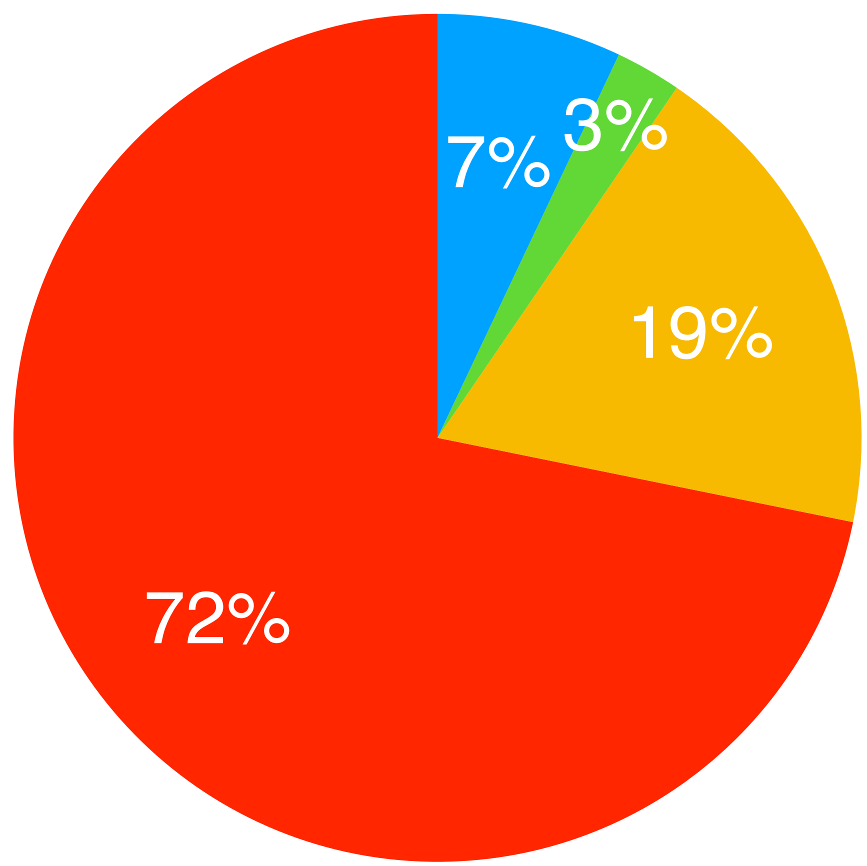

- Z+jet Control Region
  - $40 < m_Z < 65$ or
  - $105 < m_Z < 150$

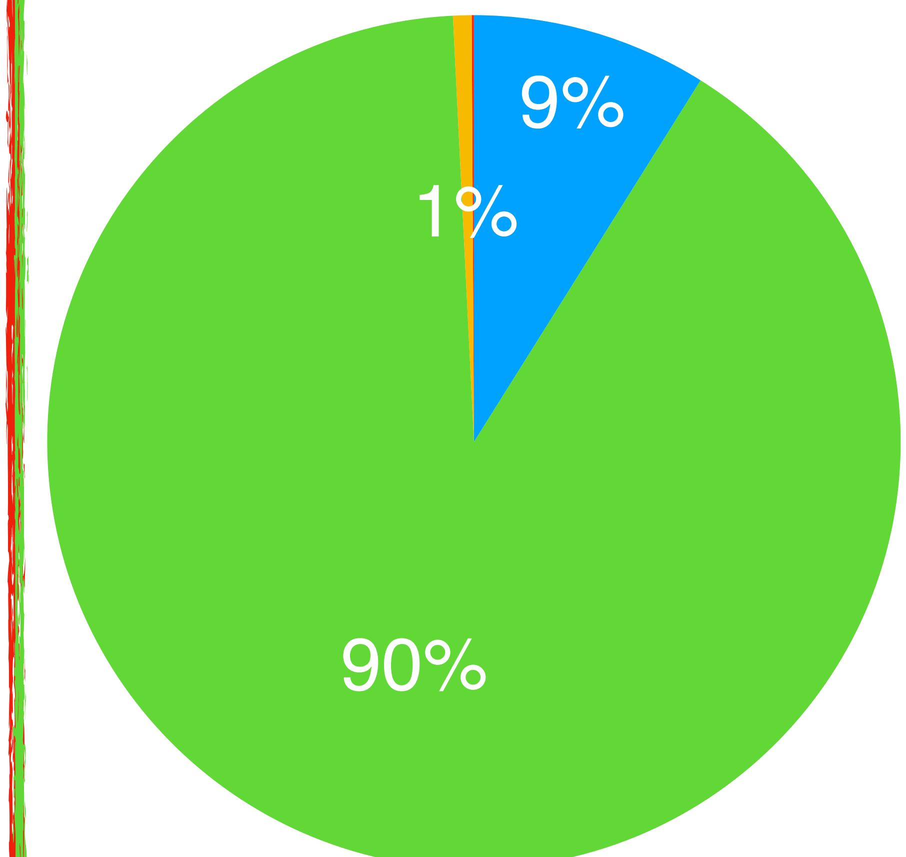

Diboson Z+jet top W+jet

TTbar Control Region

Lepton p_T

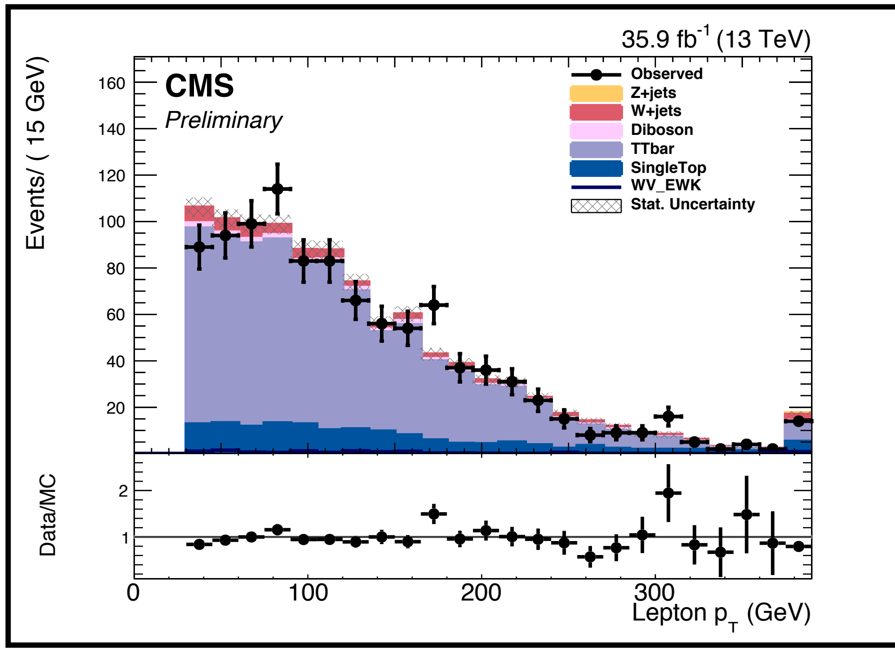

pfMET

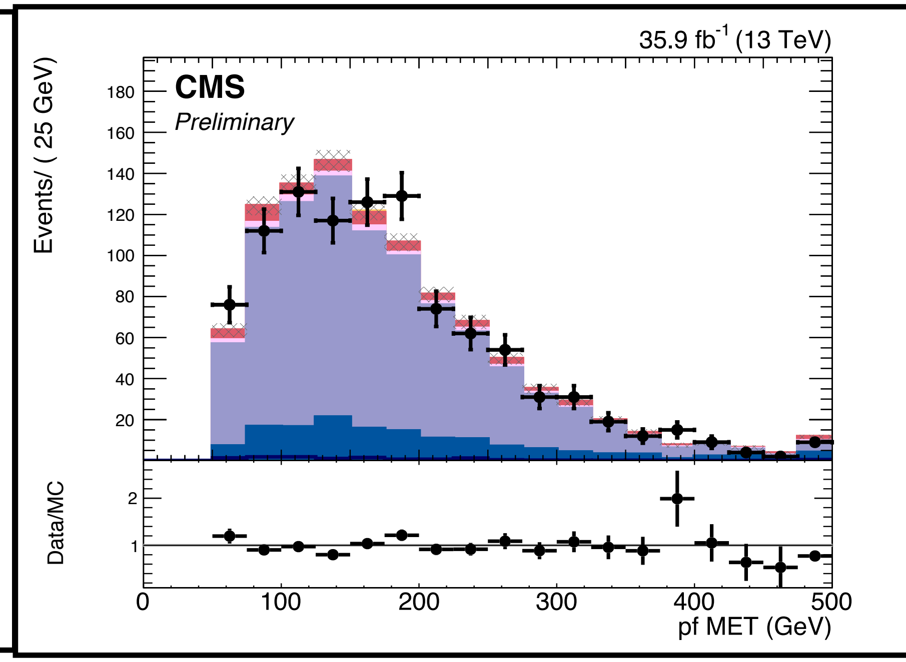

Mass of diboson system

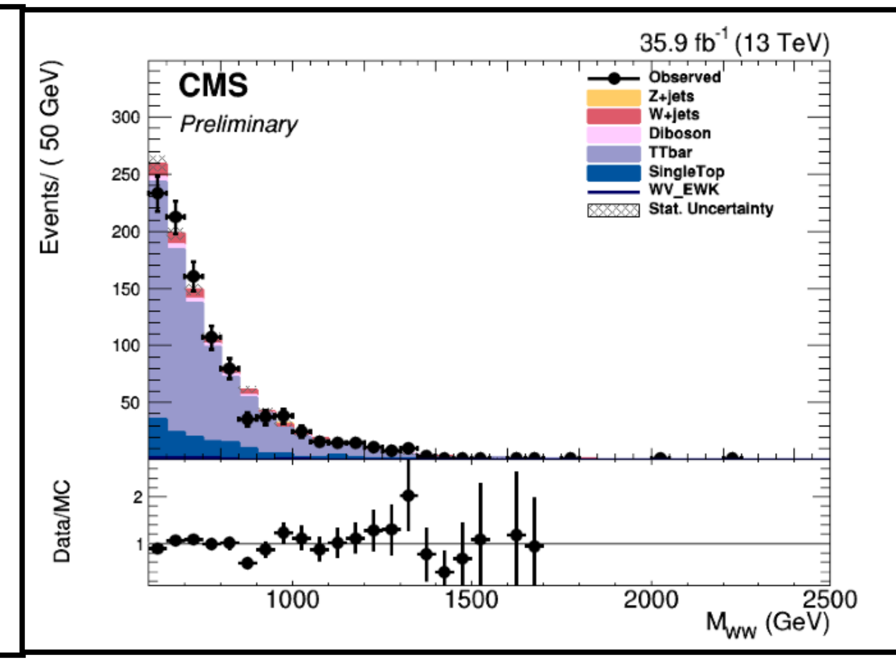

AK8 jet p_T

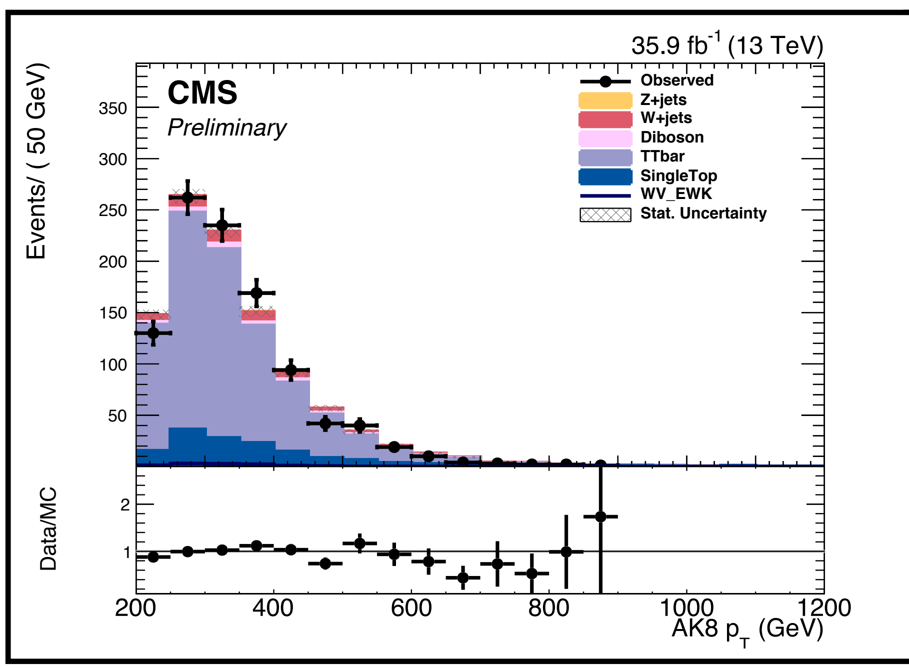

VBF di-jet Invariant mass

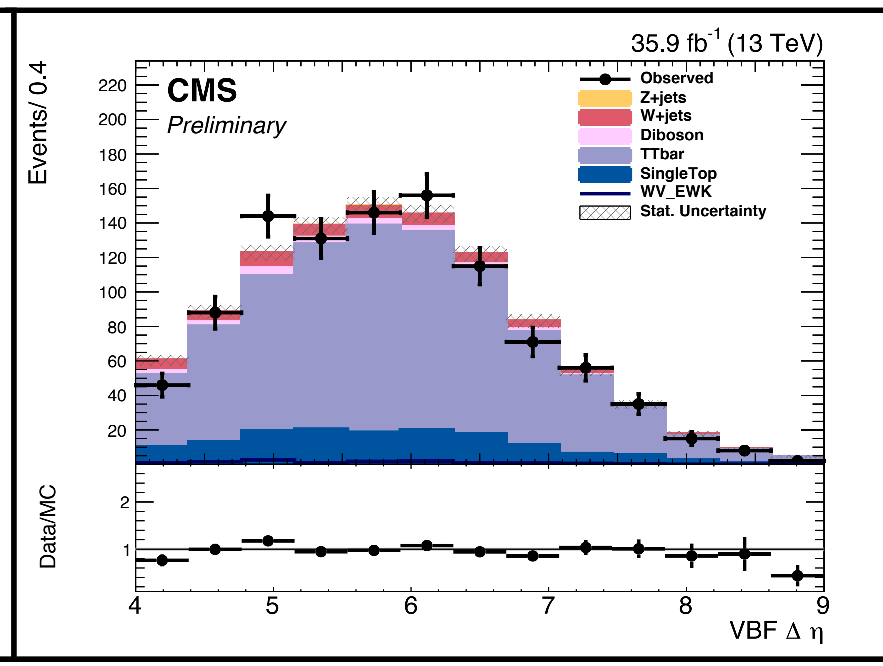

VBF Pseudo-Rapidity Gap

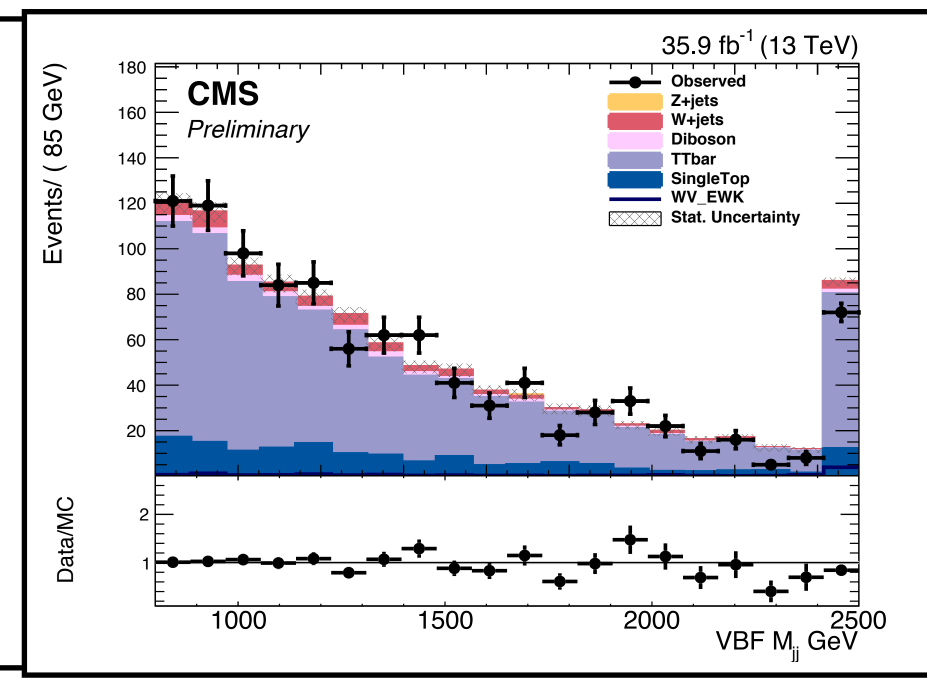

W+jet Control Region

Lepton p_T

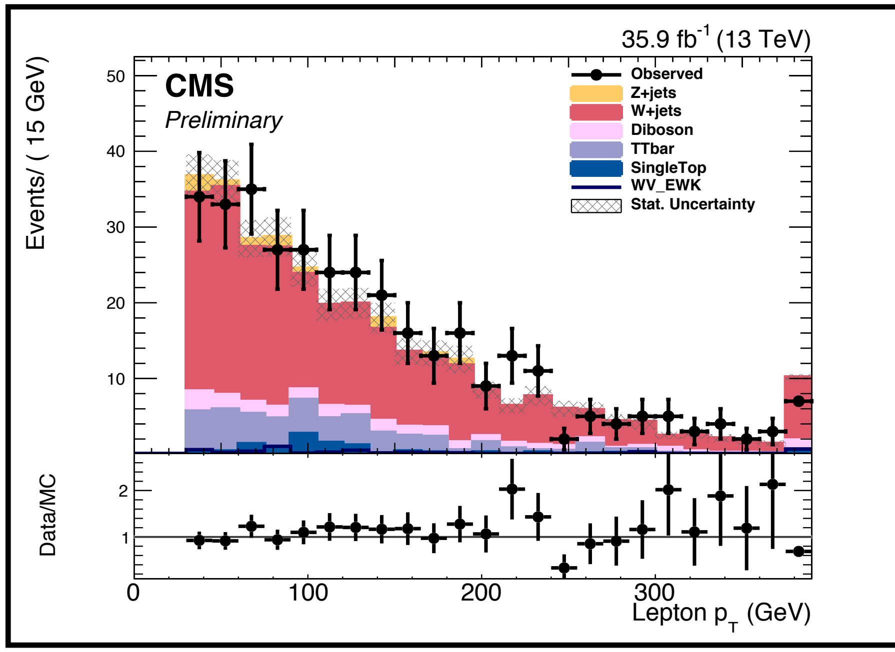

pfMET

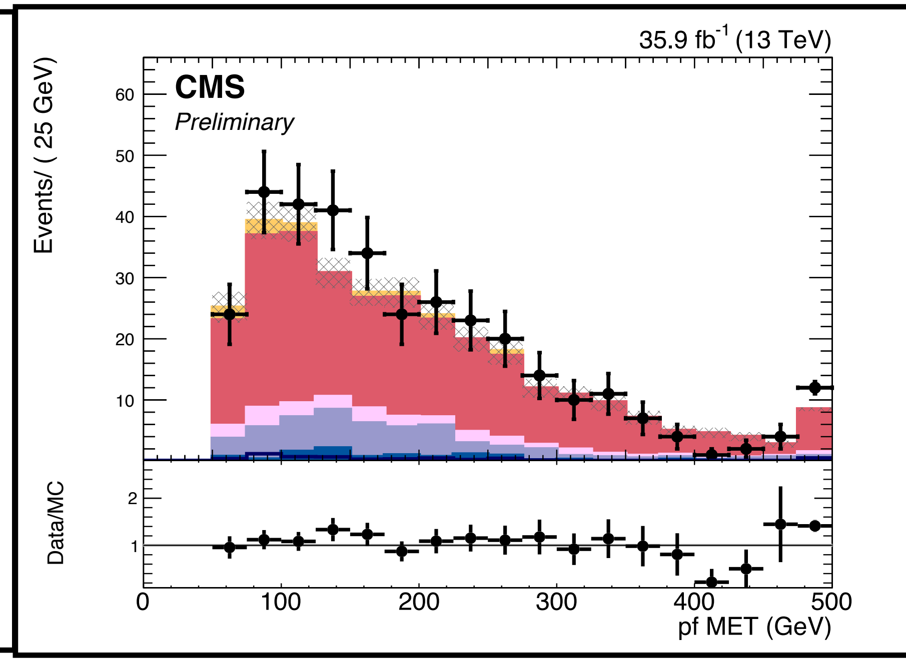

Mass of diboson system

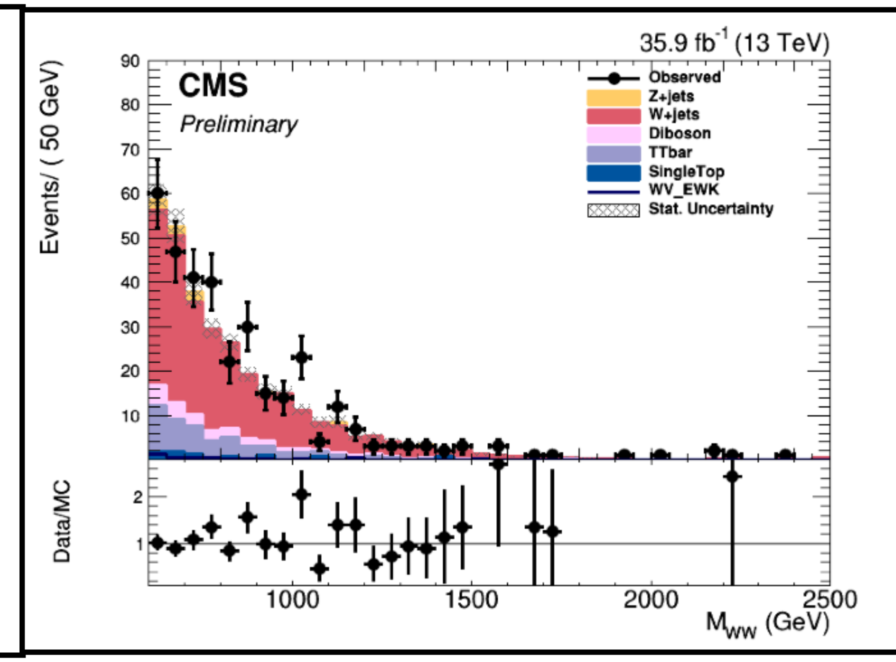

AK8 jet p_T

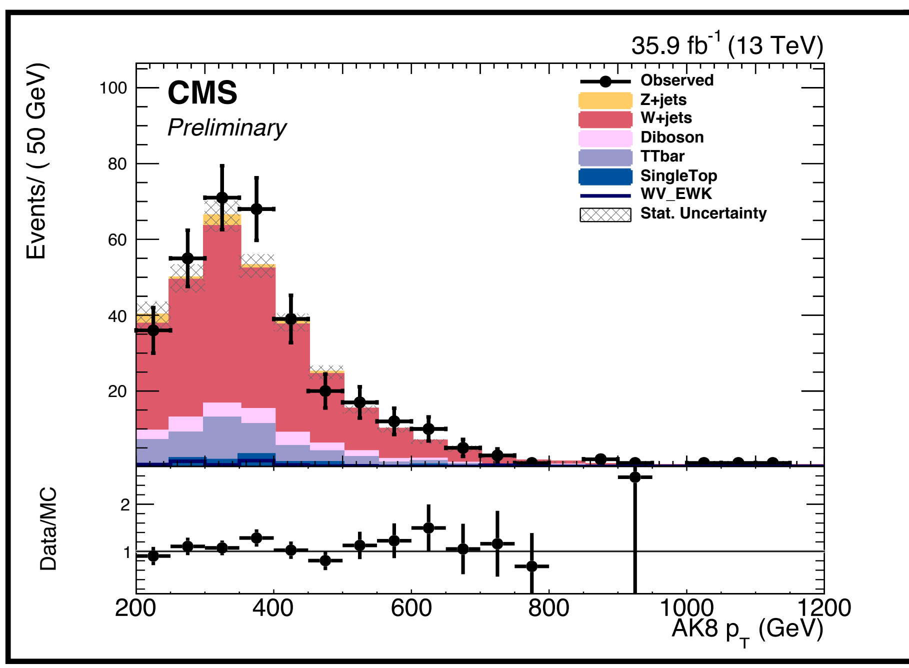

VBF di-jet Invariant mass

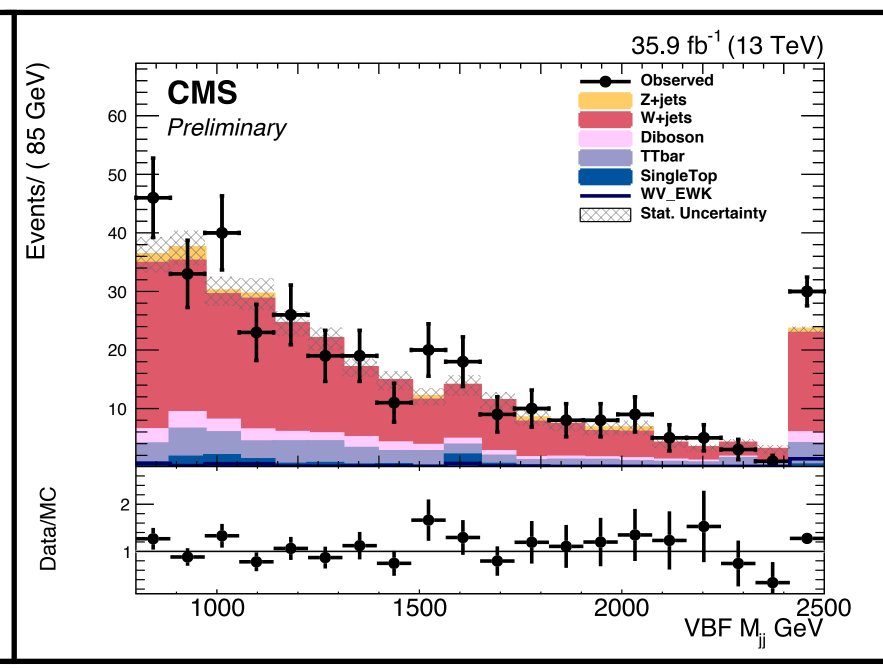

VBF Pseudo-Rapidity Gap

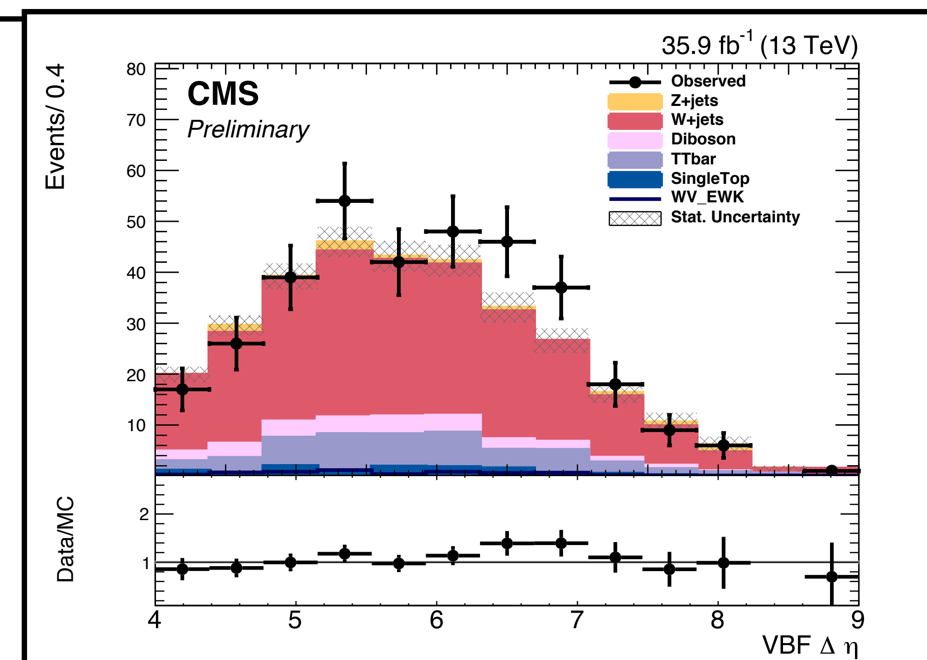

Estimated W+jet in data-driven way.

Data driven background estimation (Alpha-Ratio Method)

- **To get V+jet contribution from data in signal region:**

$$N^{Data,W+Jets}_{signal}(M_{WW}) = \alpha(M_{WW}) \times N^{Data}_{sideband}(M_{WW})$$

- **Alpha (taken from MC) is defined as:**

$$\alpha(M_{WW}) = \frac{N^{MC,W+Jets}_{signal}(M_{WW})}{N^{MC,W+Jets}_{sideband}(M_{WW})} = \frac{N^{Data}_{signal}(M_{WW})}{N^{Data}_{sideband}(M_{WW})}$$

- In this formula there are three sources of uncertainty.
  - Uncertainty in alpha (dominated by MC statistics)
  - Uncertainty coming from W+jet shape
  - Statistical uncertainty coming from data

Parametric Function For Each Background

Side-band

Diboson

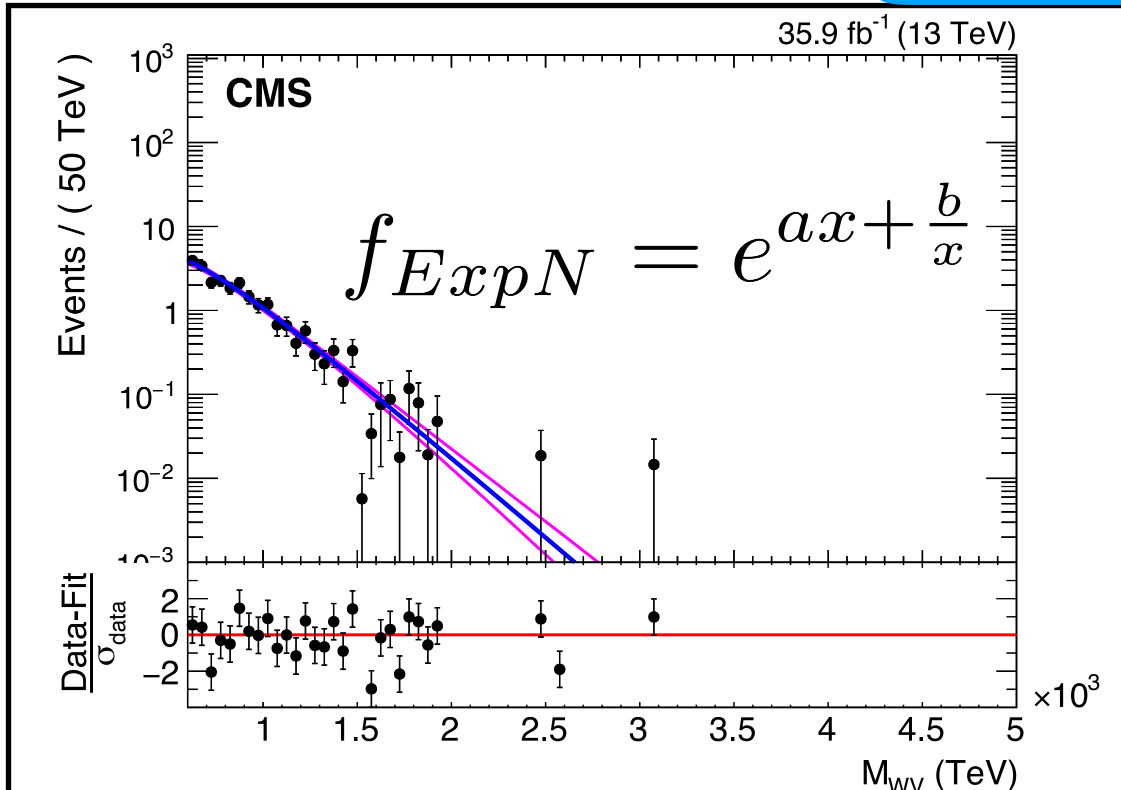

Single Top

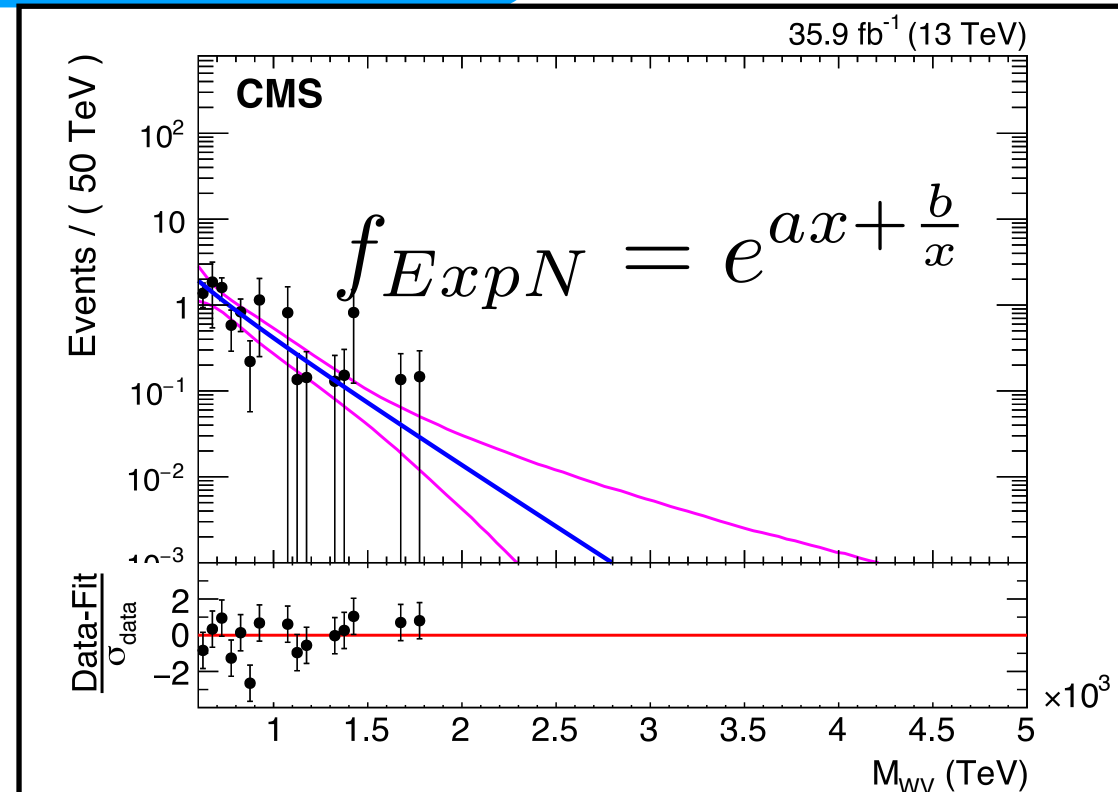

V+jet

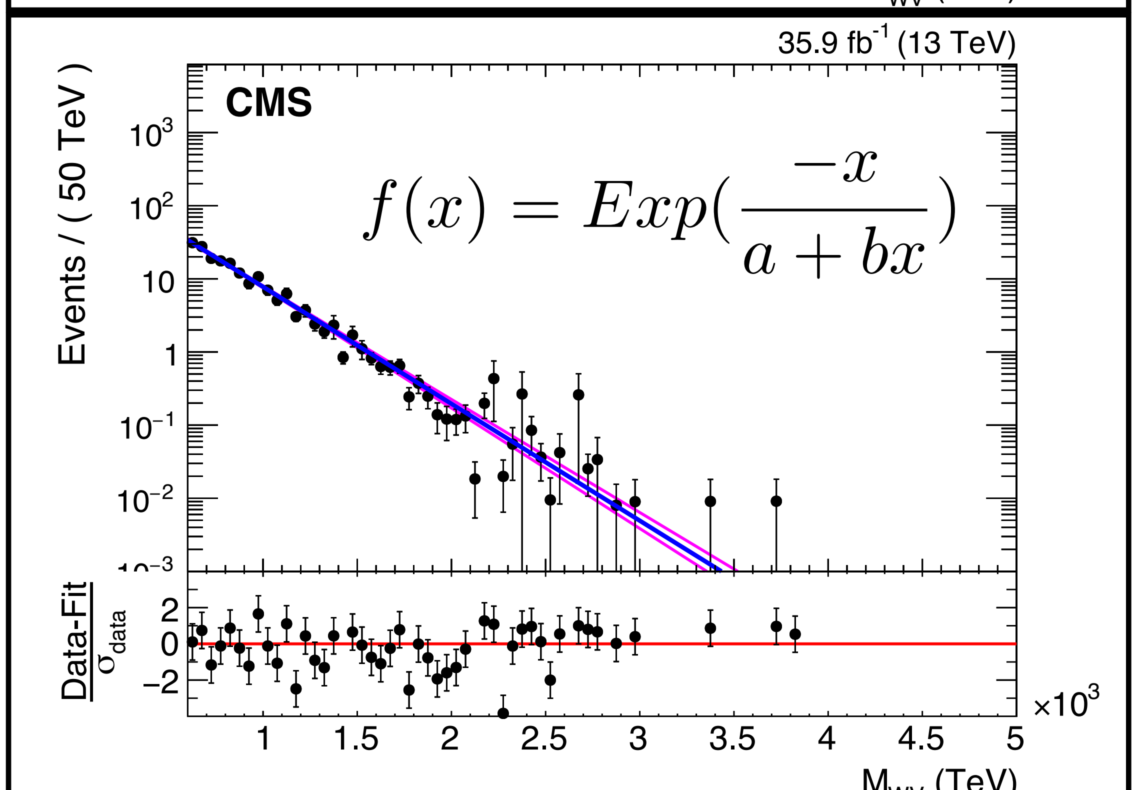

TTbar

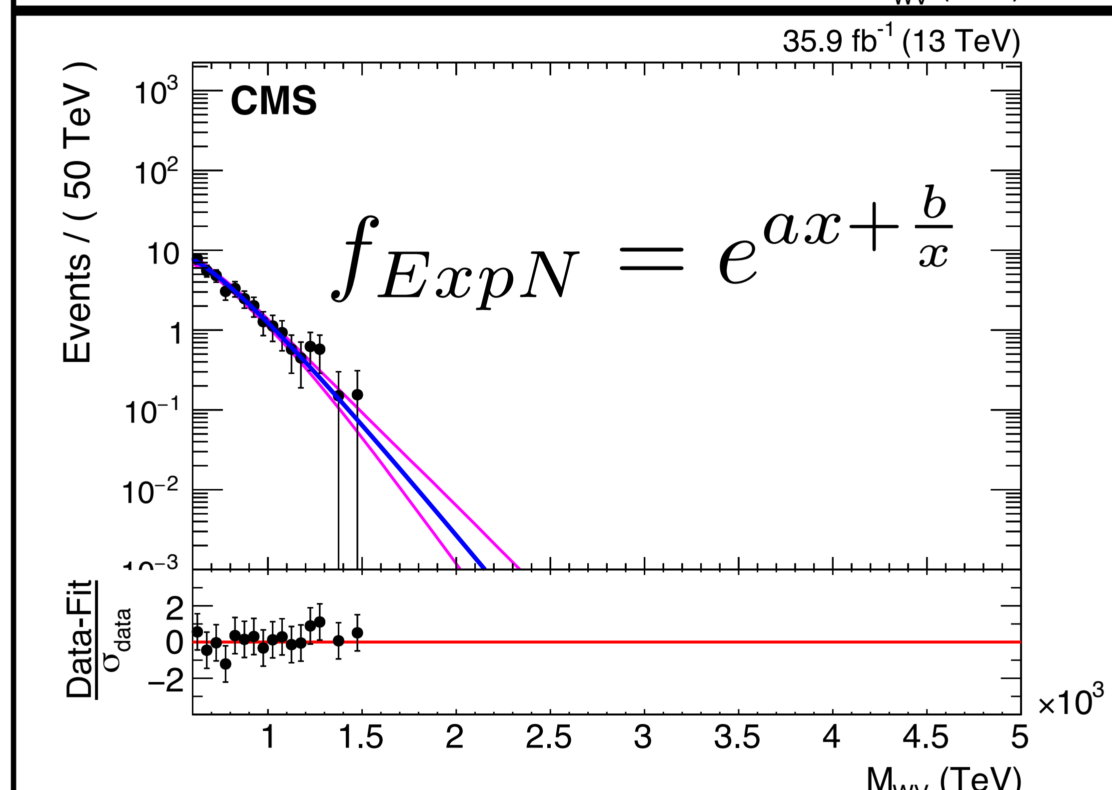

M_{WW} Fits

Log Plot

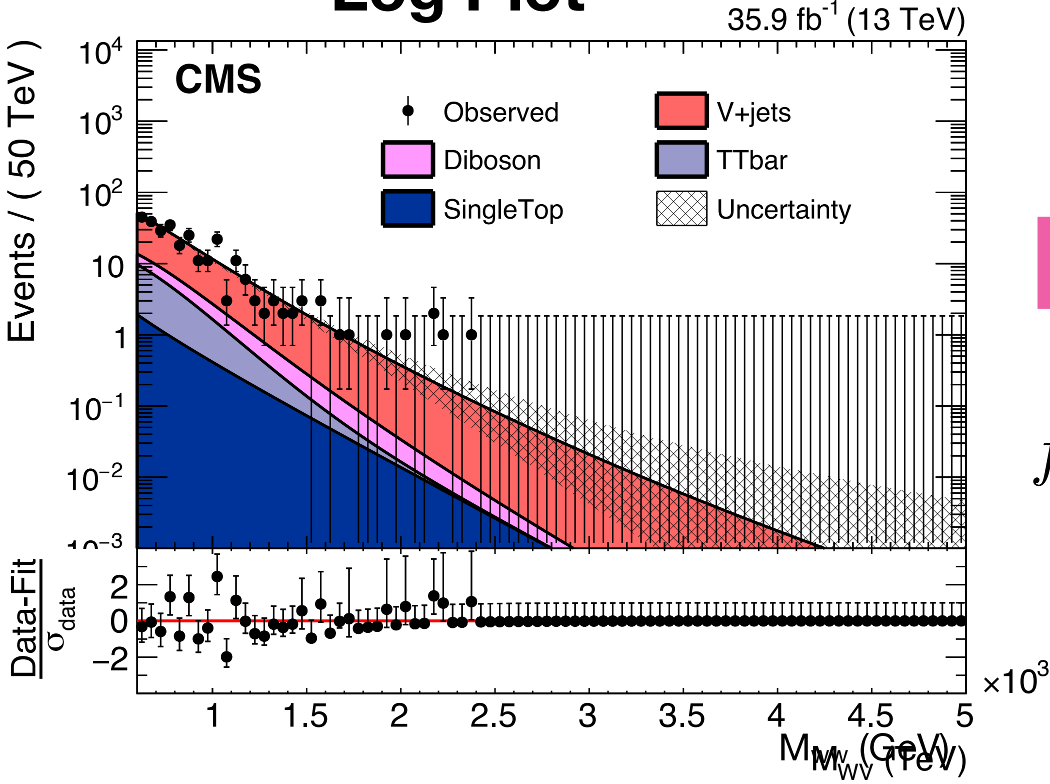

Linear Plot

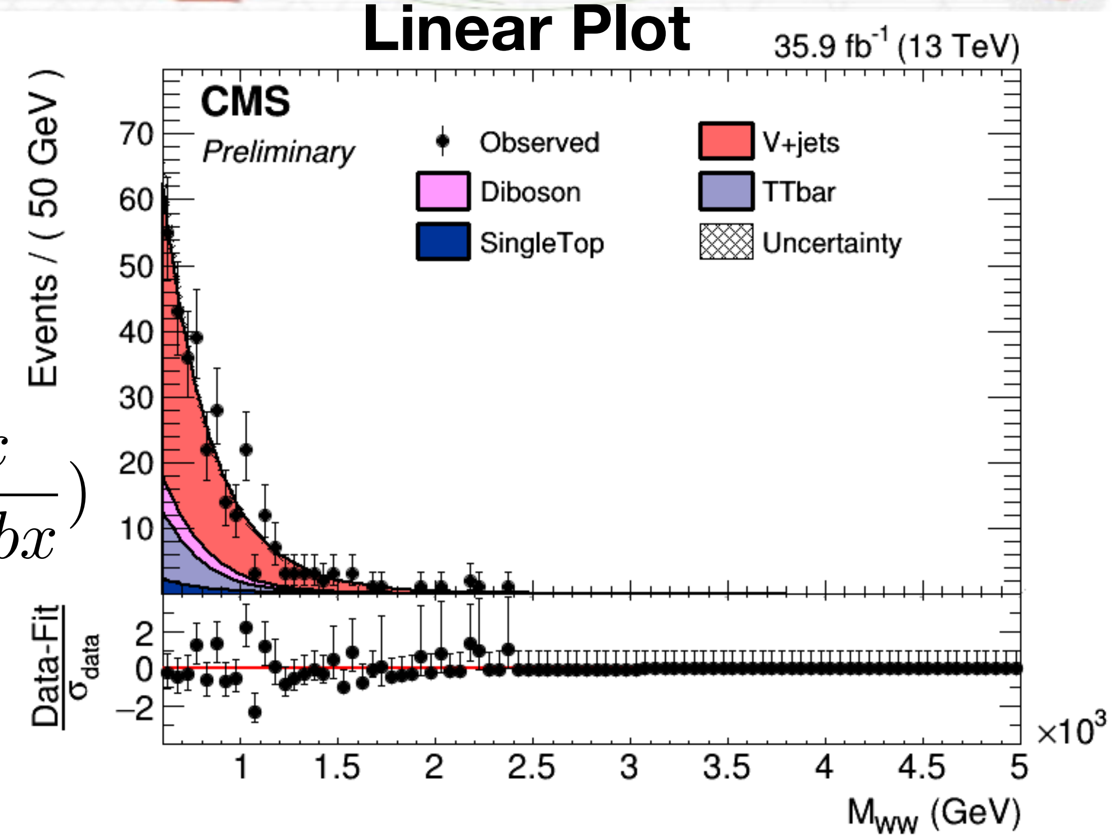

Nominal Function

$$f(x) = Exp(\frac{-x}{a+bx})$$

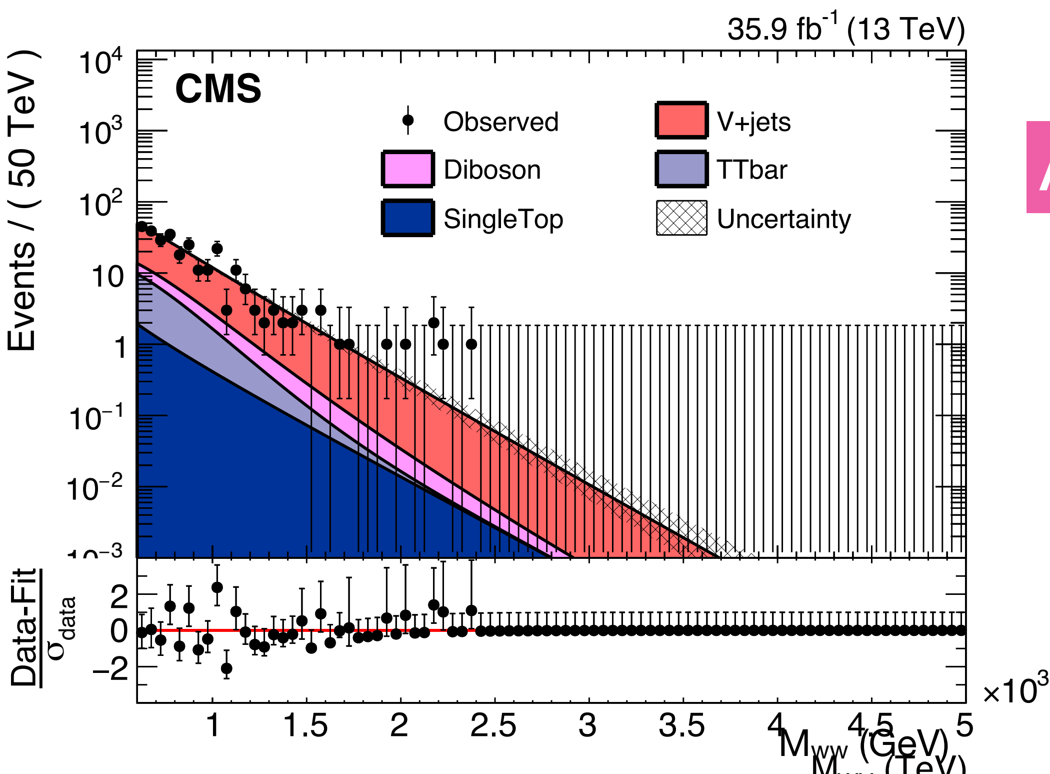

Alternate Function

$$f_{Exp} = e^{nx}$$

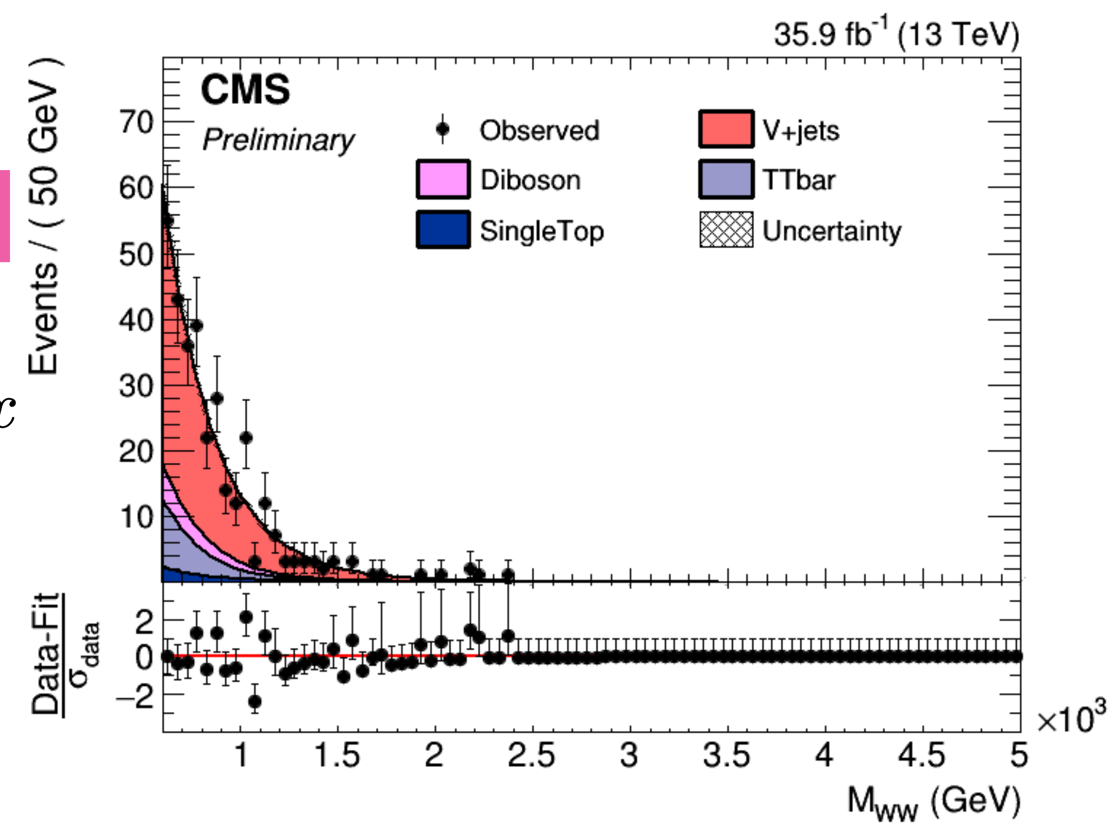

- Both V+jet normalisation as well as shape is floating in this fit.

Interference between EWK and QCD

- Interference = $| \text{EWK} + \text{QCD} |^2 - (|\text{EWK}|^2 + |\text{QCD}|^2)$.
- For interference studies, we used phantom generator.
- Applied pre-selection in phantom cards are:

Leptons:
- pt_min_lep = 20 GeV
- eta_max_lep = 3
- m_min_ll = 20 GeV
- Ptmiss_min = 25 GeV

Jets:
- pt_min_j = 20 GeV
- eta_max_lep = 5.4
- m_min_jj = 30 GeV

- Offline analysis cuts:
  - $M_{jj} > 700$ GeV, $\Delta\eta_{VBS} > 3$, $M_{WW} > 126$

EWK & QCD Interference Distributions

Comparison between EWK+QCD with and without interference

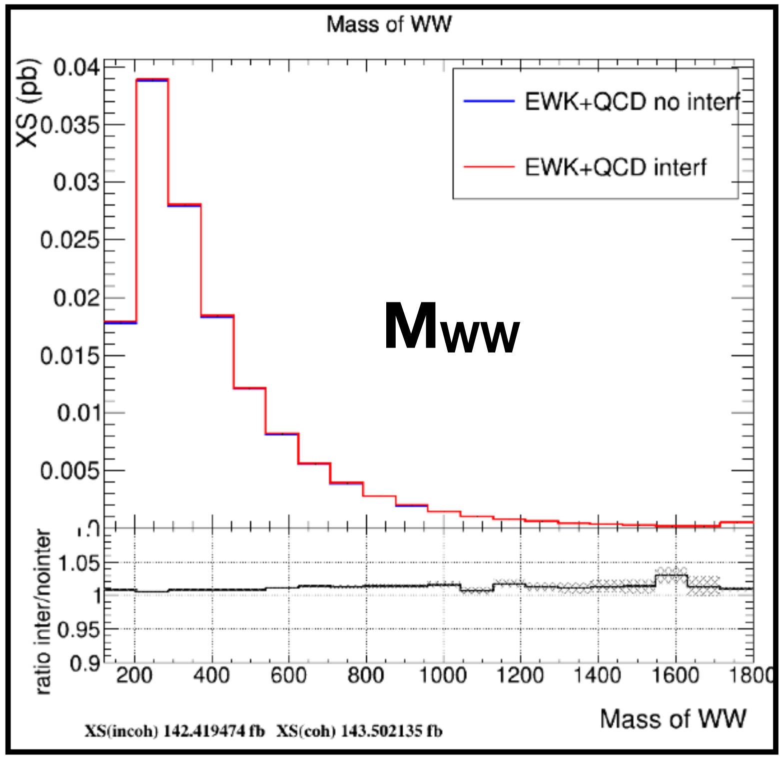

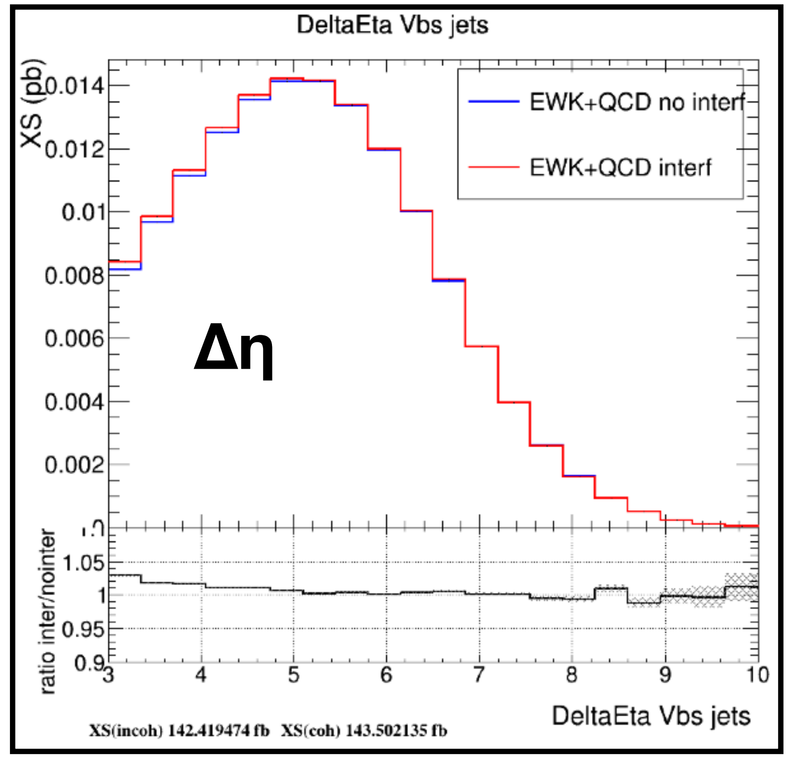

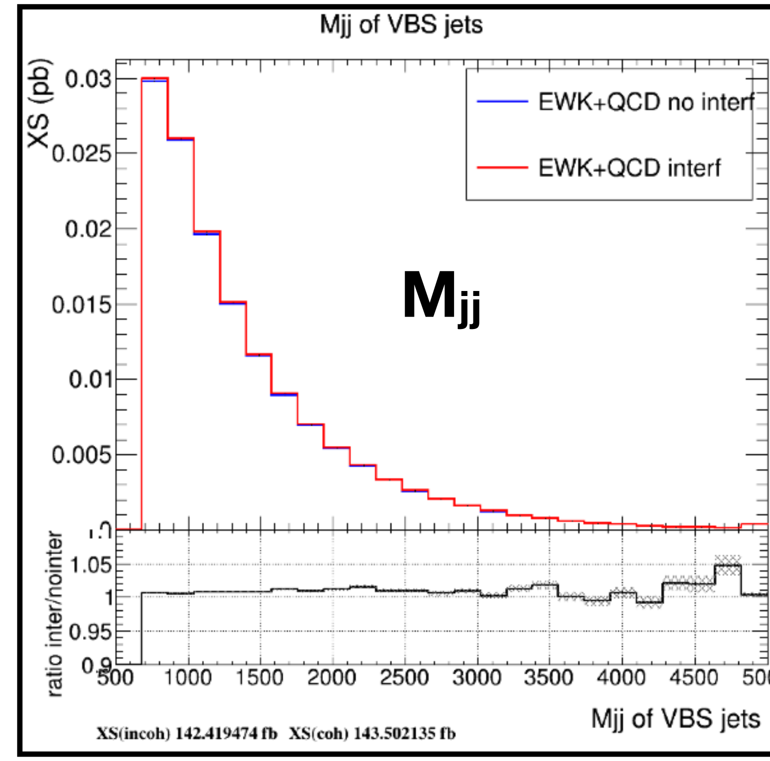

Interference distribution and ratio between interference and signal

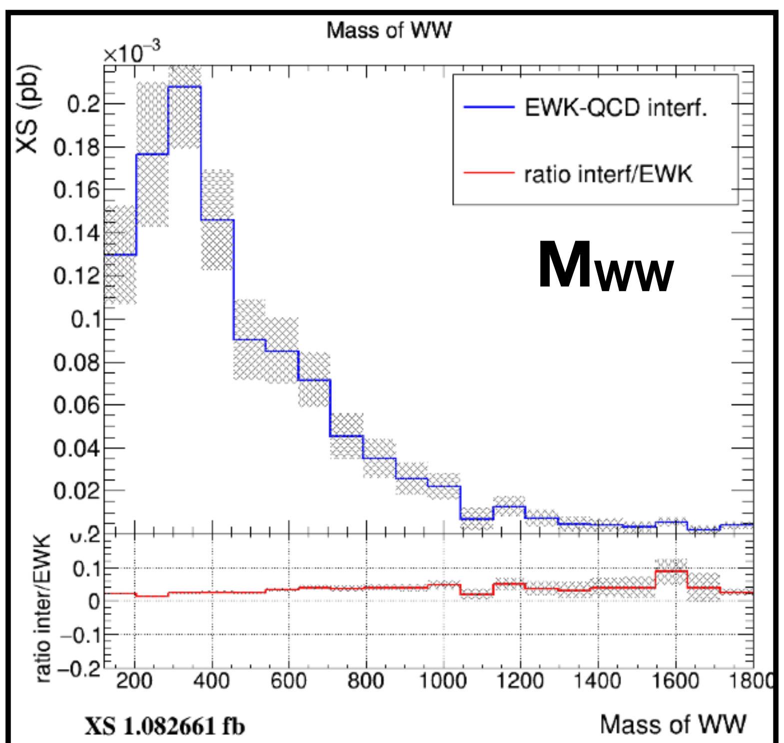

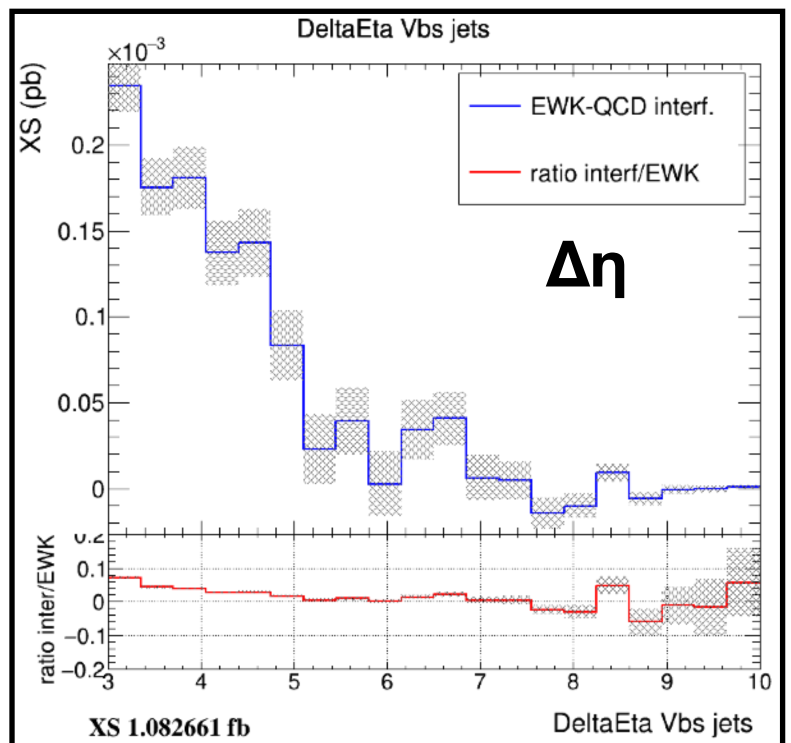

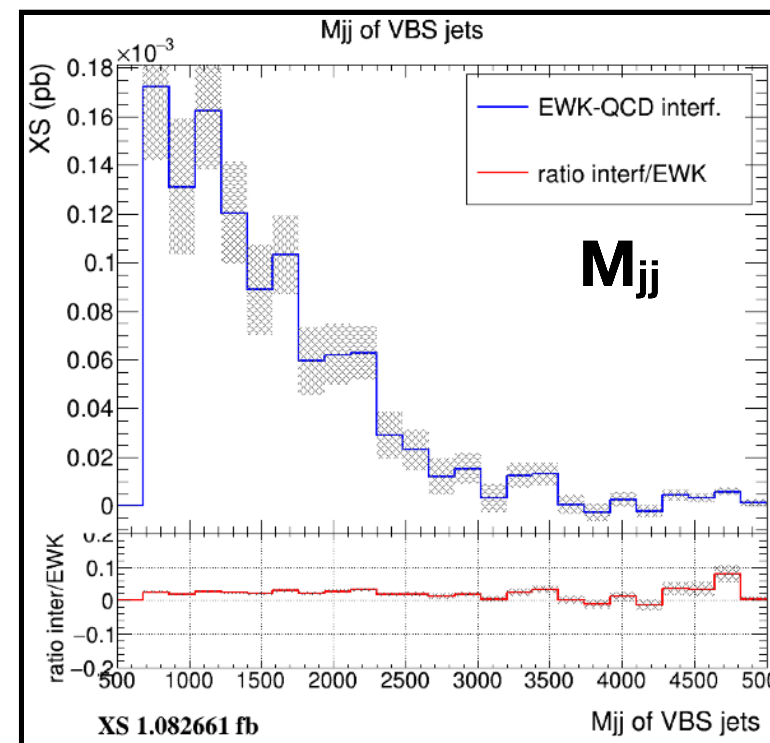

The interference is found to contribute at the level of 1% in the signal region and is therefore neglected.

Systematic Uncertainty

- Major systematics are considered as shape based.

- Following systematics are considered from background (V+Jet) estimation:
    - Wjet fit parameter variation.
    - Wjet alternate shape
    - Alpha fit parameter variation

- Also, limited MC statistics uncertainty are considered bin-wise.

Source	Signal	*W*+jet	*WV*	top	*Z*+jet
Integrated luminosity	2.5	—	2.5	—	—
Lepton efficiency	1.0	—	1.0	1.0	—
Jet momentum scale	shape	—	shape	shape	—
Lepton momentum scale	shape	—	shape	shape	—
b tagging	2.0	—	2.0	3.0	2.0
V tagging	8.0	—	8.0	8.0	—
QCD scale	22.0	—	38.0	—	—
PDF unc.	6.0	—	9.0	—	—
bkg. normalization	—	15.0	—	10.0	15.0
W+jet shape	—	shape	—	—	—
Z+jet shape	—	—	—	—	shape
Jet/MET resolution	4.0	—	3.0	2.0	
Pileup modeling	5.0	—	4.0	—	—
Limited MC stat.	shape	—	shape	shape	—

Anomalous Coupling Limits

aQGC Parameters Previous published limits		Our Limits	
		WV Channel	ZV Channel
FS0	[-7.7,7.7]	[-3.9,3.9]	[-28,28]
FS1	[-22,22]	[-4.9,4.9]	[-22,22]
FT0	[-0.46,0.44]	[-0.16,0.15]	[-0.9,0.9]
FT1	[-0.28,0.31]	[-0.16,0.17]	[-0.92,0.93]
FT2	[-0.89,1.0]	[-0.38,0.38]	[-2.1,2.3]
FM0	[-4.2,4.2]	[-0.95,0.95]	[-4.8,4.8]
FM1	[-8.7,9.1]	[-2.8,2.8]	[-15,15]
FM6	[-12,12]	[-1.9,1.9]	[-9.6,9.6]
FM7	[-13,13]	[-4.7,4.7]	[-23,23]

Reference:

1. https://twiki.cern.ch/twiki/bin/view/CMSPublic/PhysicsResultsSMPaTGC#aQGC_Results

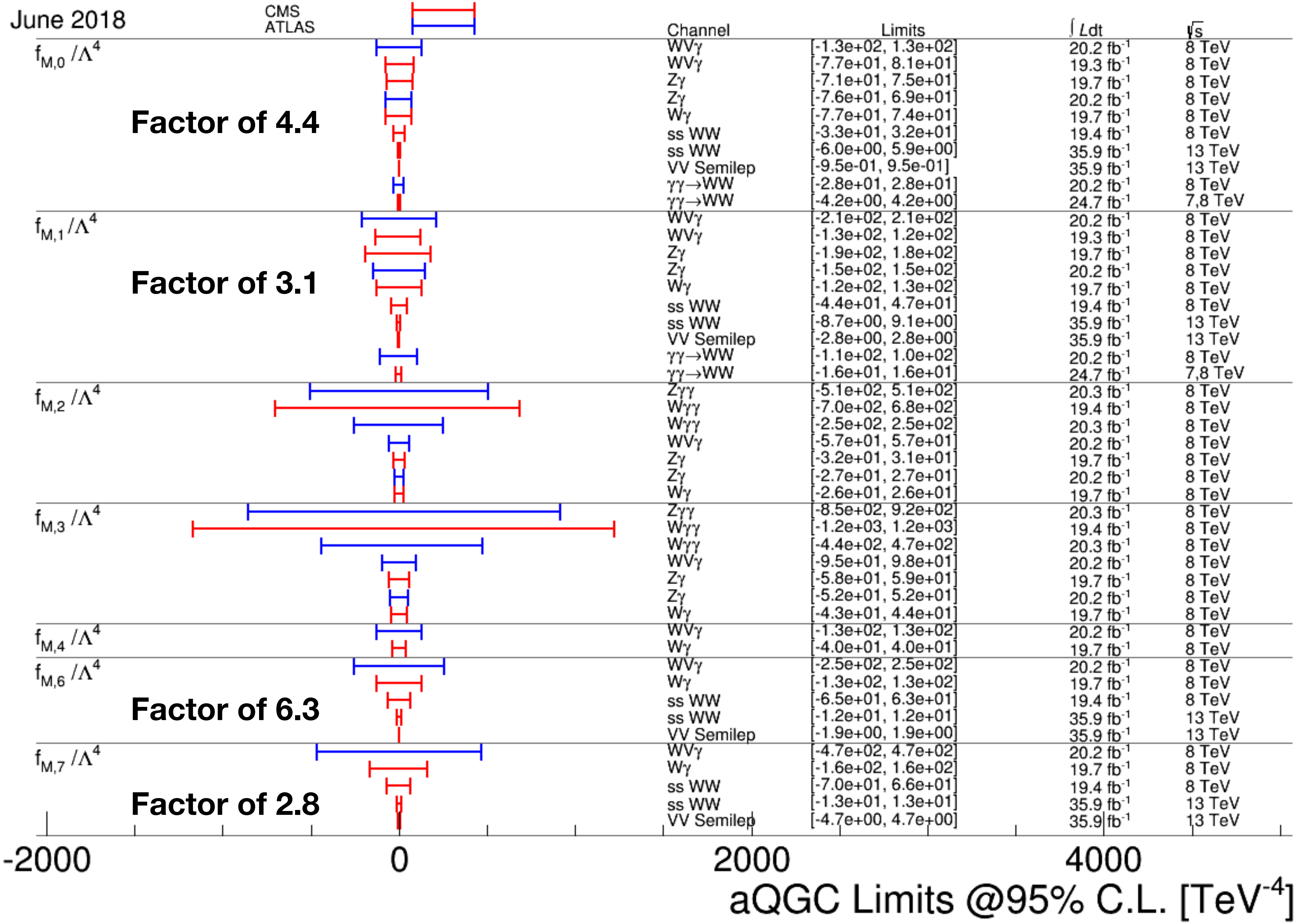
June 2018
CMS
ATLAS
Channel Limits ∫Ldt √s
fM,0 /Λ4
WVγ [-1.3e+02, 1.3e+02] 20.2 fb-1 8 TeV
WVγ [-7.7e+01, 8.1e+01] 19.3 fb-1 8 TeV
Zγ [-7.1e+01, 7.5e+01] 19.7 fb-1 8 TeV
Zγ [-7.6e+01, 6.9e+01] 20.2 fb-1 8 TeV
Wγ [-7.7e+01, 7.4e+01] 19.7 fb-1 8 TeV
ss WW [-3.3e+01, 3.2e+01] 19.4 fb-1 8 TeV
ss WW [-6.0e+00, 5.9e+00] 35.9 fb-1 13 TeV
VV Semilep [-9.5e-01, 9.5e-01] 35.9 fb-1 13 TeV
γγ→WW [-2.8e+01, 2.8e+01] 20.2 fb-1 8 TeV
γγ→WW [-4.2e+00, 4.2e+00] 24.7 fb-1 7,8 TeV
Factor of 4.4
fM,1 /Λ4
WVγ [-2.1e+02, 2.1e+02] 20.2 fb-1 8 TeV
WVγ [-1.3e+02, 1.2e+02] 19.3 fb-1 8 TeV
Zγ [-1.9e+02, 1.8e+02] 19.7 fb-1 8 TeV
Zγ [-1.5e+02, 1.5e+02] 20.2 fb-1 8 TeV
Wγ [-1.2e+02, 1.3e+02] 19.7 fb-1 8 TeV
ss WW [-4.4e+01, 4.7e+01] 19.4 fb-1 8 TeV
ss WW [-8.7e+00, 9.1e+00] 35.9 fb-1 13 TeV
VV Semilep [-2.8e+00, 2.8e+00] 35.9 fb-1 13 TeV
γγ→WW [-1.1e+02, 1.0e+02] 20.2 fb-1 8 TeV
γγ→WW [-1.6e+01, 1.6e+01] 24.7 fb-1 7,8 TeV
Factor of 3.1
fM,2 /Λ4
Zγγ [-5.1e+02, 5.1e+02] 20.3 fb-1 8 TeV
Wγγ [-7.0e+02, 6.8e+02] 19.4 fb-1 8 TeV
Wγγ [-2.5e+02, 2.5e+02] 20.3 fb-1 8 TeV
WVγ [-5.7e+01, 5.7e+01] 20.2 fb-1 8 TeV
Zγ [-3.2e+01, 3.1e+01] 19.7 fb-1 8 TeV
Zγ [-2.7e+01, 2.7e+01] 20.2 fb-1 8 TeV
Wγ [-2.6e+01, 2.6e+01] 19.7 fb-1 8 TeV
fM,3 /Λ4
Zγγ [-8.5e+02, 9.2e+02] 20.3 fb-1 8 TeV
Wγγ [-1.2e+03, 1.2e+03] 19.4 fb-1 8 TeV
Wγγ [-4.4e+02, 4.7e+02] 20.3 fb-1 8 TeV
WVγ [-9.5e+01, 9.8e+01] 20.2 fb-1 8 TeV
Zγ [-5.8e+01, 5.9e+01] 19.7 fb-1 8 TeV
Zγ [-5.2e+01, 5.2e+01] 20.2 fb-1 8 TeV
Wγ [-4.3e+01, 4.4e+01] 19.7 fb-1 8 TeV
fM,4 /Λ4
WVγ [-1.3e+02, 1.3e+02] 20.2 fb-1 8 TeV
Wγ [-4.0e+01, 4.0e+01] 19.7 fb-1 8 TeV
fM,6 /Λ4
WVγ [-2.5e+02, 2.5e+02] 20.2 fb-1 8 TeV
Wγ [-1.3e+02, 1.3e+02] 19.7 fb-1 8 TeV
ss WW [-6.5e+01, 6.3e+01] 19.4 fb-1 8 TeV
ss WW [-1.2e+01, 1.2e+01] 35.9 fb-1 13 TeV
VV Semilep [-1.9e+00, 1.9e+00] 35.9 fb-1 13 TeV
Factor of 6.3
fM,7 /Λ4
WVγ [-4.7e+02, 4.7e+02] 20.2 fb-1 8 TeV
Wγ [-1.6e+02, 1.6e+02] 19.7 fb-1 8 TeV
ss WW [-7.0e+01, 6.6e+01] 19.4 fb-1 8 TeV
ss WW [-1.3e+01, 1.3e+01] 35.9 fb-1 13 TeV
VV Semilep [-4.7e+00, 4.7e+00] 35.9 fb-1 13 TeV
Factor of 2.8
-2000
0
2000
4000
aQGC Limits @95% C.L. [TeV-4]

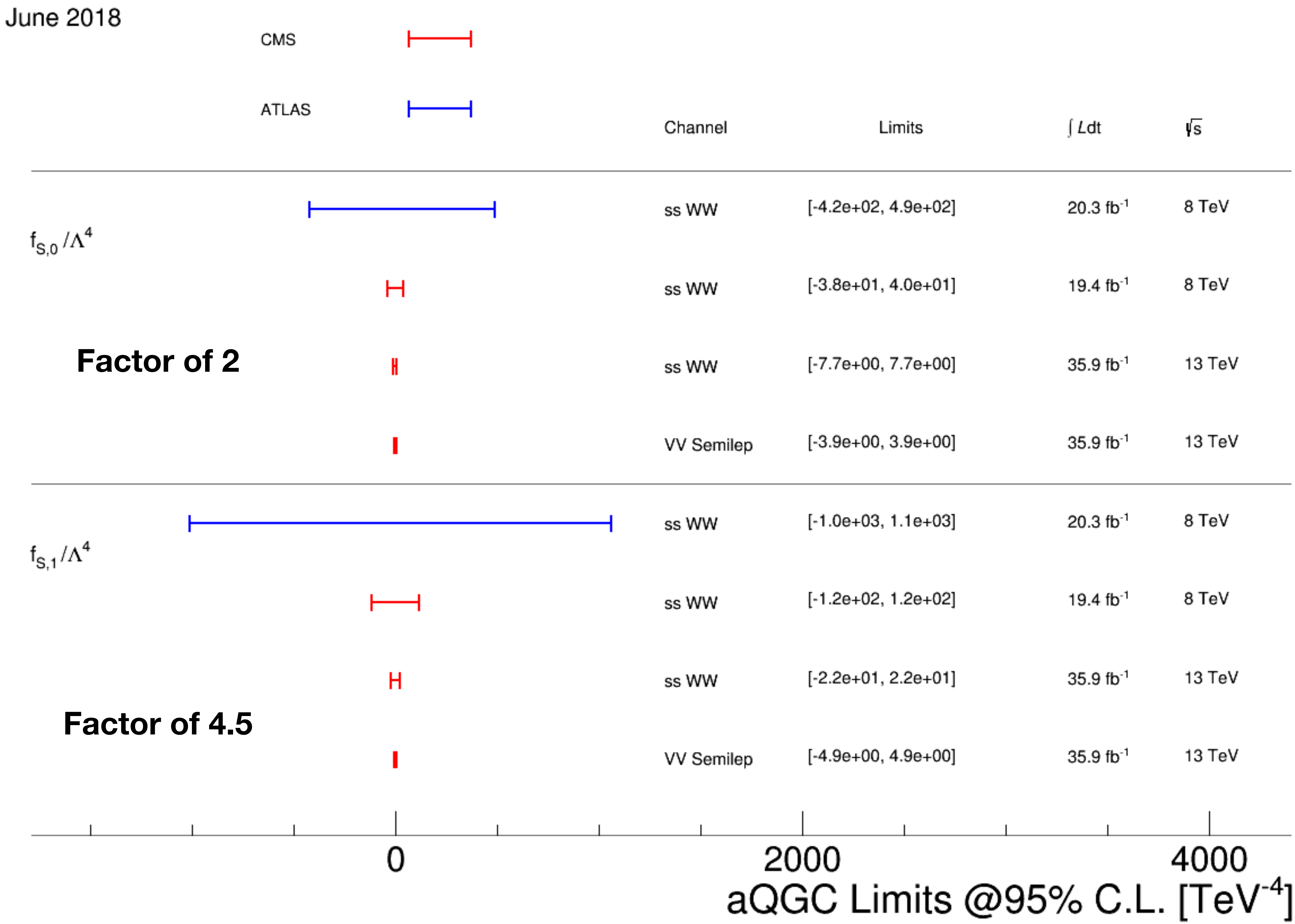

June 2018
CMS
ATLAS
Channel
Limits
$\int L dt$
$\sqrt{s}$
$f_{S,0}/\Lambda^4$
ss WW [-4.2e+02, 4.9e+02] 20.3 fb^{-1} 8 TeV
ss WW [-3.8e+01, 4.0e+01] 19.4 fb^{-1} 8 TeV
ss WW [-7.7e+00, 7.7e+00] 35.9 fb^{-1} 13 TeV
VV Semilep [-3.9e+00, 3.9e+00] 35.9 fb^{-1} 13 TeV
Factor of 2
$f_{S,1}/\Lambda^4$
ss WW [-1.0e+03, 1.1e+03] 20.3 fb^{-1} 8 TeV
ss WW [-1.2e+02, 1.2e+02] 19.4 fb^{-1} 8 TeV
ss WW [-2.2e+01, 2.2e+01] 35.9 fb^{-1} 13 TeV
VV Semilep [-4.9e+00, 4.9e+00] 35.9 fb^{-1} 13 TeV
Factor of 4.5
0
2000
4000
aQGC Limits @95% C.L. [TeV^{-4}]

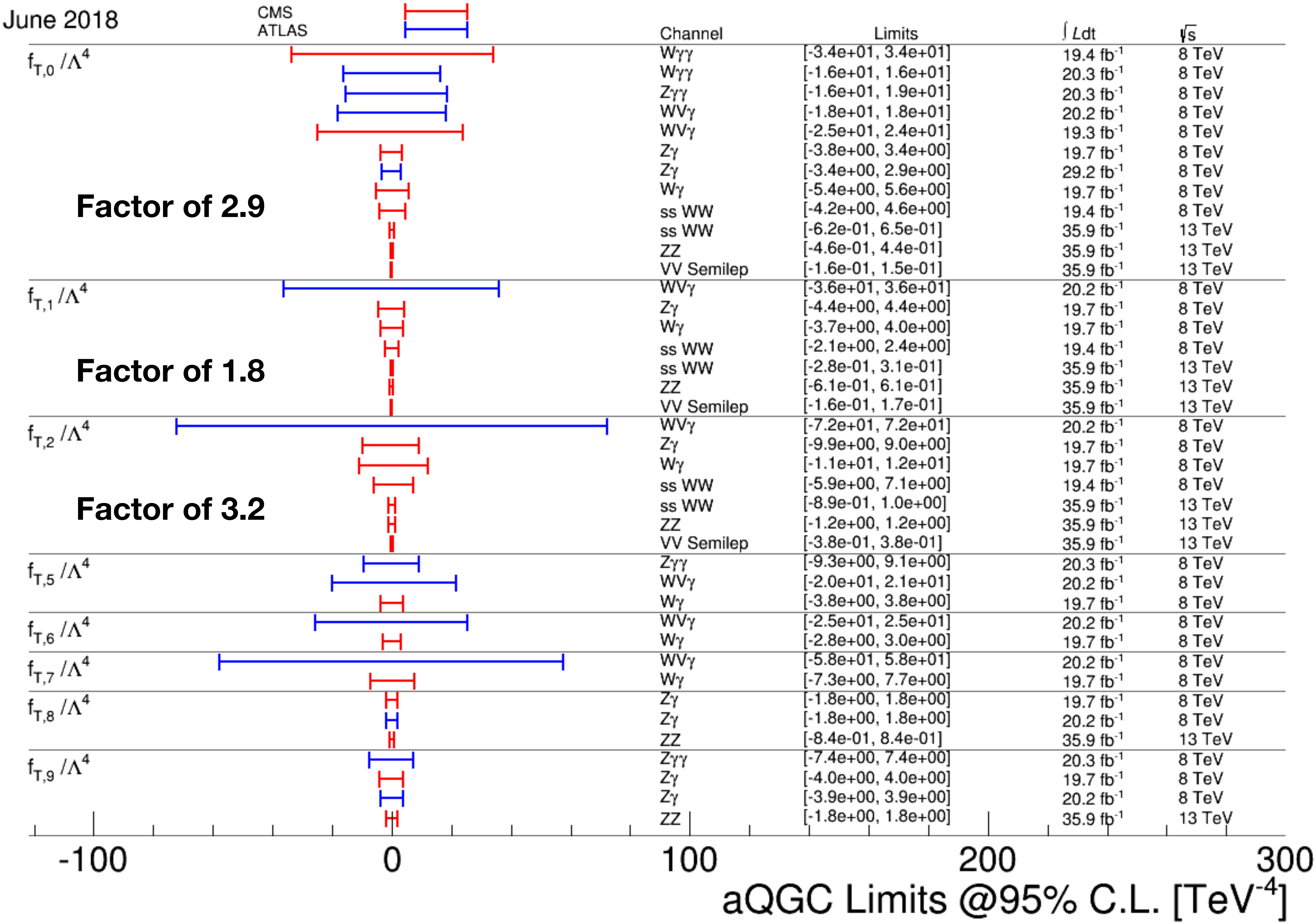

June 2018
CMS
ATLAS
Channel
Limits
∫ Ldt
√s
f_T,0 /Λ^4
Wγγ [-3.4e+01, 3.4e+01] 19.4 fb-1 8 TeV
Wγγ [-1.6e+01, 1.6e+01] 20.3 fb-1 8 TeV
Zγγ [-1.6e+01, 1.9e+01] 20.3 fb-1 8 TeV
WVγ [-1.8e+01, 1.8e+01] 20.2 fb-1 8 TeV
WVγ [-2.5e+01, 2.4e+01] 19.3 fb-1 8 TeV
Zγ [-3.8e+00, 3.4e+00] 19.7 fb-1 8 TeV
Zγ [-3.4e+00, 2.9e+00] 29.2 fb-1 8 TeV
Wγ [-5.4e+00, 5.6e+00] 19.7 fb-1 8 TeV
ss WW [-4.2e+00, 4.6e+00] 19.4 fb-1 8 TeV
ss WW [-6.2e-01, 6.5e-01] 35.9 fb-1 13 TeV
ZZ [-4.6e-01, 4.4e-01] 35.9 fb-1 13 TeV
VV Semilep [-1.6e-01, 1.5e-01] 35.9 fb-1 13 TeV
Factor of 2.9
f_T,1 /Λ^4
WVγ [-3.6e+01, 3.6e+01] 20.2 fb-1 8 TeV
Zγ [-4.4e+00, 4.4e+00] 19.7 fb-1 8 TeV
Wγ [-3.7e+00, 4.0e+00] 19.7 fb-1 8 TeV
ss WW [-2.1e+00, 2.4e+00] 19.4 fb-1 8 TeV
ss WW [-2.8e-01, 3.1e-01] 35.9 fb-1 13 TeV
ZZ [-6.1e-01, 6.1e-01] 35.9 fb-1 13 TeV
VV Semilep [-1.6e-01, 1.7e-01] 35.9 fb-1 13 TeV
Factor of 1.8
f_T,2 /Λ^4
WVγ [-7.2e+01, 7.2e+01] 20.2 fb-1 8 TeV
Zγ [-9.9e+00, 9.0e+00] 19.7 fb-1 8 TeV
Wγ [-1.1e+01, 1.2e+01] 19.7 fb-1 8 TeV
ss WW [-5.9e+00, 7.1e+00] 19.4 fb-1 8 TeV
ss WW [-8.9e-01, 1.0e+00] 35.9 fb-1 13 TeV
ZZ [-1.2e+00, 1.2e+00] 35.9 fb-1 13 TeV
VV Semilep [-3.8e-01, 3.8e-01] 35.9 fb-1 13 TeV
Factor of 3.2
f_T,5 /Λ^4
Zγγ [-9.3e+00, 9.1e+00] 20.3 fb-1 8 TeV
WVγ [-2.0e+01, 2.1e+01] 20.2 fb-1 8 TeV
Wγ [-3.8e+00, 3.8e+00] 19.7 fb-1 8 TeV
f_T,6 /Λ^4
WVγ [-2.5e+01, 2.5e+01] 20.2 fb-1 8 TeV
Wγ [-2.8e+00, 3.0e+00] 19.7 fb-1 8 TeV
f_T,7 /Λ^4
WVγ [-5.8e+01, 5.8e+01] 20.2 fb-1 8 TeV
Wγ [-7.3e+00, 7.7e+00] 19.7 fb-1 8 TeV
f_T,8 /Λ^4
Zγ [-1.8e+00, 1.8e+00] 19.7 fb-1 8 TeV
Zγ [-1.8e+00, 1.8e+00] 20.2 fb-1 8 TeV
ZZ [-8.4e-01, 8.4e-01] 35.9 fb-1 13 TeV
f_T,9 /Λ^4
Zγγ [-7.4e+00, 7.4e+00] 20.3 fb-1 8 TeV
Zγ [-4.0e+00, 4.0e+00] 19.7 fb-1 8 TeV
Zγ [-3.9e+00, 3.9e+00] 20.2 fb-1 8 TeV
ZZ [-1.8e+00, 1.8e+00] 35.9 fb-1 13 TeV
-100
0
100
200
300
aQGC Limits @95% C.L. [TeV-4]

Conclusions

- Analysed both WV and ZV channel for aQGC.
- **Best constraint on 9 parameters for dimension 8 operators.**
- Test beam analysis performed for the GE1/1 detector studied and gave us very good results:
    - Efficiency $\geq$ 98%
    - Time resolution ~5-8ns
    - Space resolution ~200-300μm
- GEM foils produced in India shows very good electrical and optical properties
    - Having $\cong$ 0.13% defects only.

List of Publications

Journal Publication:

- "Development, characterization and qualification of first GEM foils produced in India", Aashaq Shah,...,**Ram Krishna Sharma**,..., Md. Naimuddin, ..., et. al.. In: Nuclear Instruments and Methods in Physics Research Section A: Accelerators, Spectrometers, Detectors and Associated Equipment 892 (2018), pp. 10-17

- "Search for anomalous electroweak production of WW/WZ/ZZ boson pairs in association with two jets in proton-proton collision at 13 TeV", Md. Naimuddin,...,**Ram Krishna Sharma**,..., et.al..
  To be submitted in: Physics Letters B

CMS Analysis Note:

- "Search for anomalous electroweak production of WW/WZ/ZZ boson pairs in association with two jets in proton-proton collision at 13 TeV", Md. Naimud- din,..., **Ram Krishna Sharma**, ...et. al. CMS Analysis Note-2017/236

CMS Detector Note:

- "Test beam studies of Gas Electron Multiplier (GEM) detectors for the upgrade of CMS endcap muon system", Md. Naimuddin,..., **Ram Krishna Sharma**, ...et. al. CMS Detector Note-16/017.

Conference Proceedings/Poster Presentations

- "Test Beam Study of Gas Electron Multiplier (GEM) Detectors for the Upgrade of CMS Endcap Muon System", **Ram Krishna Sharma**.
  Talk presented at the **XXII DAE High Energy Physics Symposium**, held at University of Delhi, India, December 12-16, 2016.

- "Charged particle detection performance of Gas Electron Multiplier (GEM) detectors for the upgrade of CMS endcap muon system at the CERN LHC", **Ram Krishna Sharma**.
  Poster presented at the **2015 IEEE Nuclear Science Symposium and Medical Imaging Conference (NSS/MIC)**, held at Town and Country Hotel, San Diego, California, USA, 31 October-7 November 2015.


Thank You...

LHC

EHEP Instruments

Accelerator

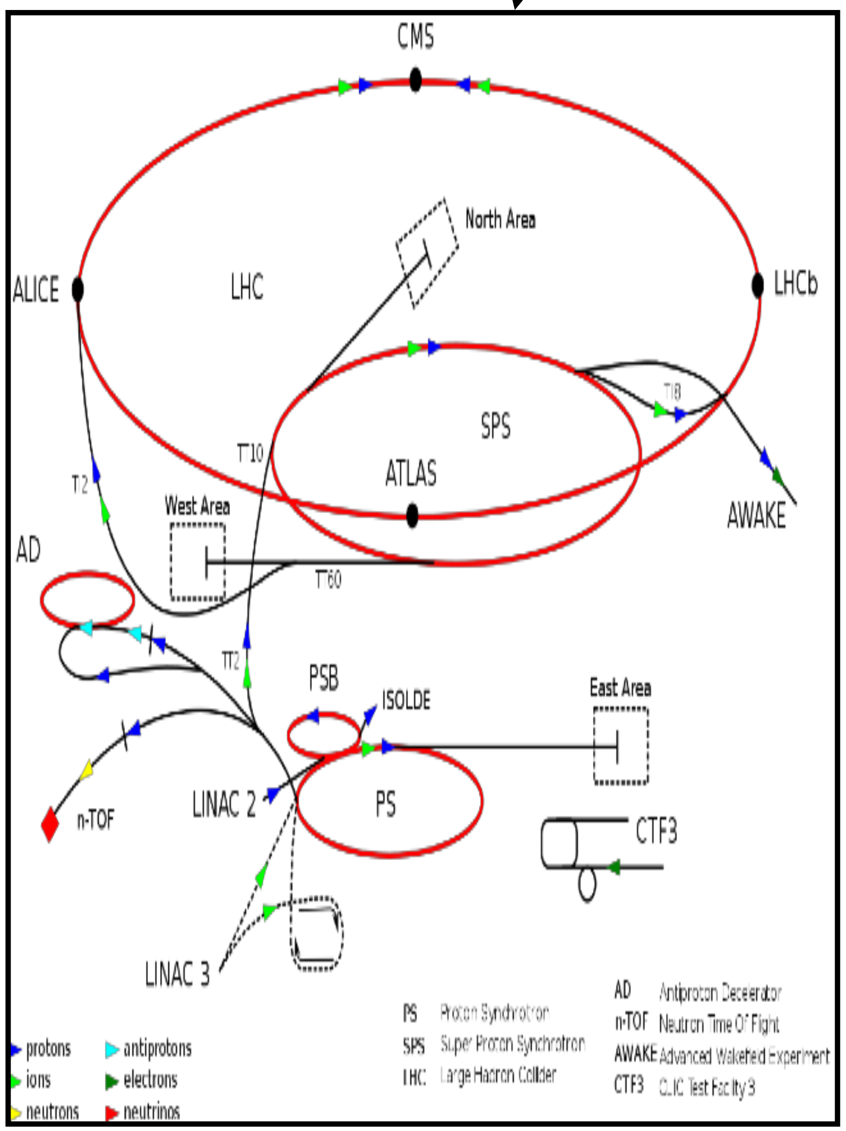

Multipurpose Detector

The particles that reach Detector are

$e^{\pm}, \mu^{\pm}, \gamma, \pi^{\pm}, k^{\pm}, p, n, k_L \text{ and } k_S$

Muon System

Electromagnetic Interaction → **Electromagnetic Calorimeter**

Strong interaction → **Hadronic Calorimeter**

Apart form above listed sub-detector:One need a detector that don't do the destructive measurement and help us to reconstruct the collision point (i.e. vertex)

Other Experiments at LHC Accelerating Chain

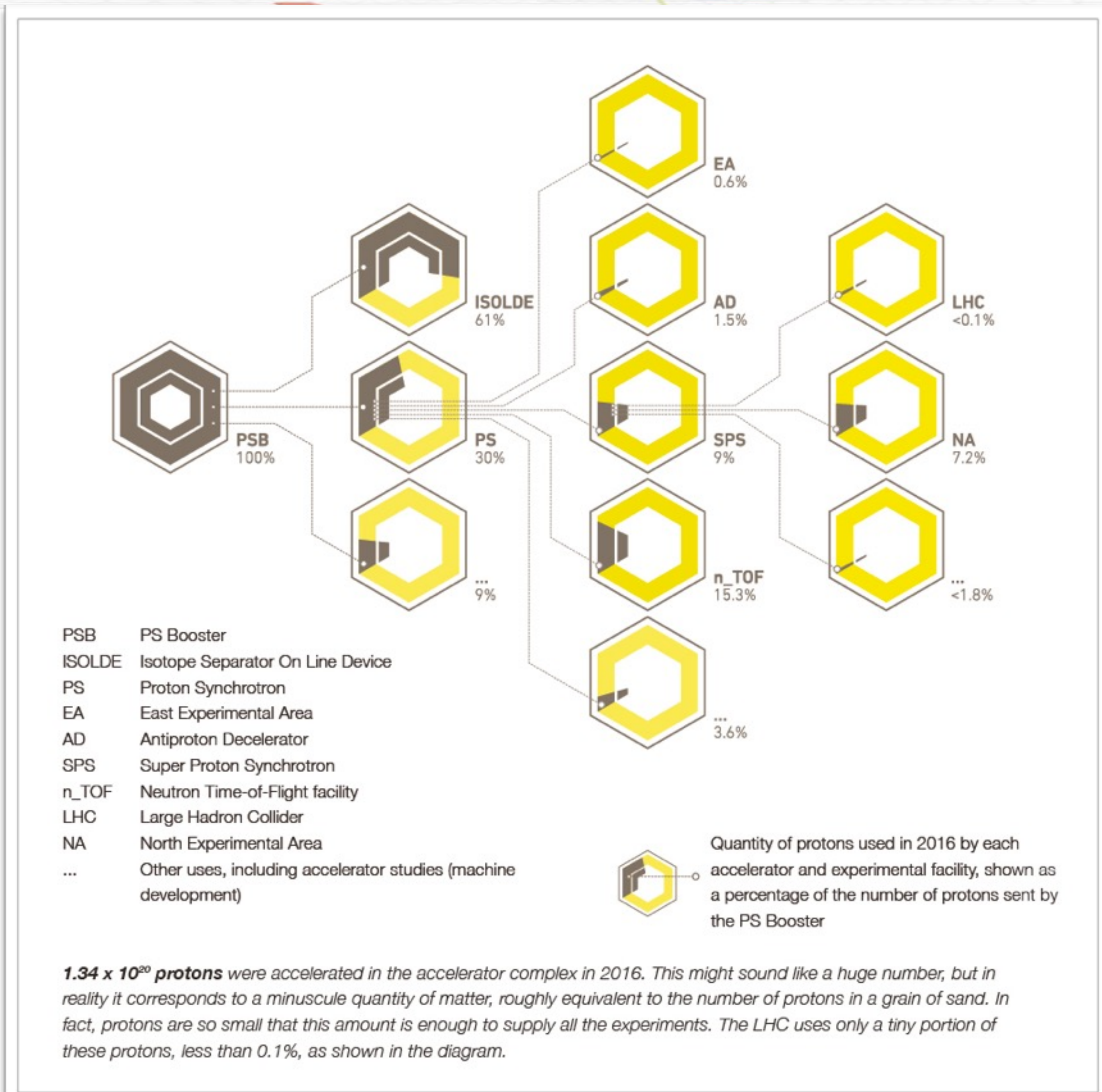

Backgrounds at LHC

Background sources:

1. Particles originating from cascade by the proton-proton collisions.

2. Particle entering the detector from accelerator.

    1. Generated by the interaction of upstream collimators: (known as beam-halo).

    2. Interaction by the residual gas molecules inside the vacuum pipe.

CMS

CMS Coordinate System

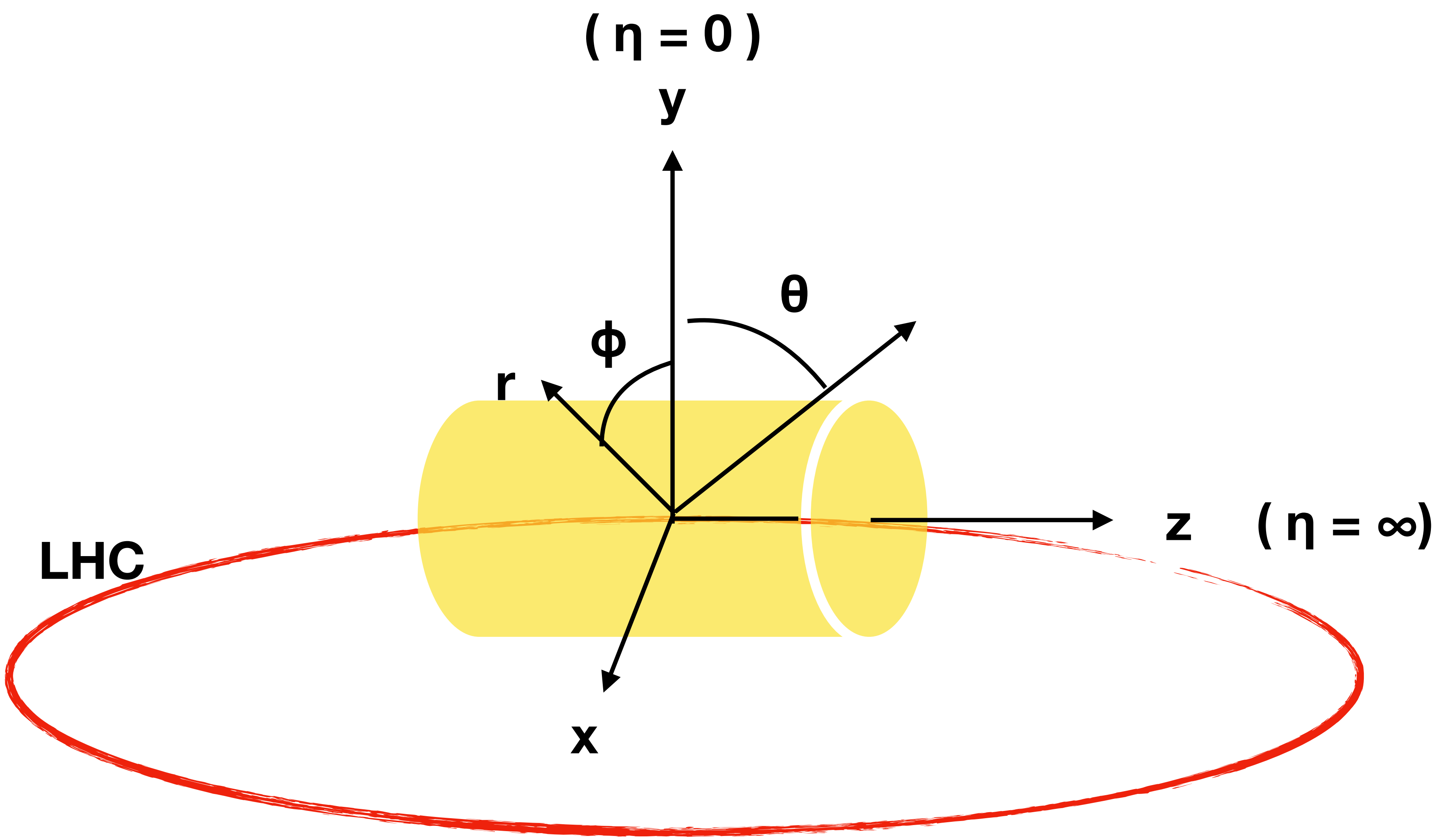

CMS

- Length = 28.7 m
- Diameter = 15 m
- Weight = ~14 kTonnes
    - 12.5 kTonnes = steel return yoke
- CMS detector was constructed in 15 sections at ground level before lowered into an underground cavern.

CMS Magnet

- Inner diameter = 6 meter
- Length = 12.5 m
- Magnetic field = 3.8 Tesla
    - Earth magnetic field at surface = 25-65 Tesla
= 0.25-0.65 gauss
- Stored energy = 2.6 GJ
- Weight of yoke = 12.5 kTonnes
    - Consists of 5 wheel and 2 endcap
- Niobium titanium coil carries 18000 A current

ECAL

- Lead tungstate ($PbW0_4$) crystal (0.8903 cm radiation length)
- Coverage : $|\eta|<3.0$
- Detection of scintillation light
    - Avalanche Photo Diode (APD) in barrel
    - Vacuum Photo Triodes (VPT) in endcap
- Pre-shower installed in front of ECAL for π^0 rejection
- Thickness : 25 radiation length

Lead Tungstate Properties

Quantity	Value	Units	Value	Units
<Z/A>	0.41315			
Density	8.30	g cm^{-3}		
Mean excitation energy	600.7	eV		
Minimum ionization	1.229	MeV g^{-1}cm^{2}	10.20	MeV cm^{-1}
Nuclear collision length	100.6	g cm^{-2}	12.12	cm
Nuclear interaction length	168.3	g cm^{-2}	20.27	cm
Pion collision length	126.2	g cm^{-2}	15.21	cm
Pion interaction length	199.5	g cm^{-2}	24.04	cm
Radiation length	7.39	g cm^{-2}	0.8903	cm
Critical energy	9.64	MeV (for e^-)	9.31	MeV (for e^+)
Molière radius	16.26	g cm^{-2}	1.959	cm
Plasma energy $\hbar\omega_p$	53.36	eV		
Muon critical energy	170.	GeV		
Melting point	1396.	K	1123.	C
Index of refraction (@ STP, Na D)	2.20			

Composition:

Elem	Z	Atomic frac*	Mass frac*
Pb	82	1.00	0.455347
W	74	1.00	0.404011
O	8	4.00	0.140462

* calculated from mass fraction data.

HCAL

- Brass/scintillator sampling calorimeter
- Coverage : $|\eta|<3.0$
- Scintillation light is converted by wavelength shifting (WLS) fibres embedded in scintillator tiles and channeled to photodetectors via clear fibres.
- "*Tail-catcher*" is added in barrel region (HO) to ensure hadronic showers are sampled with nearly 11 hadronic interaction lengths.
- To increase coverage of $|\eta|<5.0$ a iron/quartz fibre calorimeter is added to ensure the full geometric coverage for the measurement of transverse energy in the event.
- Thickness : 7-11 interaction length depending on η.
    - 10-15 interaction length with HO included.

GEM

Gain Vs Outer Hole Diameter

NIM-A 438.2-3 (1999), pp. 376–408

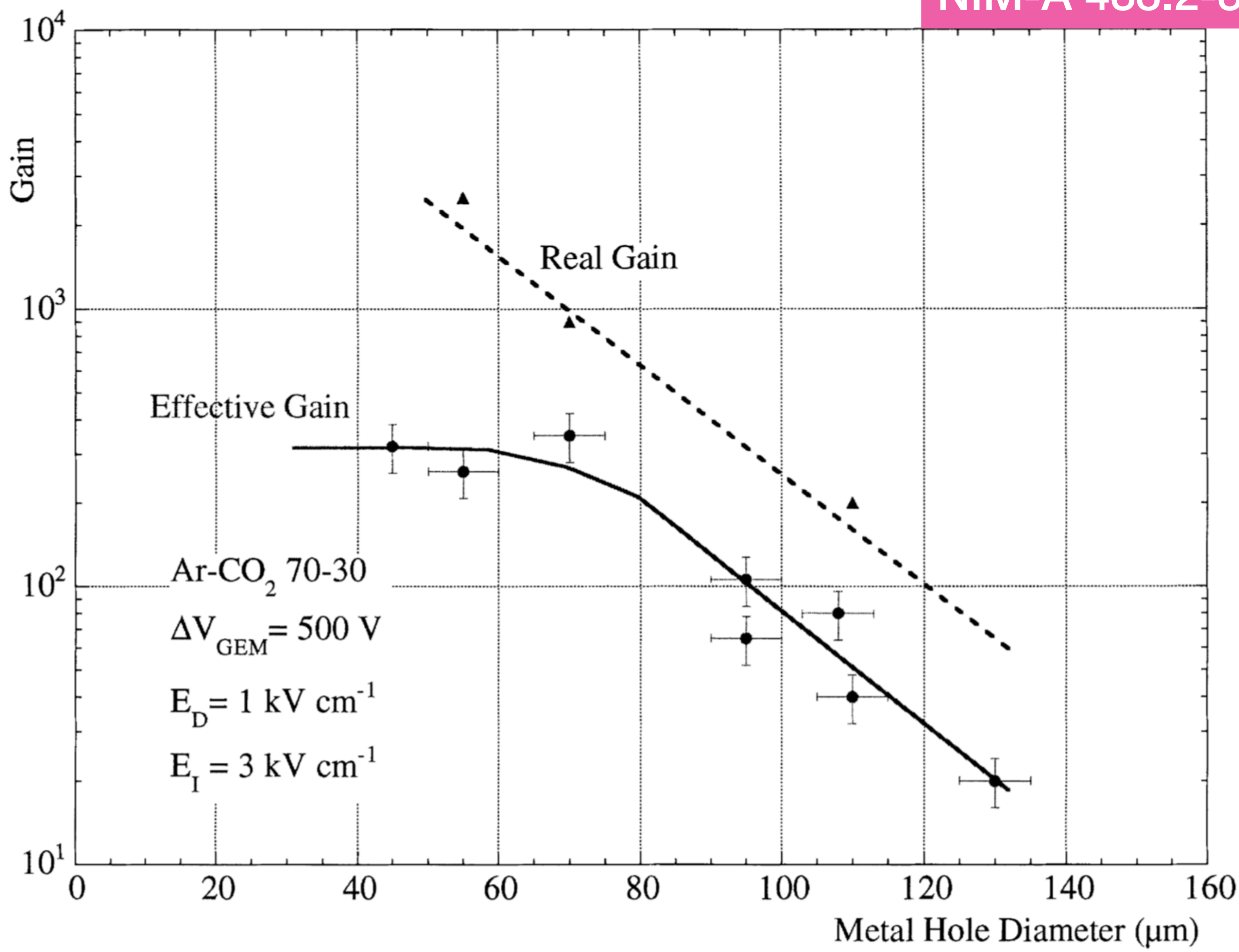

Real gain and effective gain variation with GEM hole diameter having a foil thickness of 60 μm (= 50 μm + 5μm + 5 μm). As the hole diameter decreases, the effective gain increases till 70 μm and after that it reaches saturation. This is due to loss of generated electrons in the avalanche to the bottom of the GEM electrode when hole diameter is reduced below the foil thickness.

CMS Forward Muon System

- Originally CMS muon system is designed with high redundancy
  - Resistive plate chamber (RPC) extended upto |η| = 2.4
  - However, at the time of construction CMS RPCs were not validated for rates in forward region
- For all of Run 1 & Run 2, Cathode Strip Chambers (CSC) provided muon triggers at |η| > 1.6
- CSC system was pushed to performance limit during Run I & Run II
- Muon Bremsstrahlung and large neutron backgrounds (at high instantaneous luminosity) became a problem
- Solution to handle increased pile-up, particle rate, and backgrounds is to provide the original redundancy CMS was designed with!!

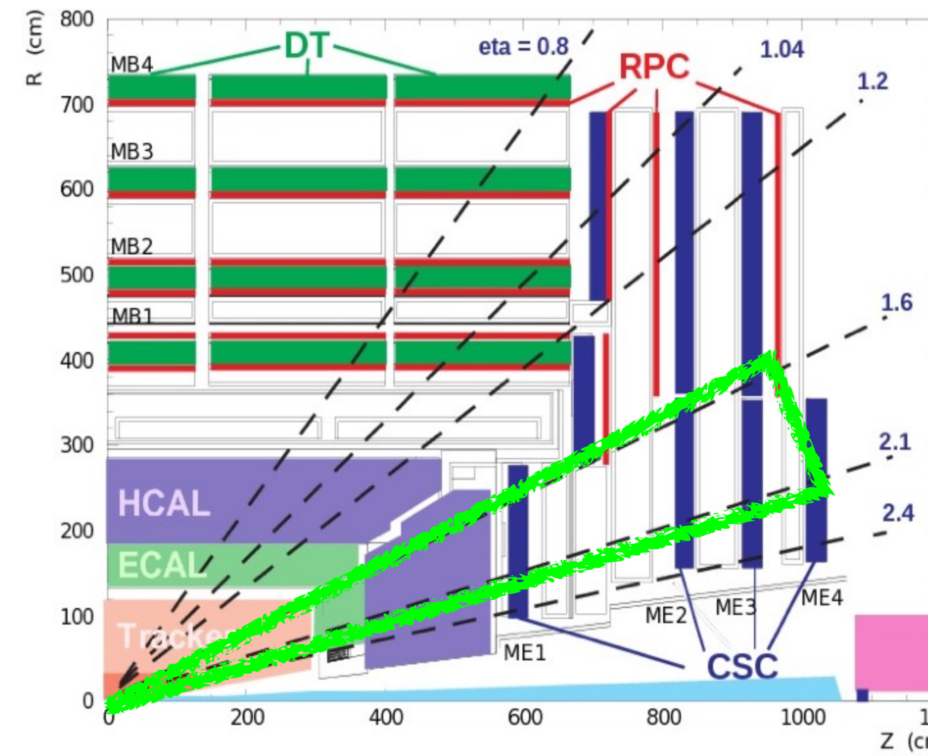

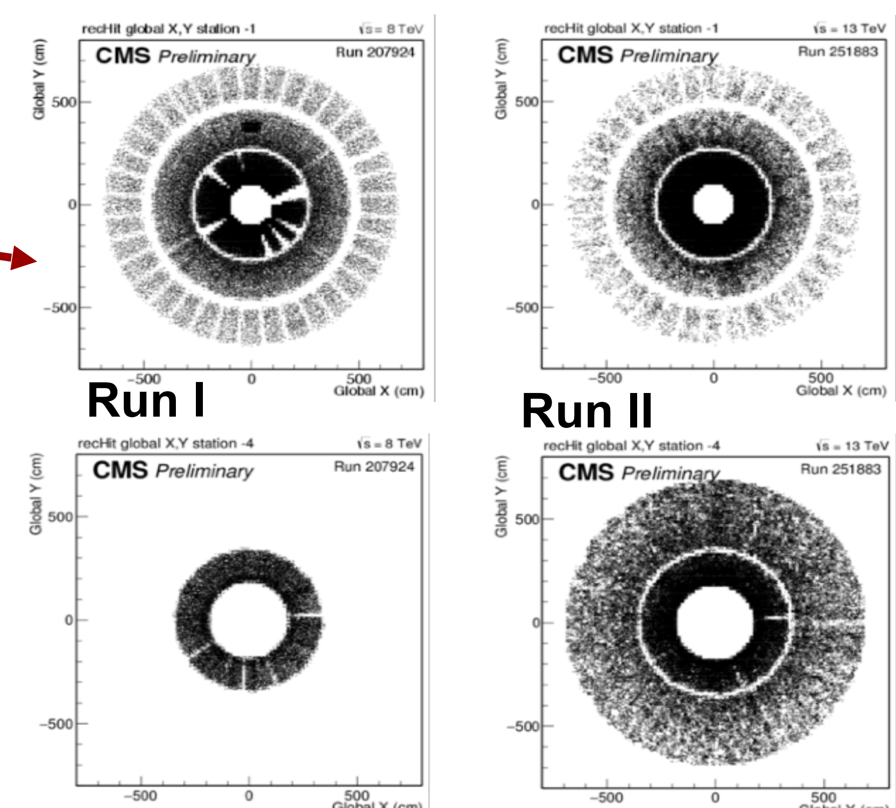

Ref: arxiv:1510.08908

Most promising for Forward Muon Upgrade : Gas Electron Multiplier (GEM)

Physics Motivation For Muon System Upgrade (1/ 2)

Impact On Trigger:

- Reduce trigger rate in high η region which is currently suffering from highest background rates and a non-uniform magnetic field.
- Allow us to keep low p_T muons
- Improves measurement of bending angle using the combination of GEM+CSC.

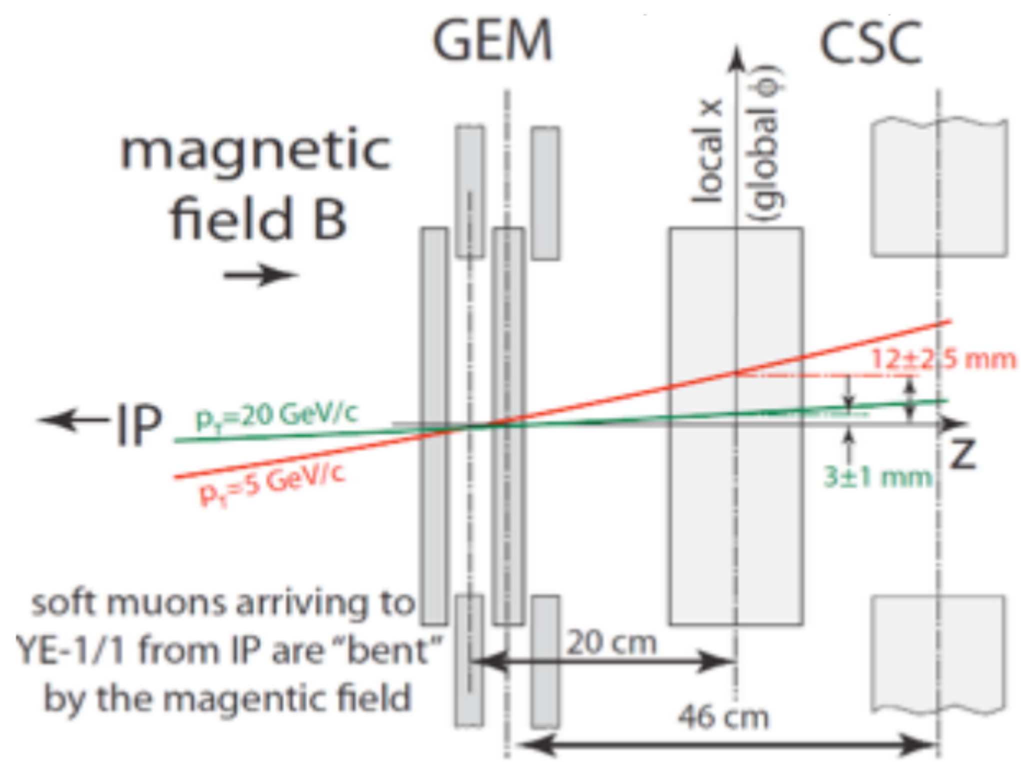

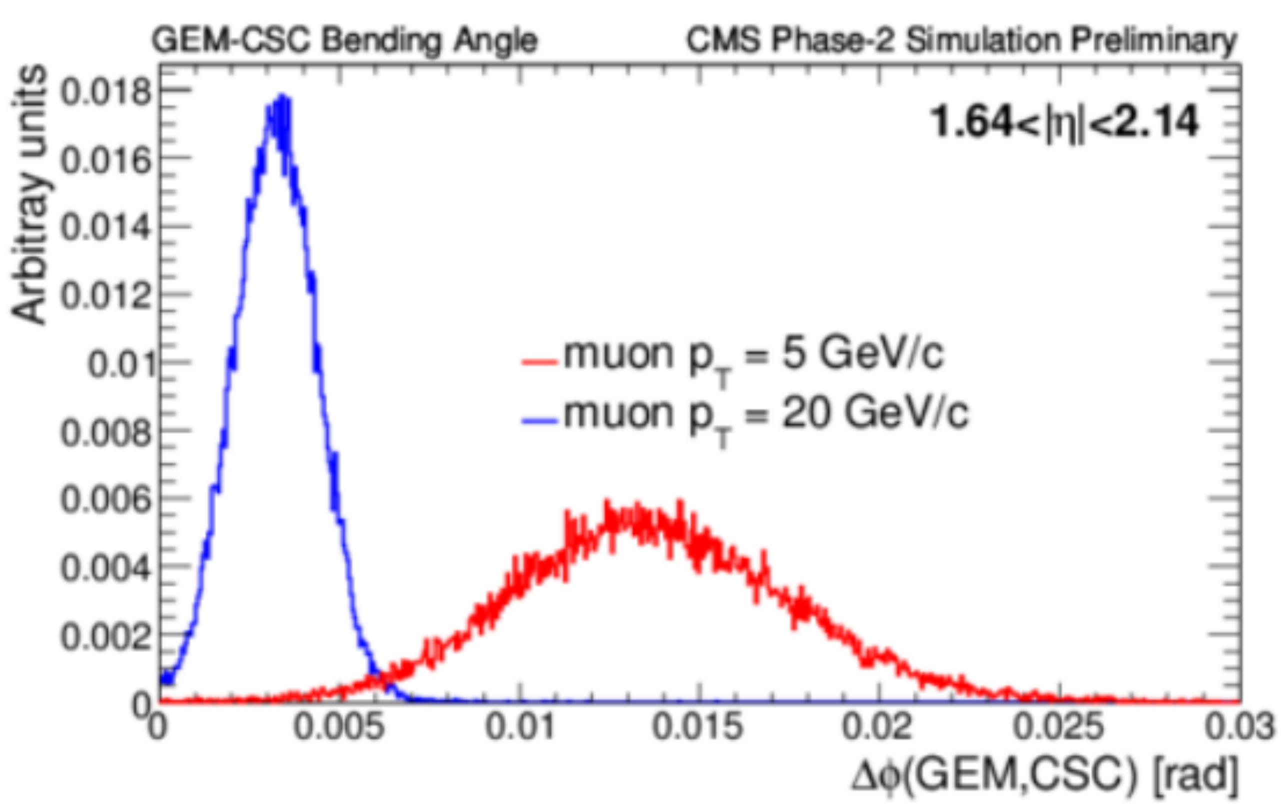

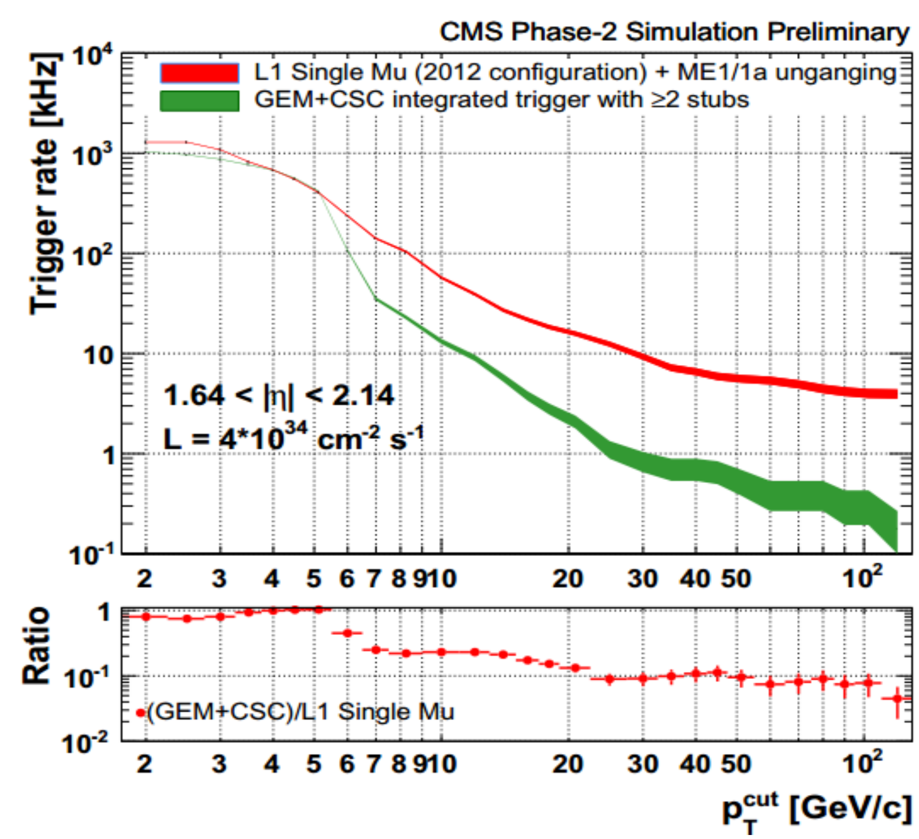

Micropack GEM

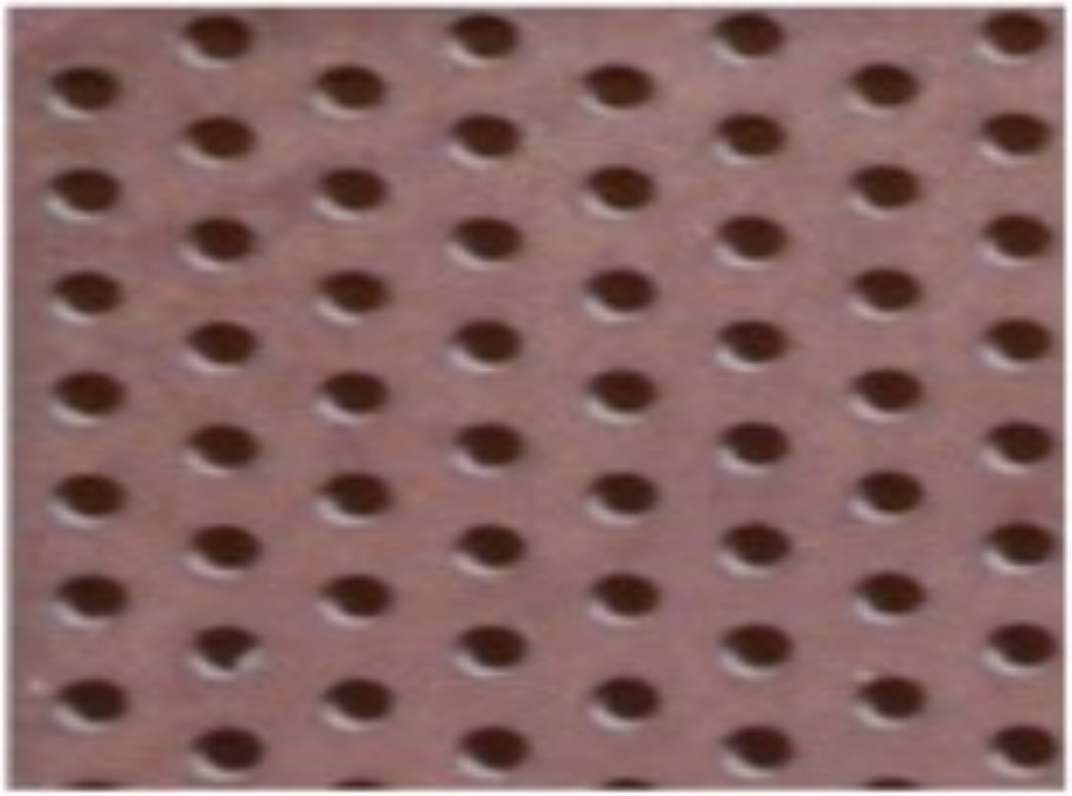

Close view of the Micropack Foil

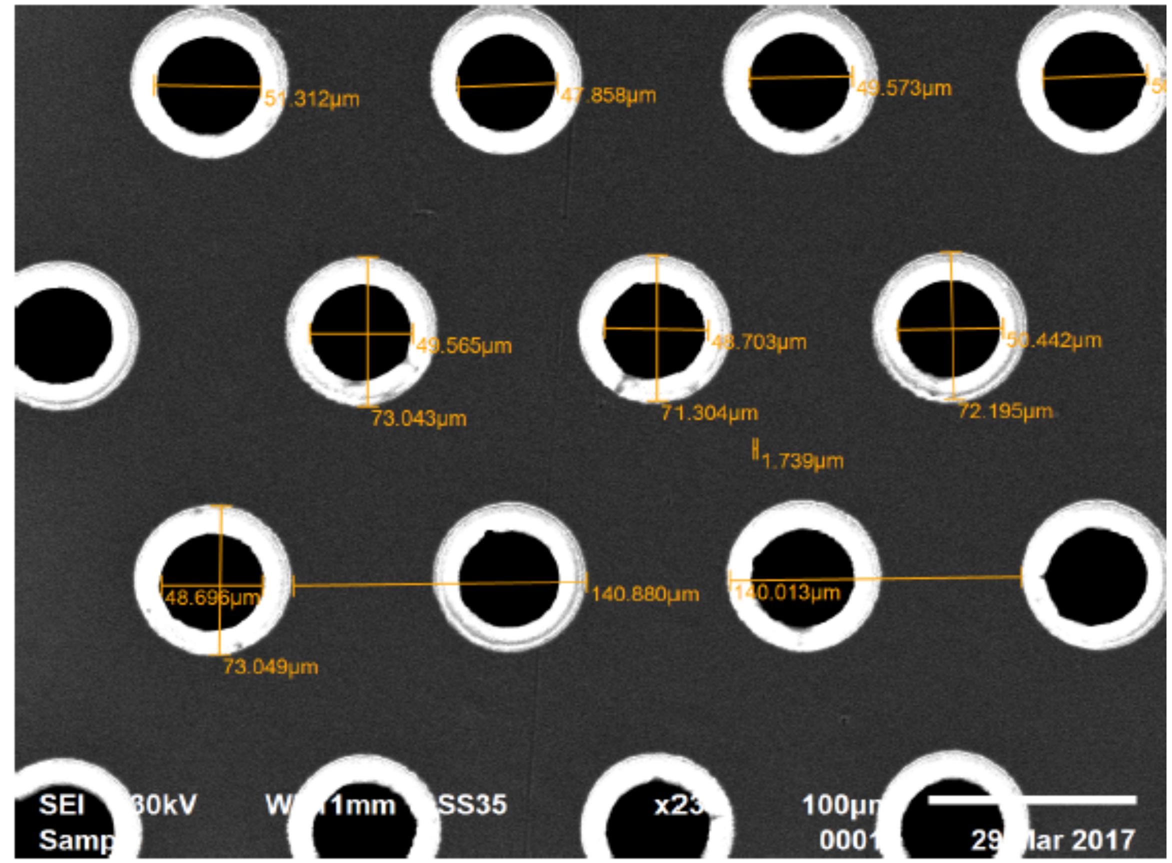

SEM Image Taken at DU

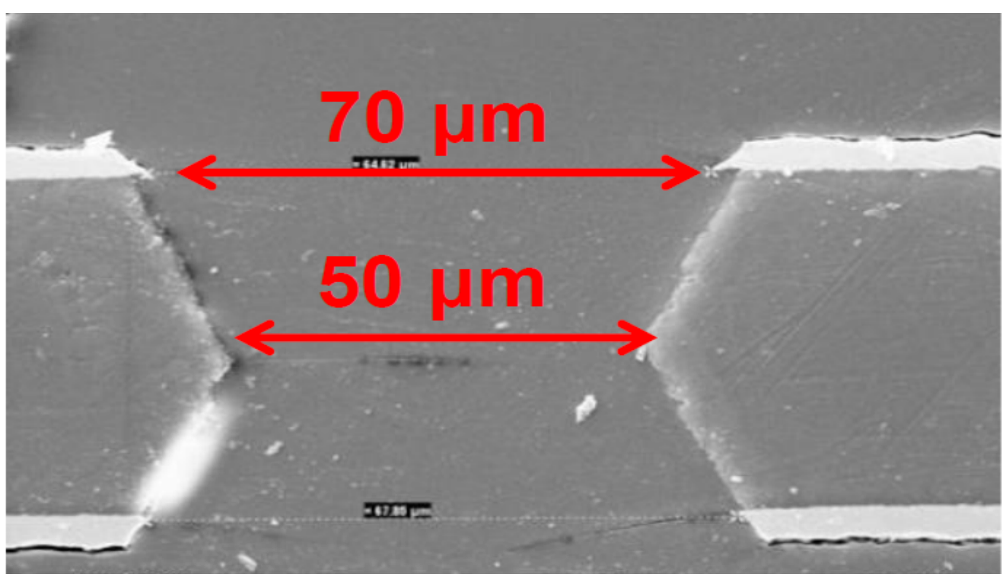

Cross-Sectional view for Double Conical GEM

- Its hard to study 600,000 holes manually for each Foil
- Each Sector were further divided into 9 subsectors
- Processed each subsector's image through MATLAB Image Processing Tool
- Obtained data were plotted in ROOT

Comparison of Single, Double, & Triple GEM

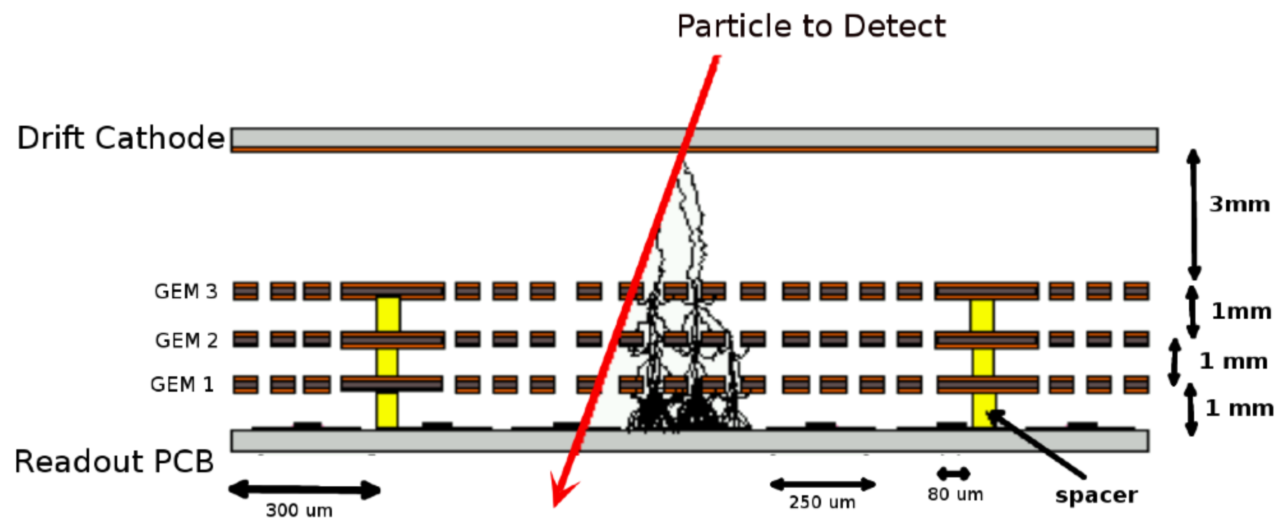

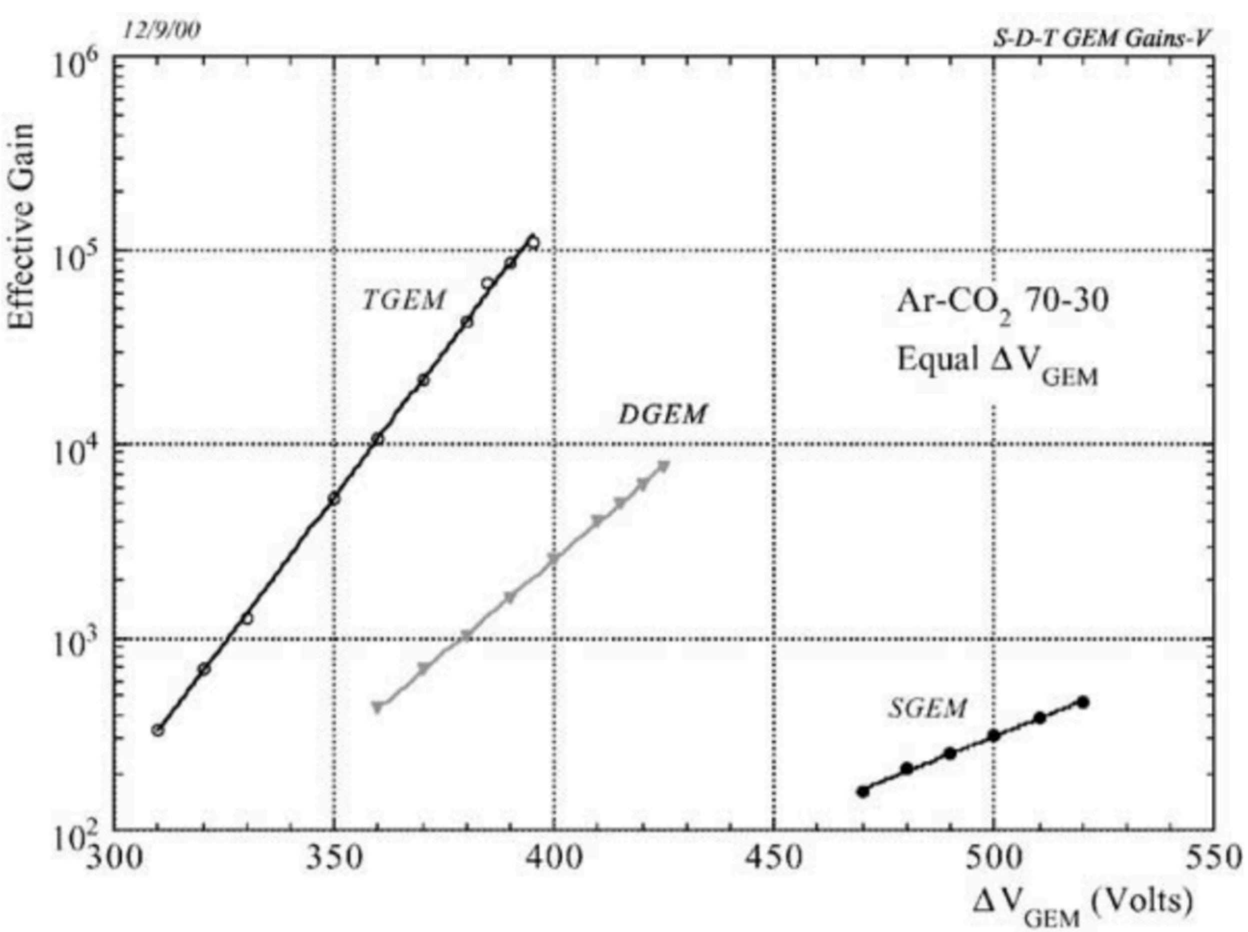

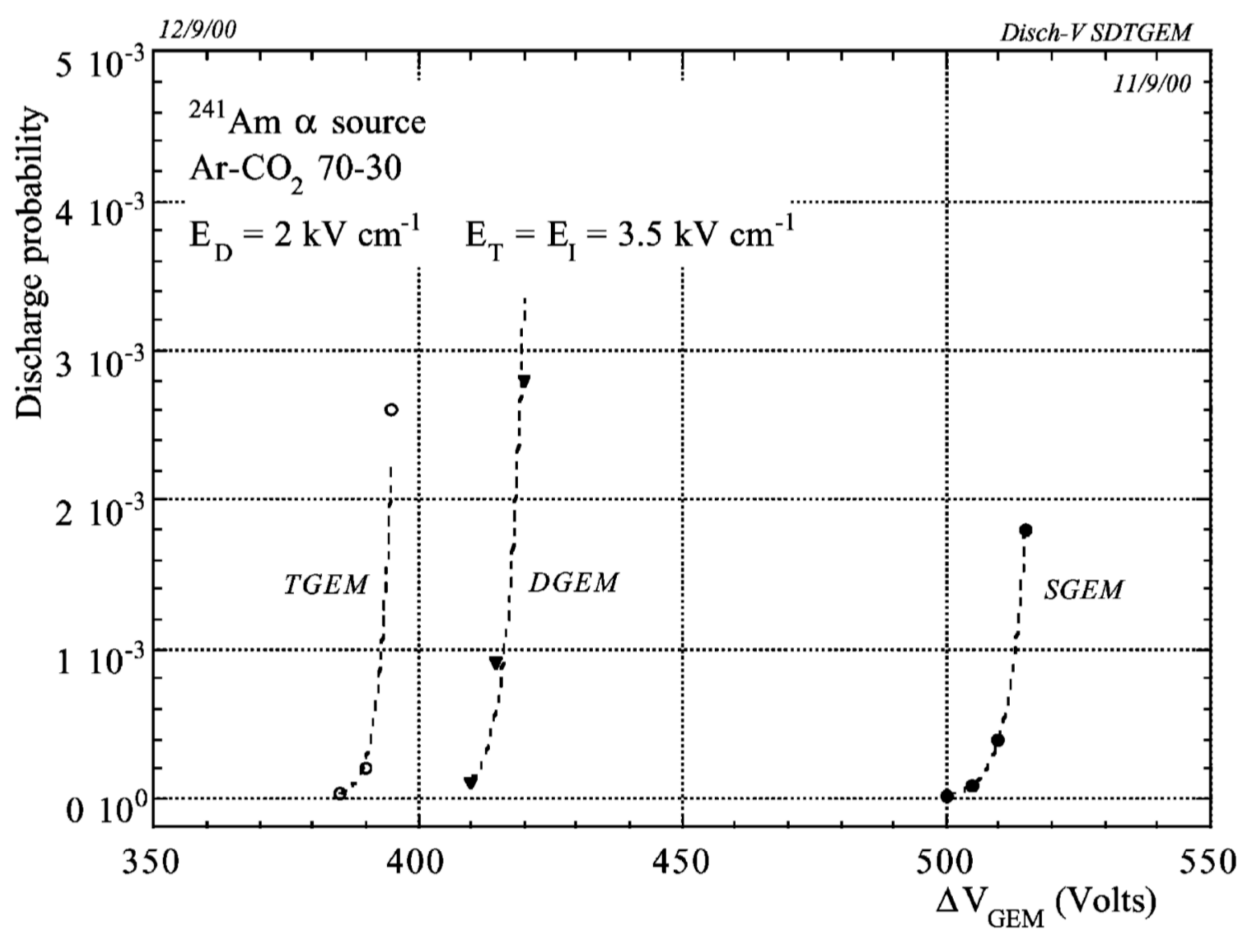

What is GEM?

- Gas electron multiplier (GEM) is a micro-patterned gaseous detector.

- CMS GEM configuration is a triple-GEM detector, i.e. it contains 3 GEM foils, as shown in image.

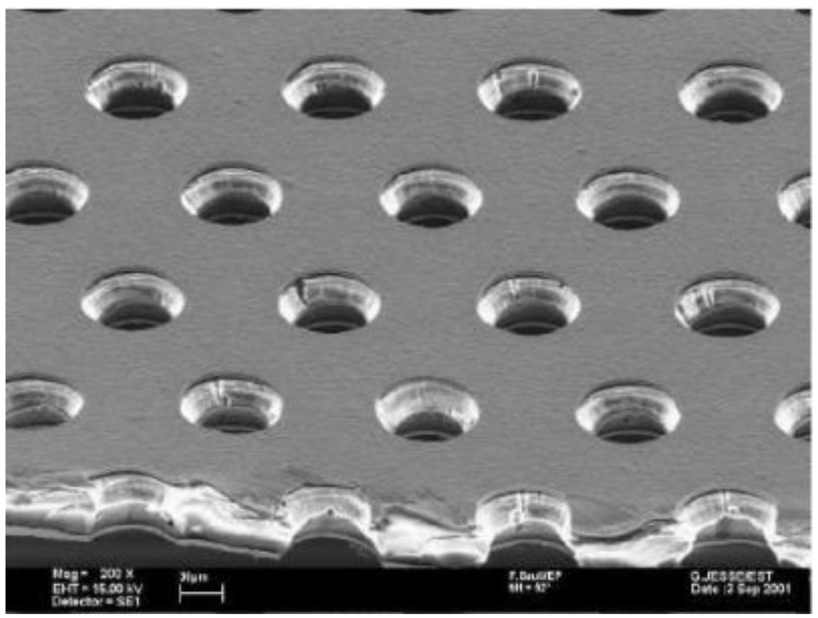

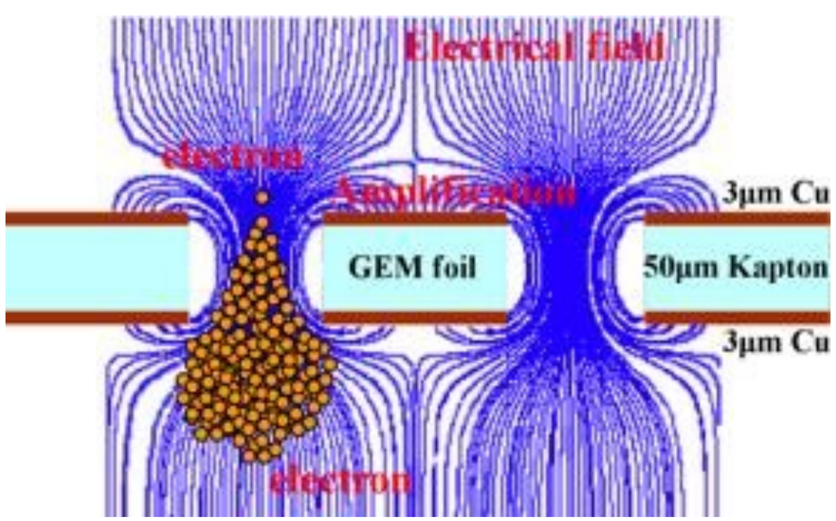

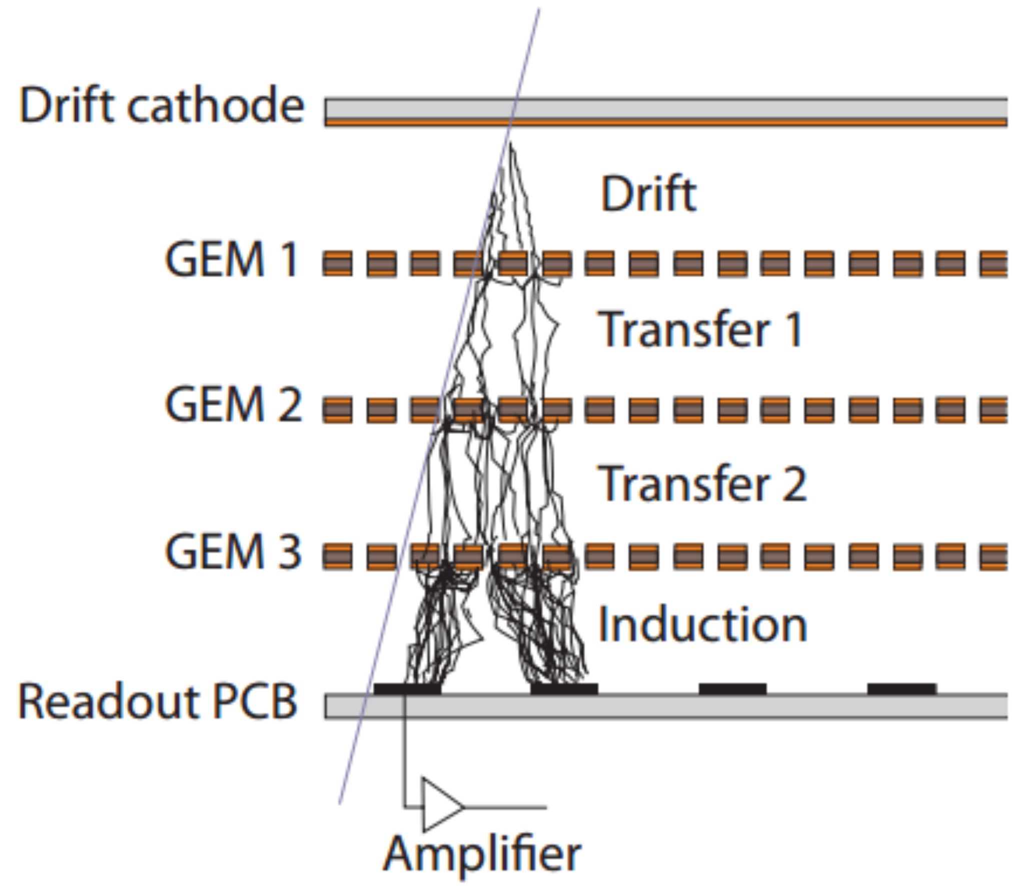

Figure: Cascade of three GEM foil

Why 3 GEM foil?

- Gain = 20x20x20 ~ 8000
- Reduce discharge probability

GE1/1 Generations

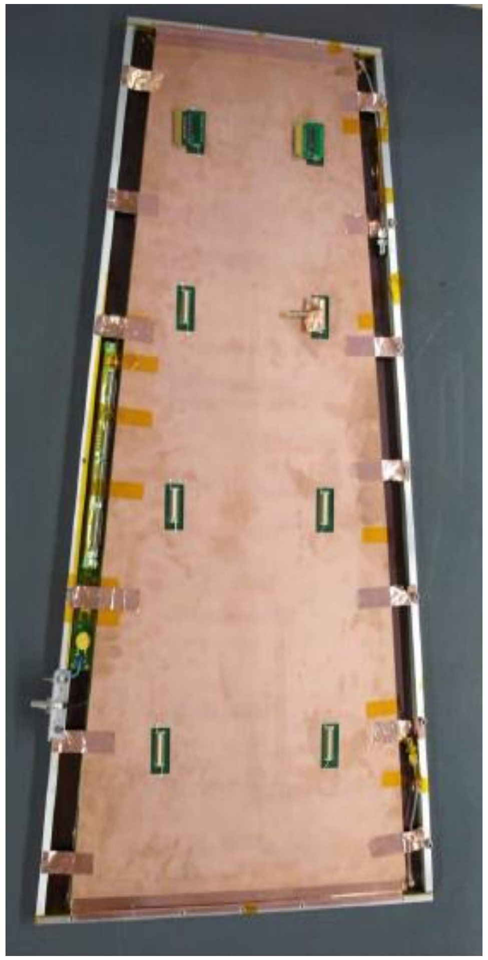

GE1/1- I (2010)

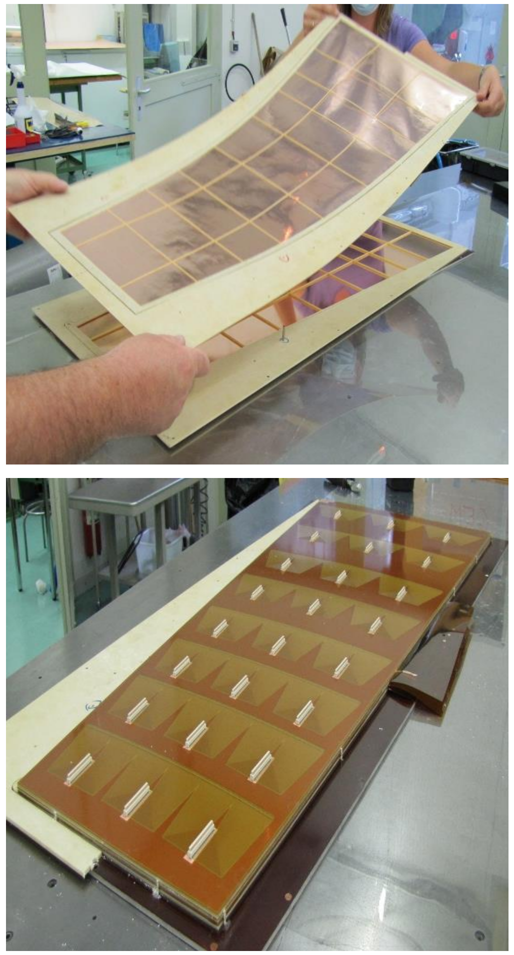

GE1/1- II (2011)

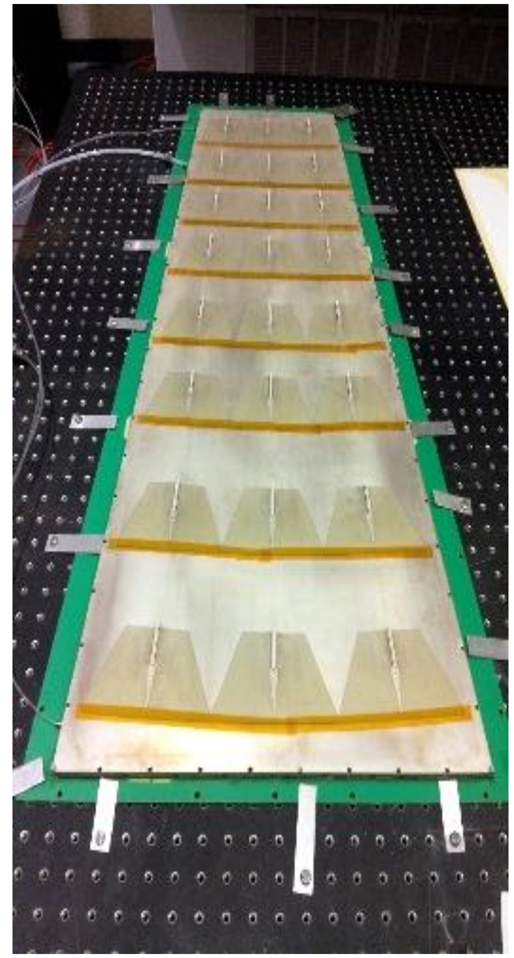

GE1/1- III (2012)

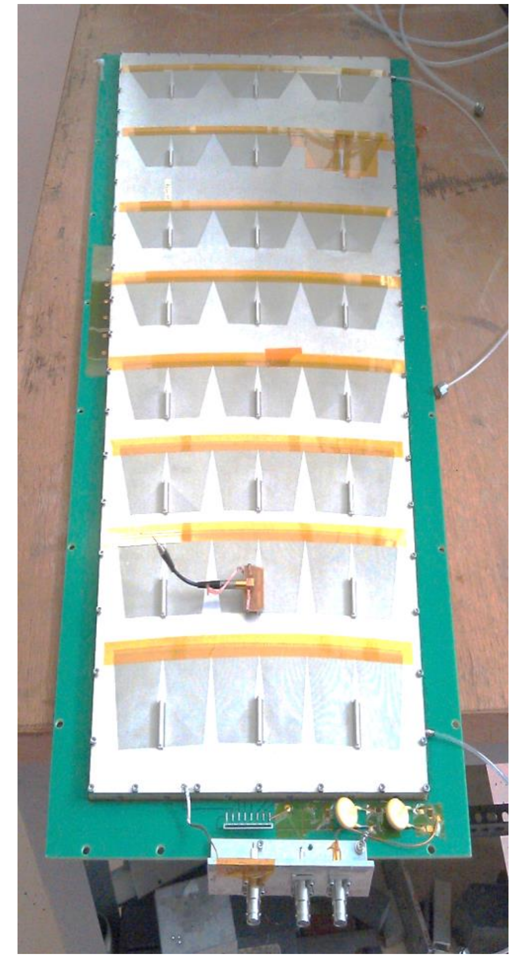

GE1/1- IV (2013)

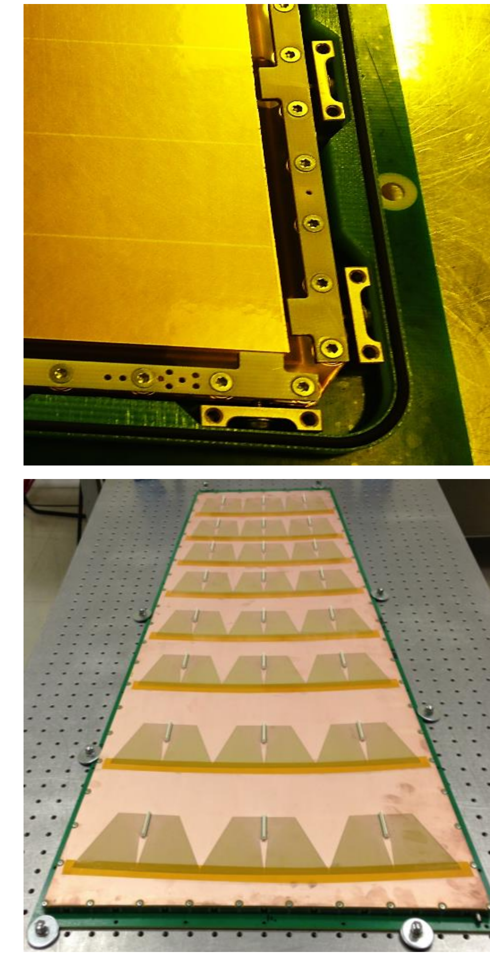

GE1/1-V-short (2014)

The cluster size is greater in (η,ϕ) = (5,2) region for both the detectors due to the uniformity in readouts channels.The GE1/1 4th generation prototype used suffered from the significant bending in the readout and drift PCB. This affects GE1/1 properties like primary charge created, uniformity, transparency of bottom of third GEM foil, charge collection by the readout, etc. Thus, it is expected that non-uniformity in the cluster size distribution in (η,ϕ) sector (1,2), (5,2), and (8,2) is a consequence of this. This issue is improved in the next version of GE1/1 prototype known as GE1/1-V.

Physics Analysis

SM: Electroweak gauge boson self-interaction

- Non-abelian nature of electroweak interaction allows the self-coupling between gauge bosons.

- **Triple-gauge couplings (TGC)**

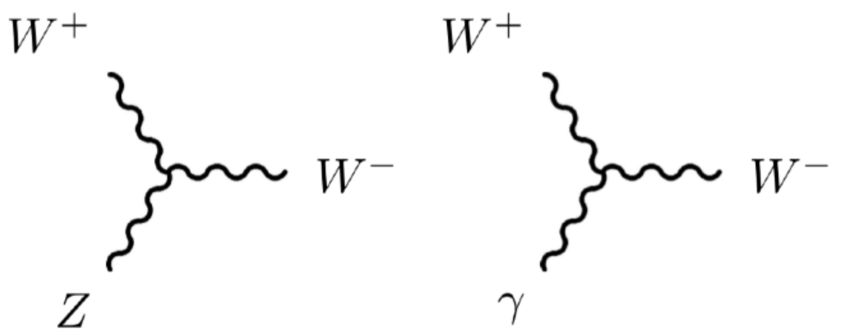

- **Quartic gauge couplings (QGC)**

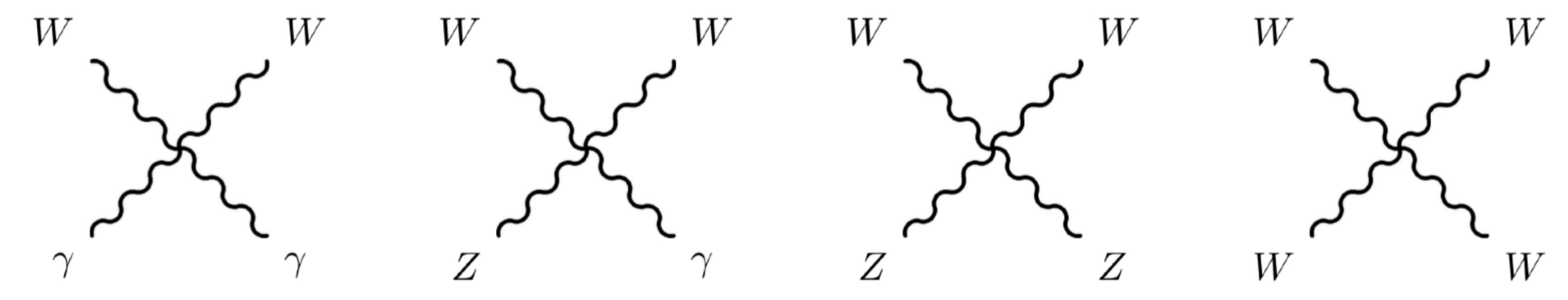

- **No neutral self-couplings**

6 Fermions Final State at α_{EW}^{6}

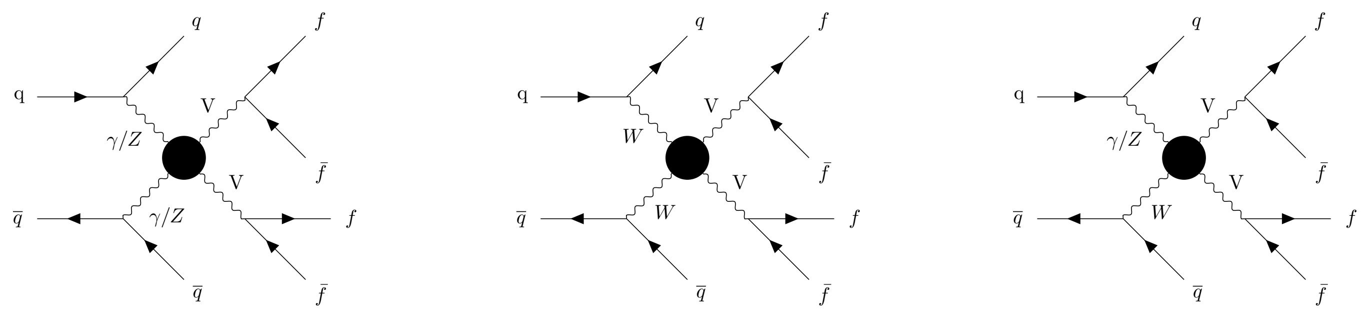

VV fusion

Higgs

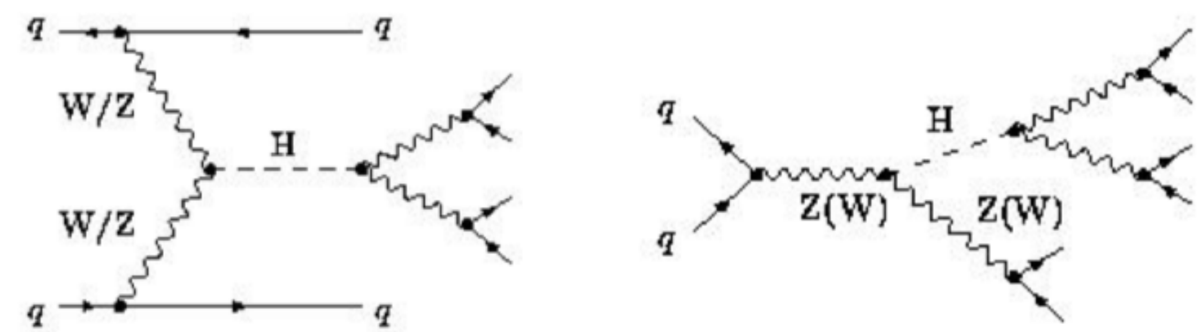

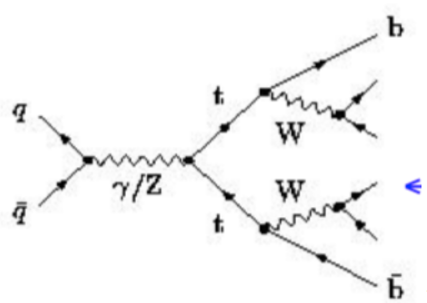

Top-top (EW)

TGC & QGC

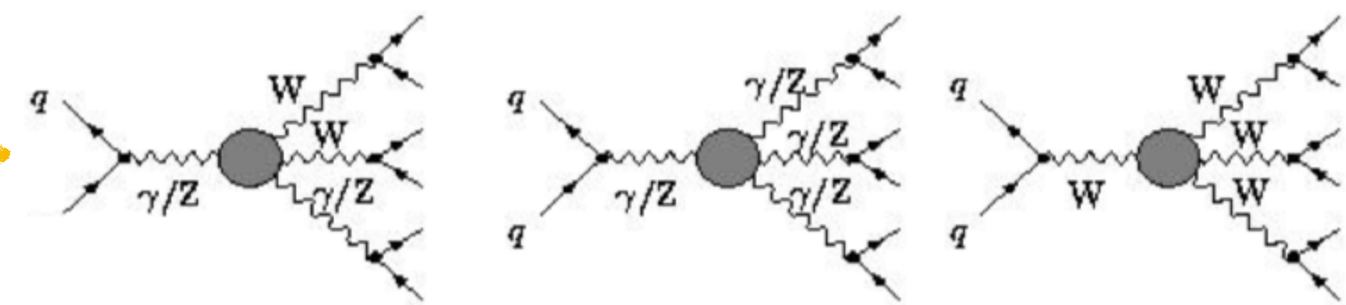

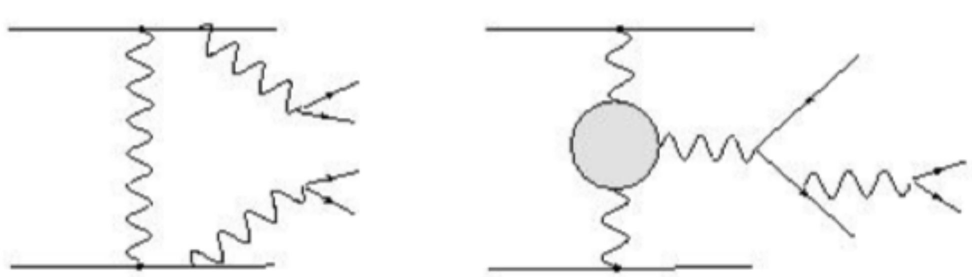

VV and non-resonant

And $\alpha_s^2\,\alpha_{EW}^4$

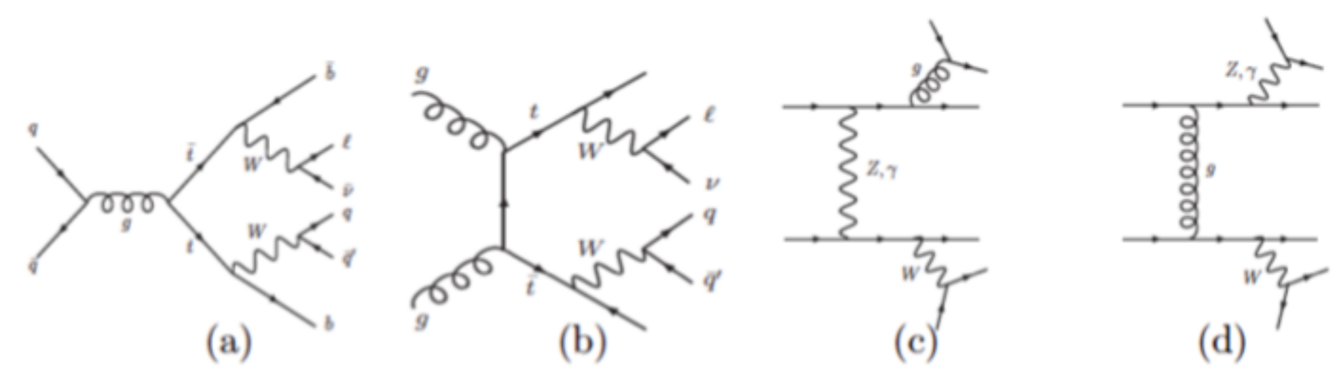

Neutrino $p_{\nu z}$ calculation

(To reconstruct leptonic W-boson invariant mass)

$$p_{\nu z} = \frac{1}{2 \times A}[-b \pm \sqrt{b^2 - 4 \times A \times C}]$$

Where,

$$A = 4(E_l^2 - p_{lz}^2)$$

$$b = -4ap_{lz}$$

$$C = 4E_l^2 p_{\nu T}^2 - a^2$$

$$a = M_w^2 - M_l^2 + 2(p_{lx}p_{\nu x} + p_{ly}p_{\nu y})$$

Full calculation: link

- Picked solution which is closest to lepton p_z.
- If roots are complex then take real part.

Green Color => Expected solution (Closest to truth)					
Truth	Two solution of Quadratic Equation		type0	type2	Expected soultion
	Sol1	Sol2			
-46.9578	-44.3851	356.671	-44.3851	-44.3851	-44.3851
-191.942	-73.9132	-151.143	-73.9132	-73.9132	-151.143
22.3573	21.8648	-65.1082	21.8648	21.8648	21.8648
-303.521	-9.42494	-302.584	-9.42494	-9.42494	-302.584
-16.178	-322.663	-17.0433	-322.663	-17.0433	-17.0433
67.6159	66.1042	612.37	66.1042	66.1042	66.1042
4.17889	10.4376	-2.88399	10.4376	-2.88399	10.4376
-15.4736	-13.8728	-195.284	-13.8728	-13.8728	-13.8728
69.4457	19.0206	19.0206	19.0206	19.0206	19.0206
62.0216	26.9113	83.577	26.9113	26.9113	83.577
-99.9548	-345.875	-101.363	-345.875	-101.363	-101.363
-413.859	-97.7227	-412.187	-97.7227	-97.7227	-412.187
-5.3027	-54.0724	-5.91689	-54.0724	-5.91689	-5.91689
32.2772	27.1372	129.69	27.1372	27.1372	27.1372
-152.767	-152.604	-46.7698	-152.604	-46.7698	-152.604
74.2368	54.4799	82.3299	54.4799	54.4799	82.3299
-349.738	-348.888	-1240.64	-348.888	-348.888	-348.888
497.871	499.738	1918.88	499.738	499.738	499.738
41.7177	45.963	371.922	45.963	45.963	45.963
-57.2105	-59.9833	24.8473	-59.9833	24.8473	-59.9833
-150.235	-154.518	-226.908	-154.518	-154.518	-154.518
19.3429	25.8074	-82.0508	25.8074	25.8074	25.8074
-432.564	-430.914	-1714.05	-430.914	-430.914	-430.914
-73.6094	-73.7716	254.694	-73.7716	-73.7716	-73.7716
-59.3917	-58.8027	159.863	-58.8027	-58.8027	-58.8027
-221.099	-150.217	-193.318	-150.217	-150.217	-193.318

Object Selection

- Electron (Muon) Selection
  - Cut based tight ID
  - pT > 30 GeV, |η| < 2.4 (2.5),
  - Loose lepton veto for 3rd lepton; p_T > 20 GeV
  - Muons: trkIso/p_T < 0.1
- Selected type-1 pfMET
- Hadronic V-jet (Puppi jets are selected):
  - 40 GeV < Softdrop mass < 150 GeV, pt>200 GeV, |η| < 2.4
  - |ΔR(AK8jet, lepton) | > 1.0
  - AK8 jet Closest to W-boson mass
- VBF jets (AK4 jets):
  - pT > 30 GeV, Mjj > 500 GeV
  - |ΔR(AK4jet, lepton) | > 0.3
  - |ΔR(AK8jet, AK4jet) | > 0.8
  - Cut based loose ID
  - Select highest mjj pair
- B-tag AK4 jets:
  - Loose CSVv2
  - pT > 30 GeV, |η| < 2.4

Boson Centrality (Phys. Rev. D 95, 032001)

$$\xi_V = min\{\Delta\eta_-, \Delta\eta_+\}$$

where,

$$\Delta\eta_- = min\{\eta(V_{had}), \eta(V_{lep})\} - min\{\eta_{j1}, \eta_{j2}\},$$

$$\Delta\eta_+ = max\{\eta_{j1}, \eta_{j2}\} - max\{\eta(V_{had}), \eta(V_{lep})\}$$

- **ζ > 0 : Both W's should be within VBF jets**
- **ζ < 0 : One or both lepton are at larger |η| than the VBF jets**

Zeppenfeld w.r.t. Leptonic W (Phys. Rev. D 54, 6680)

$$Z_{Wlep} = \frac{\eta_{Wlep} - \frac{\eta_{j1}+\eta_{j2}}{2}}{|\eta_{j1} - \eta_{j2}|}$$

Electron ID

Barrel

Variable	Veto	Loose	Medium	Tight
Full 5x5 $\sigma_{i\eta i\eta}$	0.0115	0.0110	0.00998	0.00998
$\Delta\eta_{seed}$	0.00749	0.00477	0.00311	0.00308
$\Delta\varphi_{in}$	0.228	0.222	0.103	0.0816
H/E	0.356	0.298	0.253	0.0414
Relative combined PF Isolation	0.175	0.0994	0.0695	0.0588
|1/E - 1/p|	0.299	0.241	0.134	0.0129
dxy	N/A	N/A	N/A	N/A
dz	N/A	N/A	N/A	N/A
Conversion Veto	yes	yes	yes	yes
Missing hits	2	1	1	1

Endcap

Variable	Veto	Loose	Medium	Tight
Full 5x5 $\sigma_{i\eta i\eta}$	0.0370	0.0314	0.0298	0.0292
$\Delta\eta_{seed}$	0.00895	0.00868	0.00609	0.00605
$\Delta\varphi_{in}$	0.213	0.213	0.0450	0.0394
H/E	0.211	0.101	0.0878	0.0641
Relative combined PF Isolation	0.159	0.107	0.0821	0.0571
|1/E - 1/p|	0.150	0.140	0.130	0.0129
dxy	N/A	N/A	N/A	N/A
dz	N/A	N/A	N/A	N/A
Conversion Veto	yes	yes	yes	yes
Missing hits	3	1	1	1

IDs for Jets

For -2.7 <= eta <= 2.7			
PF Jet ID	Loose	Tight	TightLepVeto
Neutral Hadron Fraction	< 0.99	< 0.90	< 0.90
Neutral EM Fraction	< 0.99	< 0.90	< 0.90
Number of Constituents	> 1	> 1	> 1
Muon Fraction	-	-	< 0.8
And for -2.4 <= eta <= 2.4 in addition apply			
Charged Hadron Fraction	> 0	> 0	> 0
Charged Multiplicity	> 0	> 0	> 0
Charged EM Fraction	< 0.99	< 0.99	< 0.90

For 2.7 < abs(eta) <= 3.0		
PF Jet ID		
Neutral EM Fraction	> 0.01	> 0.01
Neutral Hadron Fraction	< 0.98	< 0.98
Number of Neutral Particles	> 2	>2

For abs(eta) > 3.0		
PF Jet ID	Loose	Tight
Neutral EM Fraction	< 0.90	< 0.90
Number of Neutral	> 10	>10

What is Jet?

- Jet: An object reconstructed from the shower of particles produced from a quark or a gluon.
- Each particle belong to a jet is known as constituent.
    - Each has a 4-vector that can be used for further analysis.
- Algorithm to reconstruct jet from the particle in the shower:
    - Iteratively find the two particles in the event which are closest in some distance measure and combine them.
    - Combine two particles if $d_{ij} < d_{iB}$
        - Stop when $d_{ij} > d_{iB}$

$$d_{ij} = min(p_{ti}^{2p}, p_{tj}^{2p})\frac{\Delta R_{ij}^2}{R^2}$$

$$d_{iB} = p_{ti}^{2p}$$

p=1 → kT algorithm (kT)
p=0 → Cambridge Aachen algorithm (CA)
p=-1 → anti-kT algorithm (anti-kT)

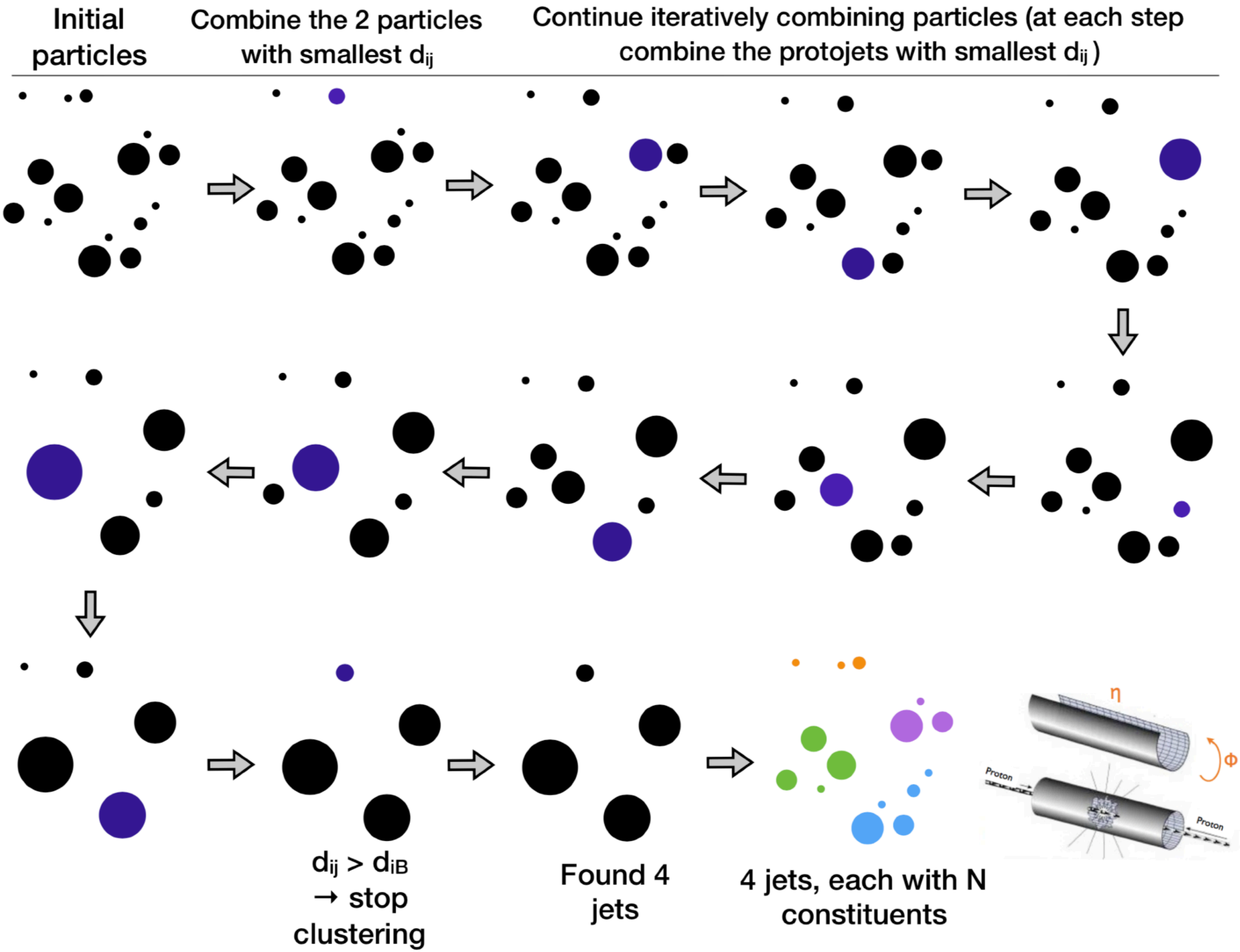

Initial particles
Combine the 2 particles with smallest d_{ij}
Continue iteratively combining particles (at each step combine the protojets with smallest d_{ij})
$d_{ij} > d_{iB}$ → stop clustering
Found 4 jets
4 jets, each with N constituents
η
Φ
Proton
Proton

Algorithm Comparison

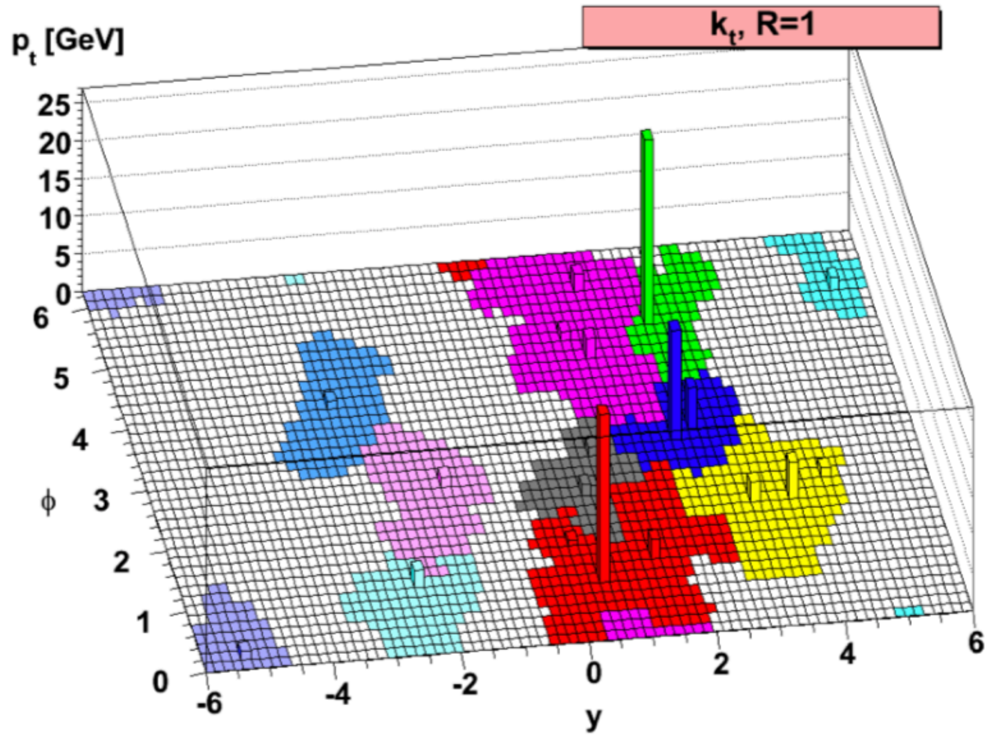

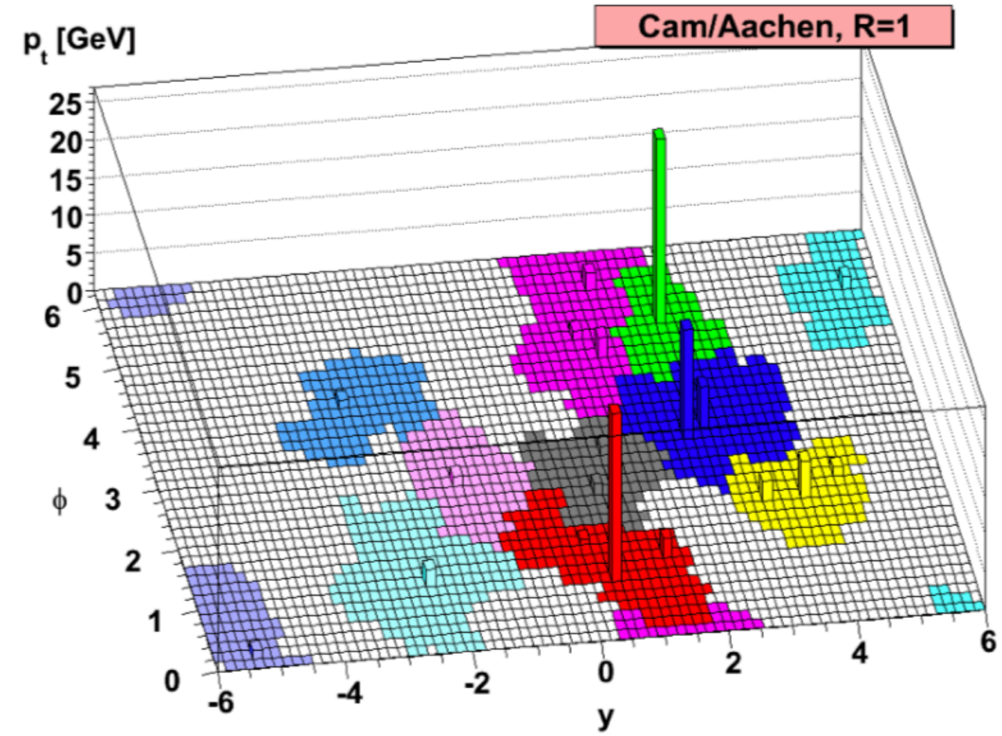

kT - soft particles clustered first

CA - angular clustering

anti-kT - hard particles clustered first

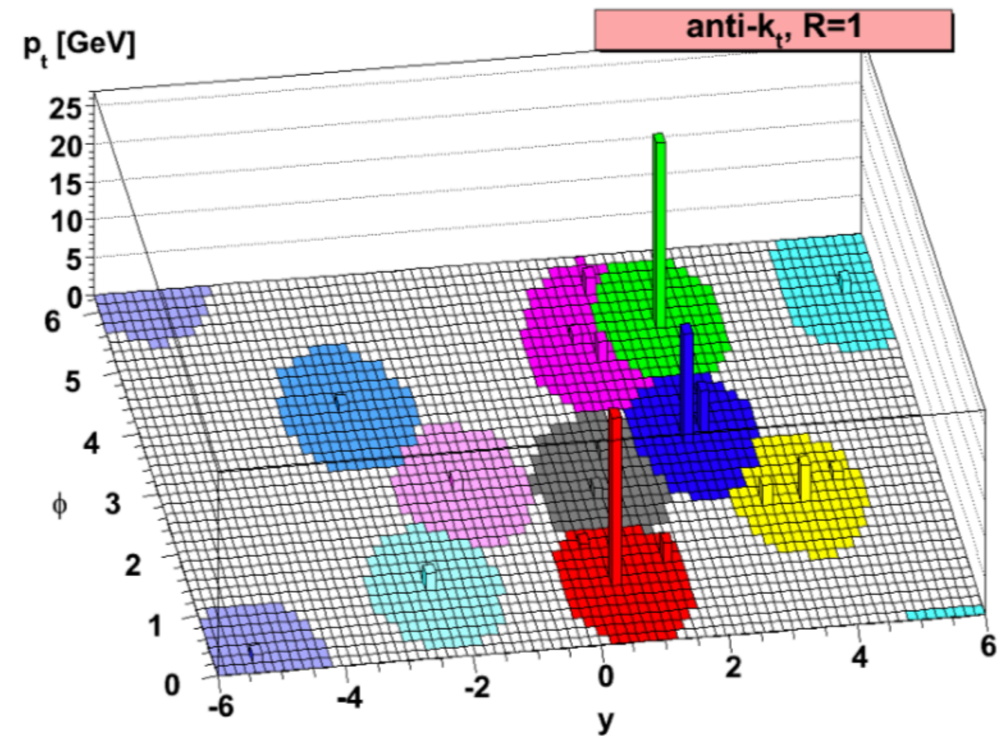

Jet Algorithm

- A good jet algorithm is infrared and collinear safe
    - The set of hard jets should be unchanged by soft emission and collinear splitting.

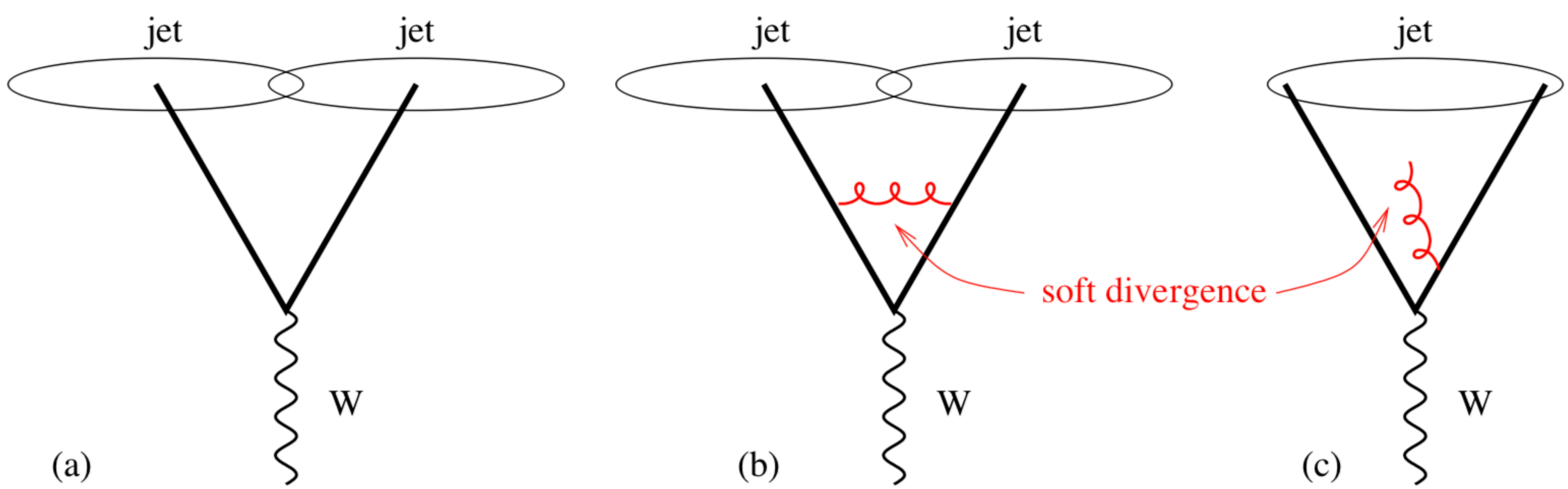

Gavin P. Salam: arXiv:0906.1833v1

Interference Studies Using MadGraph

- Electroweak sample generation:

$$generate\ pp \rightarrow W^+W^-jj\ QED = 4\ QCD = 0, W^- \rightarrow l^-\nu,\ W^+ \rightarrow jj$$

- QCD sample generation:

$$generate\ pp \rightarrow W^+W^-jj\ QED = 2\ QCD = 99, W^- \rightarrow l^-\nu,\ W^+ \rightarrow jj$$

- Electroweak + QCD generation:

$$generate\ pp \rightarrow W^+W^-jj\ QED = 4\ QCD = 99, W^- \rightarrow l^-\nu,\ W^+ \rightarrow jj$$

- In next slides upper plots are without applying any cut and bottom plots are same as above but after apply the following cuts:
  - VBF quarks pt > 30 && VBF quarks η < |4.0| && Δηjj > 4 && mWW > 300 && mjj > 300

Interference between EWK & QCD

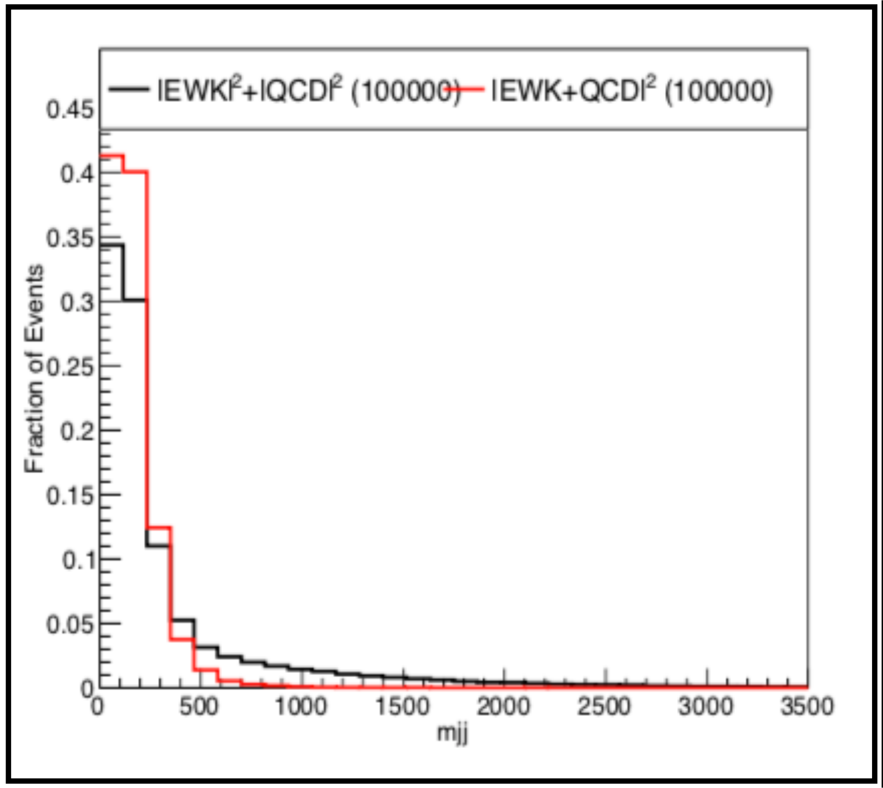

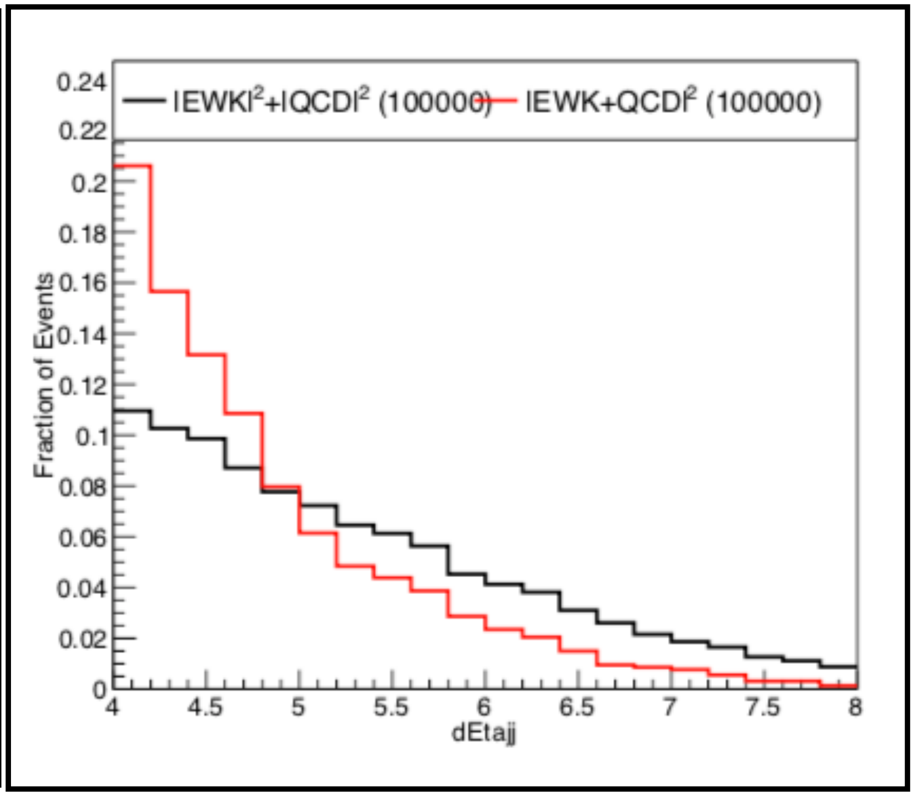

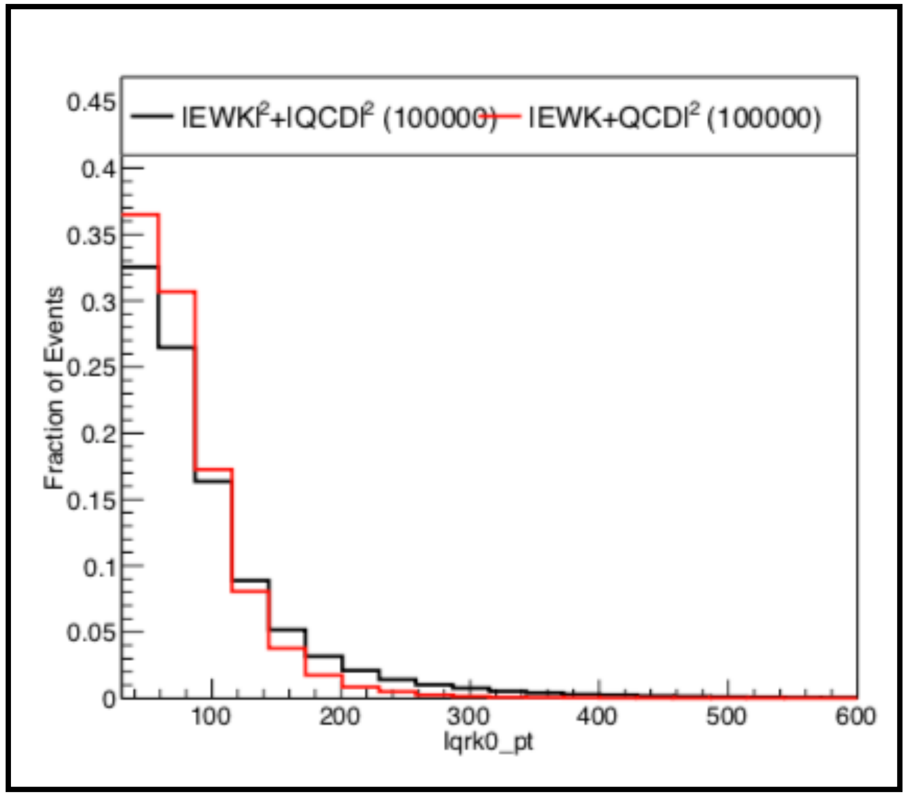

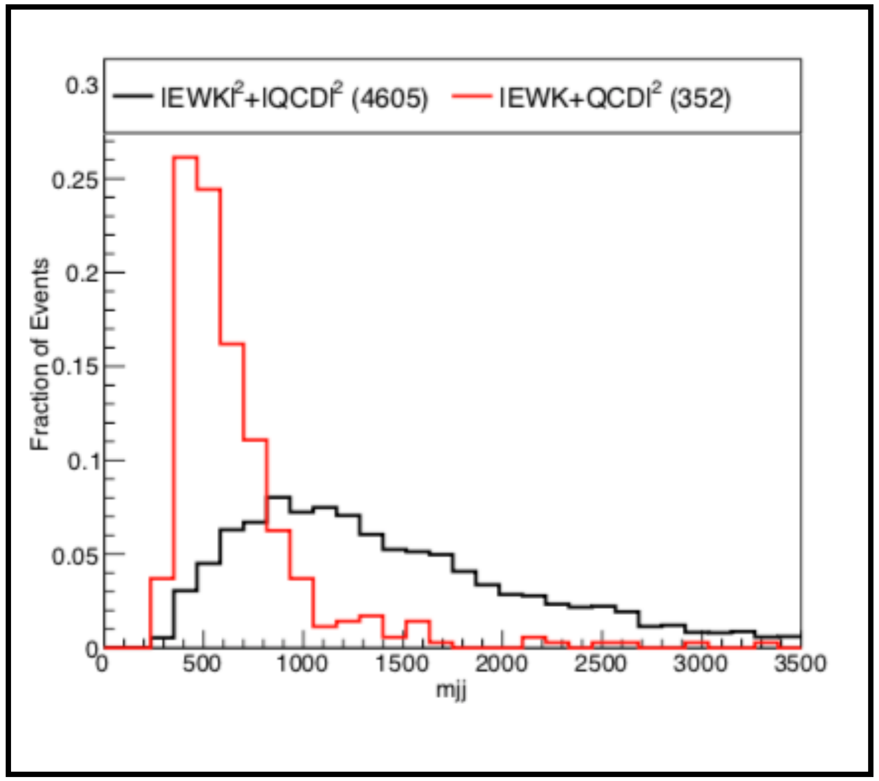

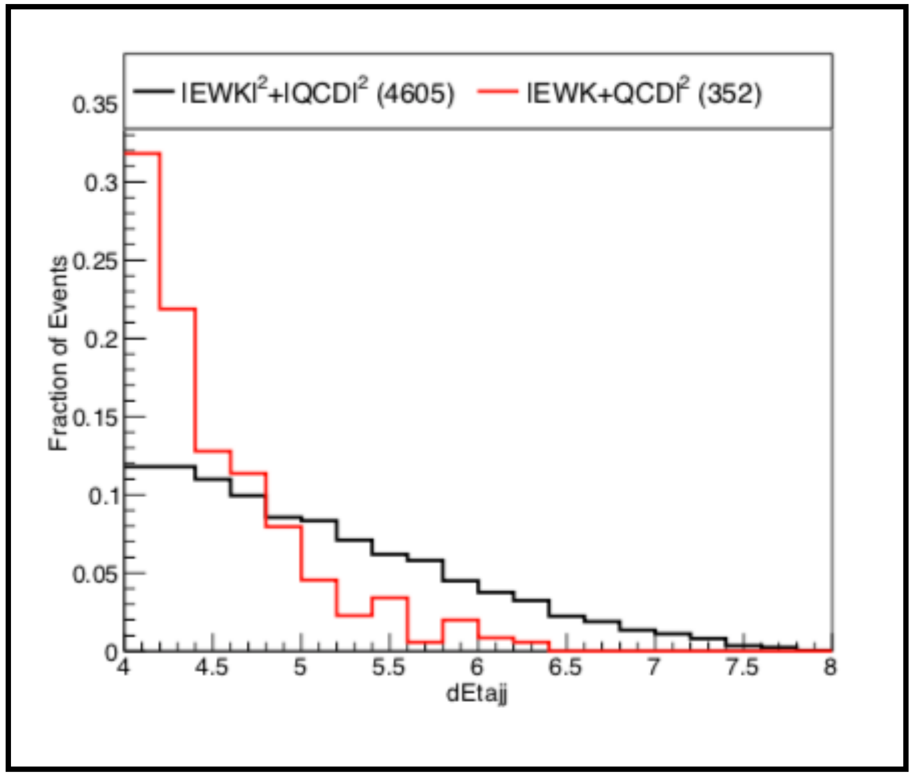

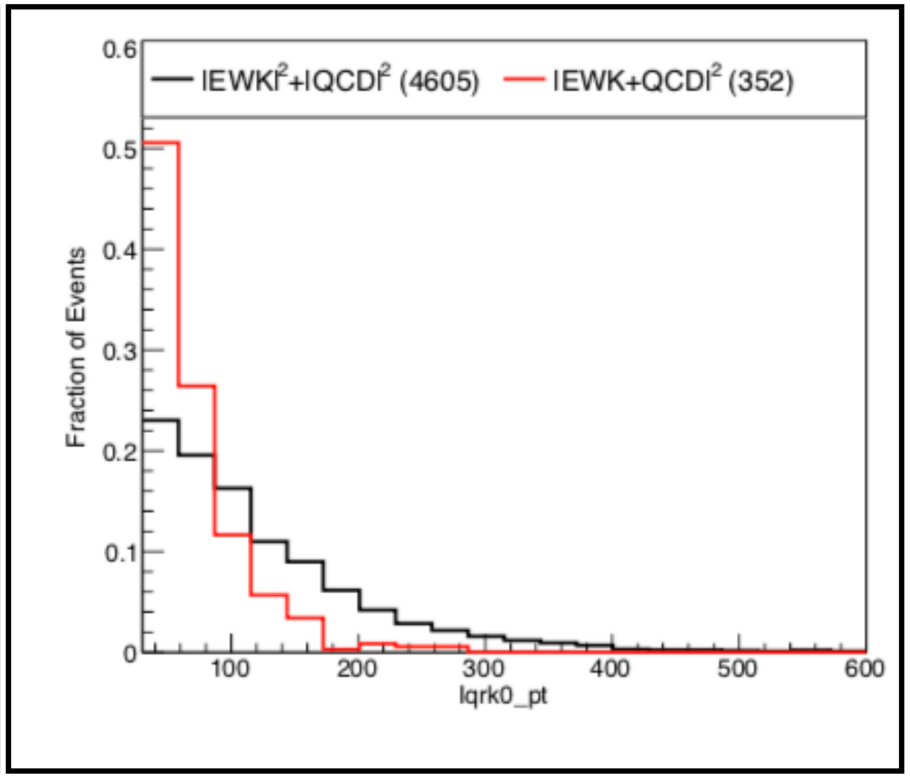

WW Scattering Cross-Section

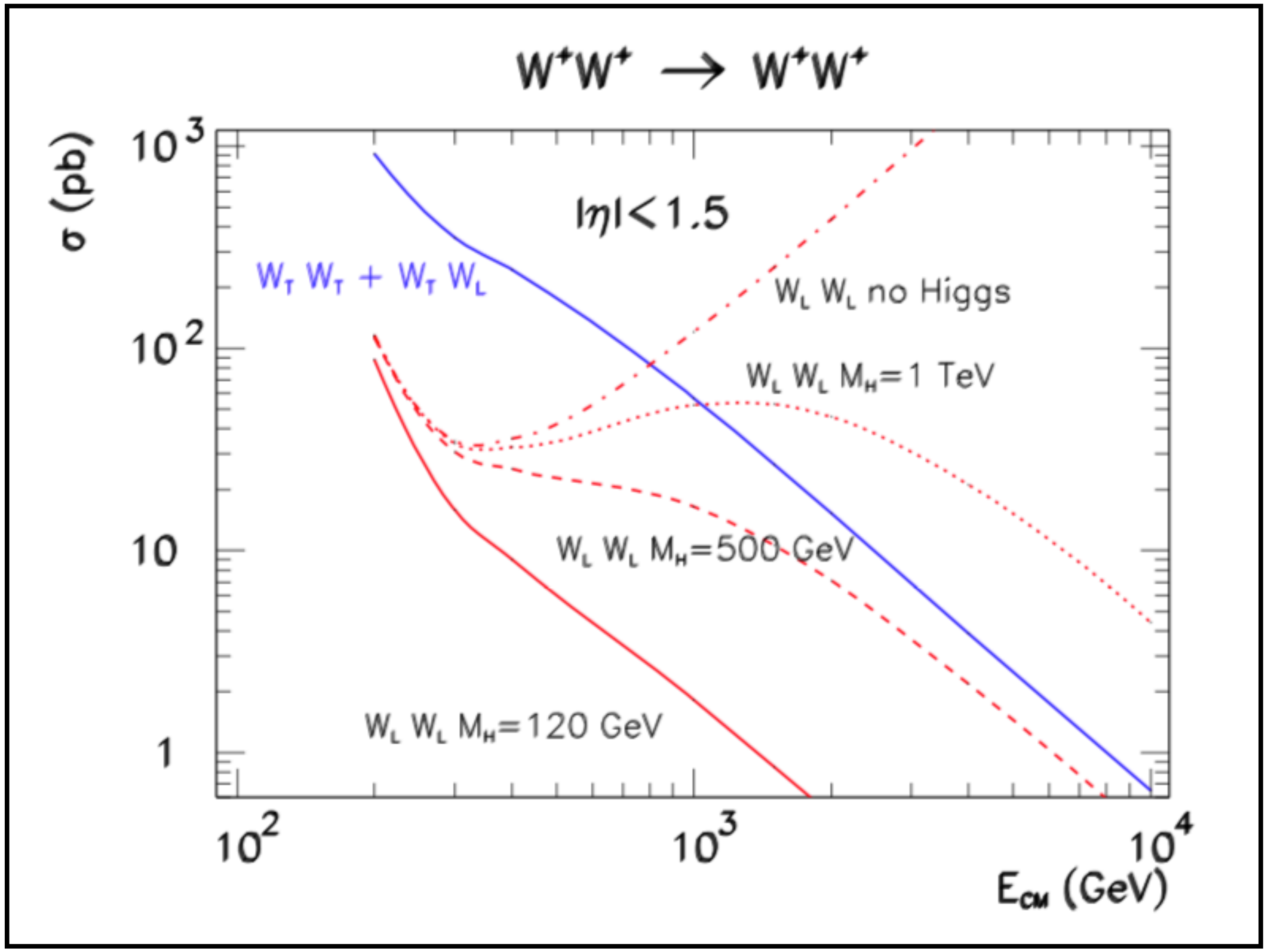

Operators containing only $D_\mu \phi$

$$\mathscr{L}_{eff} = \mathscr{L}_{SM} + \sum_{i=www,w,B,\phi W,\phi B} \frac{c_i}{\Lambda^2}\mathcal{O}_i + \sum_{j=0,1} \frac{f_{S,j}}{\Lambda^4}\mathcal{O}_{S,j} + \sum_{j=0,\ldots,9} \frac{f_{T,j}}{\Lambda^4}\mathcal{O}_{T,j} + \sum_{j=0,\ldots,7} \frac{f_{M,j}}{\Lambda^4}\mathcal{O}_{M,j}$$

$$\mathcal{O}_{S,0} = \left[(D_\mu\phi)^\dagger \times D_\nu\phi)\right] \times \left[(D^\mu\phi)^\dagger D^\nu\phi\right],$$

$$\mathcal{O}_{S,1} = \left[(D_\mu\phi)^\dagger \times D^\mu\phi)\right] \times \left[(D_\nu\phi)^\dagger D^\nu\phi\right],$$

$$D_\mu = \partial_\mu + i\frac{g'}{2}B_\mu + ig_w W^i_\mu \frac{T^i}{2}$$

$$W_{\mu\nu} = \frac{i}{2} g T^i(\partial_\mu W^i_\nu - \partial_\nu W^i_\mu + g\epsilon_{ijk} W^j_\mu W^k_\nu)$$

$$B_{\mu\nu} = \frac{i}{2} g'(\partial B_\nu - \partial_\nu B_\mu)$$

Operators containing $D_\mu\phi$ and field strength tensor

$$\mathcal{O}_{M,0} = Tr\Big[W_{\mu\nu}W^{\mu\nu}\Big] \times \Big[(D_\beta\phi)^\dagger D^\beta\phi\Big]$$

$$\mathcal{O}_{M,1} = Tr\Big[W_{\mu\nu}W^{\nu\beta}\Big] \times \Big[(D_\beta\phi)^\dagger D^\mu\phi\Big]$$

$$\mathcal{O}_{M,2} = \Big[B_{\mu\nu}B^{\mu\nu}\Big] \times \Big[(D_\beta\phi)^\dagger D^\beta\phi\Big]$$

$$\mathcal{O}_{M,3} = \Big[B_{\mu\nu}B^{\nu\beta}\Big] \times \Big[(D_\beta\phi)^\dagger D^\mu\phi\Big]$$

$$\mathcal{O}_{M,4} = \Big[(D_\mu\phi)^\dagger W_{\beta\nu}D^\mu\phi\Big] \times B^{\beta\nu}$$

$$\mathcal{O}_{M,5} = \Big[(D_\mu\phi)^\dagger W_{\beta\nu}D^\nu\phi\Big] \times B^{\beta\mu}$$

$$\mathcal{O}_{M,6} = \Big[(D_\mu\phi)^\dagger W_{\beta\nu}W^{\beta\nu}D^\mu\phi\Big]$$

$$\mathcal{O}_{M,7} = \Big[(D_\mu\phi)^\dagger W_{\beta\nu}W^{\beta\nu}D^\mu\phi\Big]$$

Operators containing field strength tensor only

$$\mathcal{O}_{T,0} = Tr\left[W_{\mu\nu}W^{\mu\nu}\right] \times Tr\left[W_{\alpha\beta}W^{\alpha\beta}\right]$$

$$\mathcal{O}_{T,1} = Tr\left[W_{\alpha\nu}W^{\mu\beta}\right] \times Tr\left[W_{\mu\beta}W^{\alpha\nu}\right]$$

$$\mathcal{O}_{T,2} = Tr\left[W_{\alpha\mu}W^{\mu\beta}\right] \times Tr\left[W_{\beta\nu}W^{\nu\alpha}\right]$$

$$\mathcal{O}_{T,5} = Tr\left[W_{\mu\nu}W^{\mu\nu}\right] \times B_{\alpha\beta}B^{\alpha\beta}$$

$$\mathcal{O}_{T,6} = Tr\left[W_{\alpha\nu}W^{\mu\beta}\right] \times B_{\mu\beta}B^{\alpha\nu}$$

$$\mathcal{O}_{T,7} = Tr\left[W_{\alpha\mu}W^{\mu\beta}\right] \times B_{\beta\nu}B^{\nu\alpha}$$

$$\mathcal{O}_{T,8} = B_{\nu\mu}B^{\nu\mu}B_{\alpha\beta}B^{\alpha\beta}$$

$$\mathcal{O}_{T,9} = B_{\alpha\mu}B^{\mu\beta}B_{\beta\nu}B^{\nu\alpha}$$

Systematic Uncertainty

Systematic uncertainties are measurement errors which are not due to statistical fluctuations in real or simulated data samples.

List of typical sources of systematic uncertainties:

- Badly known detector acceptances or trigger efficiencies;
- Incorrect detector calibrations;
- Badly known detector resolutions;
- Badly known background;
- Uncertainties in the simulation or underlying theoretical models;
- Uncertainties on input parameters like cross-sections, branching fractions, life-times, the luminosity, and so on;
- Computational and software errors;
- Personal biases towards a specific outcome of an analysis;
- Other usually unknown effects on the measurements.

Impact Plot

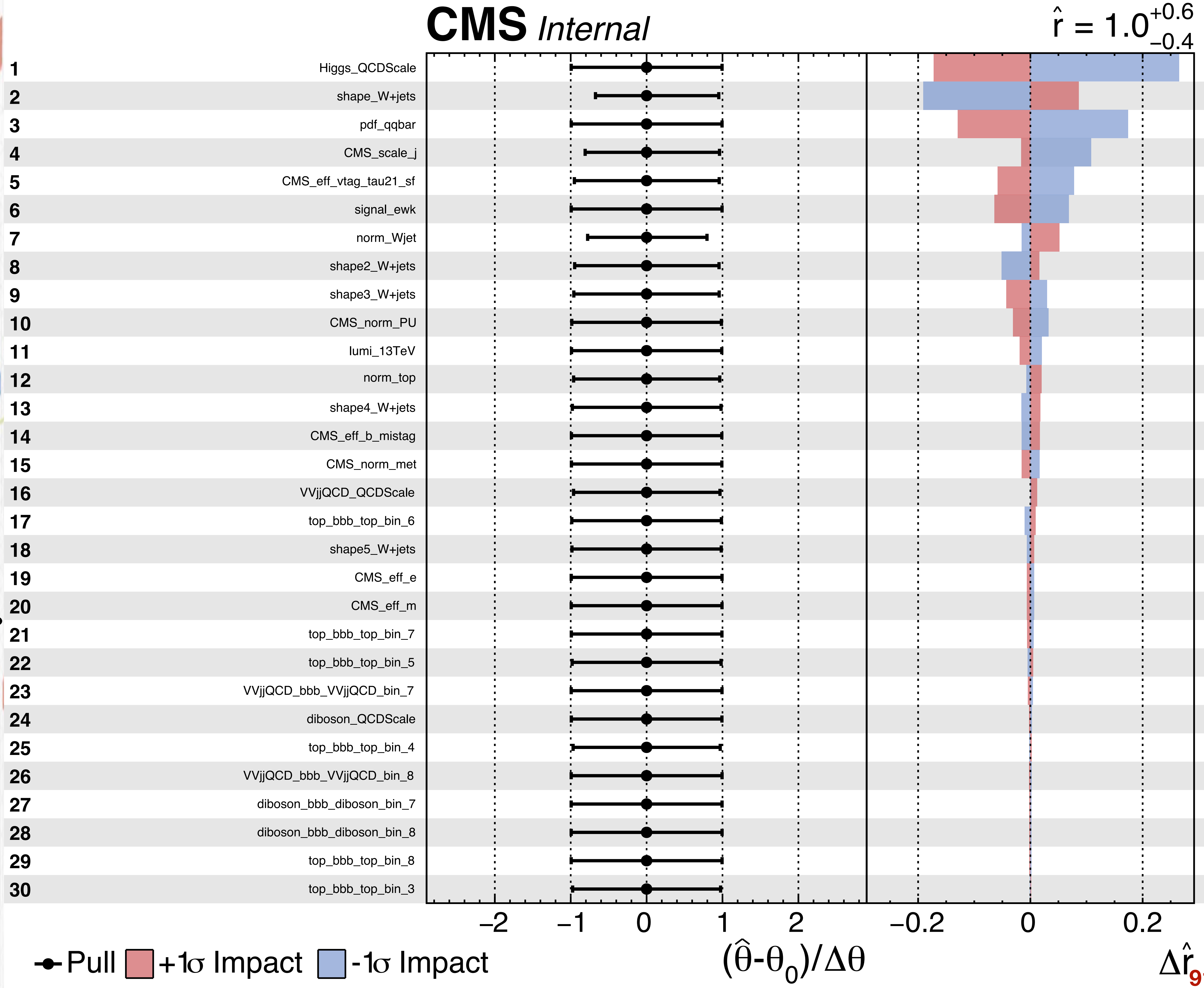

CMS Internal
r̂ = 1.0 +0.6 −0.4
1 Higgs_QCDScale
2 shape_W+jets
3 pdf_qqbar
4 CMS_scale_j
5 CMS_eff_vtag_tau21_sf
6 signal_ewk
7 norm_Wjet
8 shape2_W+jets
9 shape3_W+jets
10 CMS_norm_PU
11 lumi_13TeV
12 norm_top
13 shape4_W+jets
14 CMS_eff_b_mistag
15 CMS_norm_met
16 VVjjQCD_QCDScale
17 top_bbb_top_bin_6
18 shape5_W+jets
19 CMS_eff_e
20 CMS_eff_m
21 top_bbb_top_bin_7
22 top_bbb_top_bin_5
23 VVjjQCD_bbb_VVjjQCD_bin_7
24 diboson_QCDScale
25 top_bbb_top_bin_4
26 VVjjQCD_bbb_VVjjQCD_bin_8
27 diboson_bbb_diboson_bin_7
28 diboson_bbb_diboson_bin_8
29 top_bbb_top_bin_8
30 top_bbb_top_bin_3
−2 −1 0 1 2
−0.2 0 0.2
Pull +1σ Impact -1σ Impact
$(\hat{\theta}-\theta_0)/\Delta\theta$
$\Delta\hat{r}$

General Information

- Data Sample Used: **single electron and single muon**
- Luminosity: 35.87 fb^{-1}
- Trigger used:
  - For electrons: HLT_Ele27_WPTight_Gsf_v
  - For muons: HLT_IsoMu24_v, HLT_IsoTkMu24_v

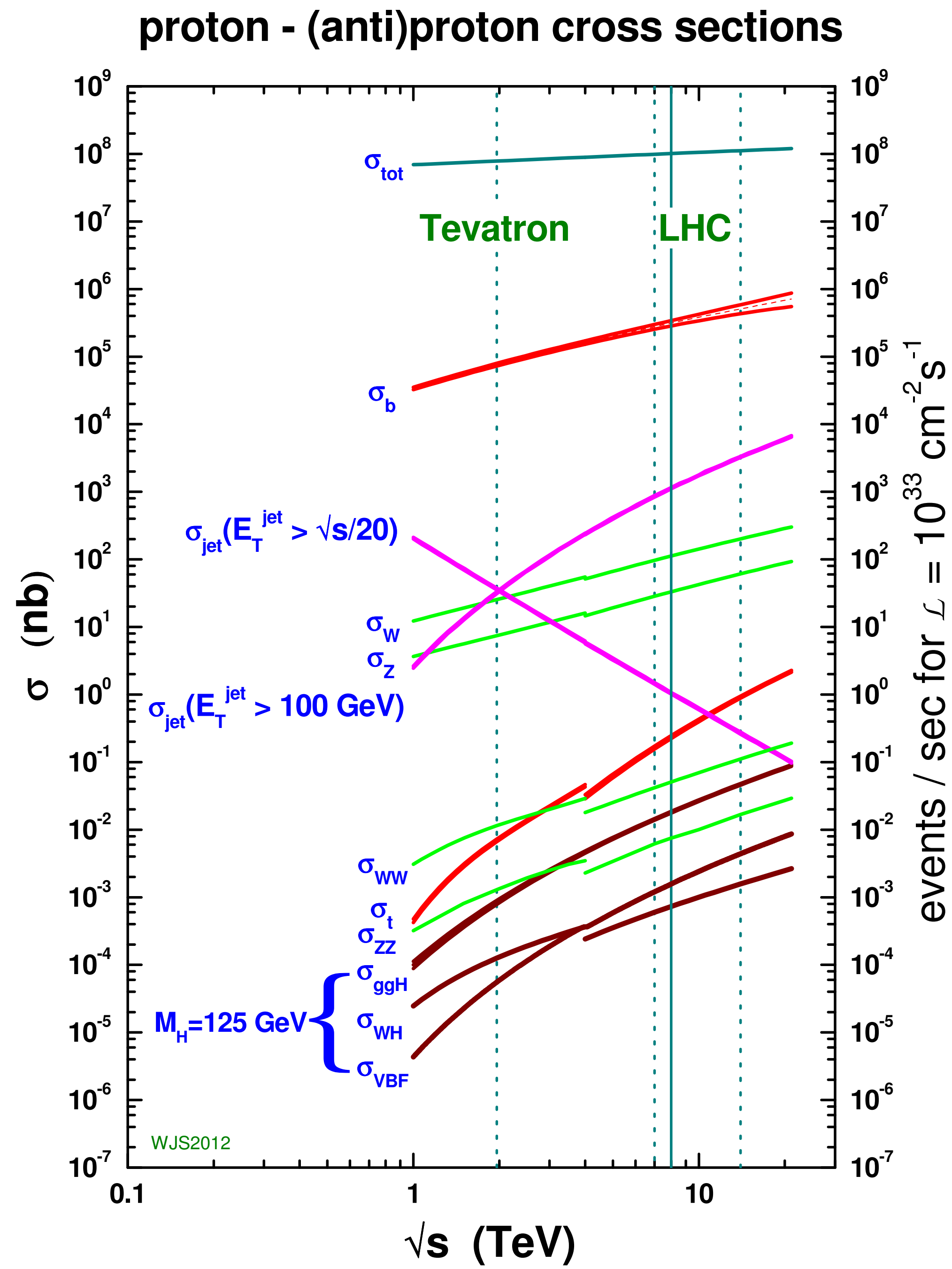

Proton proton cross-section

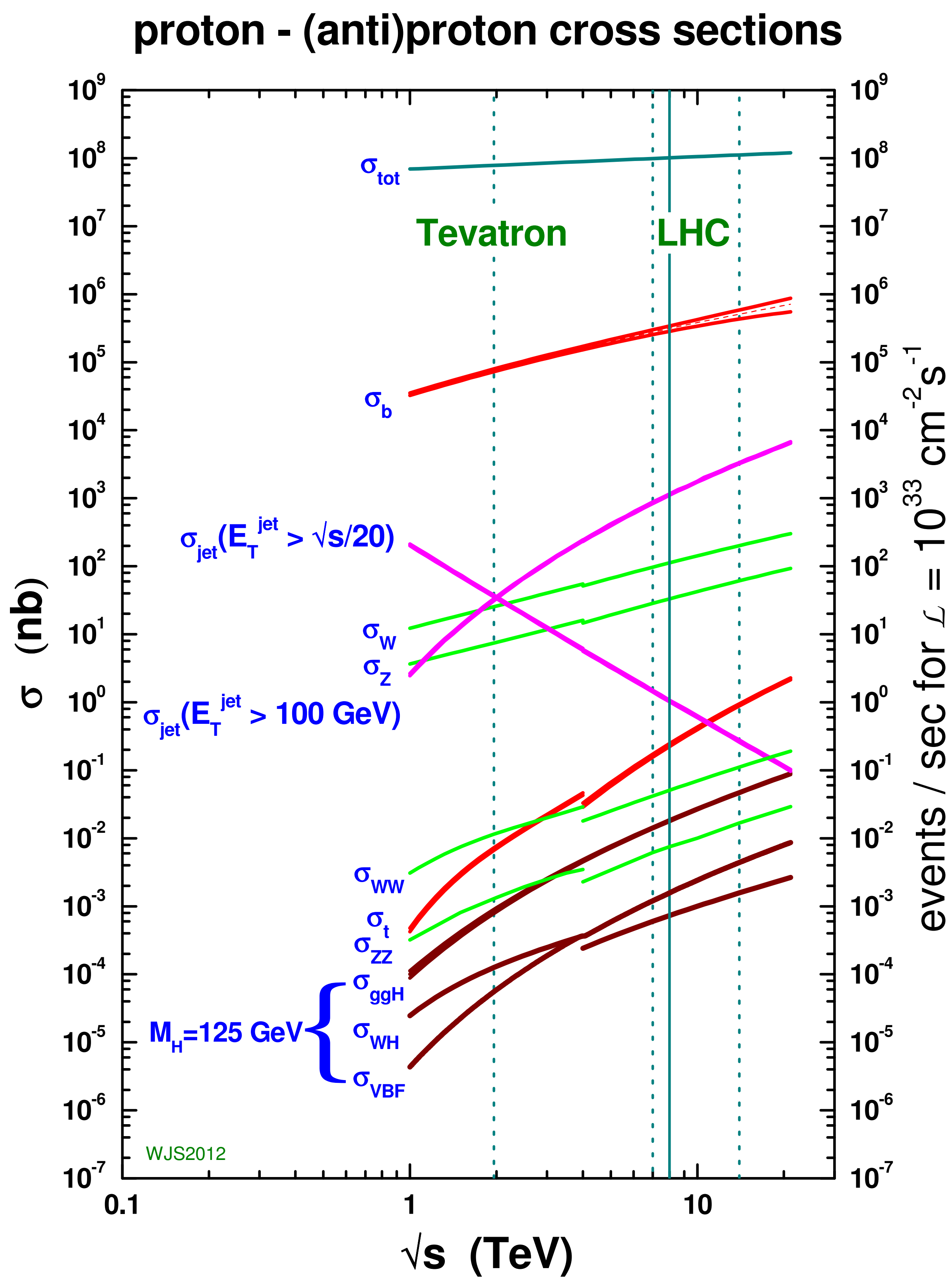

Object Identification

Electrons:

(Energy clustering to recover bremsstrahlung)

- Superclusters: are built by collecting clusters of crystals with in ϕ window

Electron seeding two complementary algorithms

- Start from the ECAL superclusters and search for compatible hits in the tracker inner layers (ECAL driven)
- Starts from tracks and finding clusters associated with them in ECAL (Tracker driven)

Jets:

- Jets are reconstructed using particle flow anti-kT algorithm with R=0.4 and R=0.8
- Particle flow (PF): Aims to reconstructing and identifying all stable particles in the event, i.e., electrons, muons, photons, charged hadrons and neutral hadrons.
- PUPPI (Pile-up per particle identification): Based on PF paradigm=> Assigns weight par particle based on how likely a particle is from PU.

Muons:

- Combine the muon segments found in the muon detector with the tracks from the tracking detector.
- Three categories: Global muons, Tracker muons and standalone muons.
- Momentum of muons determined from bending due to magnetic field in tracker and in Muon system.

MET:

- Imbalance in the momentum in the plane transverse to the beam direction constitutes MET and it signifies the undetected particles.
- MET reconstructed using particle-flow is used.